

INFORMATION TO USERS

This manuscript has been reproduced from the microfilm master. UMI films the text directly from the original or copy submitted. Thus, some thesis and dissertation copies are in typewriter face, while others may be from any type of computer printer.

The quality of this reproduction is dependent upon the quality of the copy submitted. Broken or indistinct print, colored or poor quality illustrations and photographs, print bleedthrough, substandard margins, and improper alignment can adversely affect reproduction.

In the unlikely event that the author did not send UMI a complete manuscript and there are missing pages, these will be noted. Also, if unauthorized copyright material had to be removed, a note will indicate the deletion.

Oversize materials (e.g., maps, drawings, charts) are reproduced by sectioning the original, beginning at the upper left-hand corner and continuing from left to right in equal sections with small overlaps. Each original is also photographed in one exposure and is included in reduced form at the back of the book.

Photographs included in the original manuscript have been reproduced xerographically in this copy. Higher quality 6" x 9" black and white photographic prints are available for any photographs or illustrations appearing in this copy for an additional charge. Contact UMI directly to order.

UMI

A Bell & Howell Information Company
300 North Zeeb Road, Ann Arbor, MI 48106-1346 USA
313/761-4700 800/521-0600

The Pennsylvania State University

The Graduate School

Department of Mechanical Engineering

INTELLIGENT ROBUST CONTROL OF CLUTCH-TO-CLUTCH
SHIFTS IN VEHICLE TRANSMISSION SYSTEMS

A Thesis in
Mechanical Engineering

by

Jing-Shiun Lai

© 1995 Jing-Shiun Lai

Submitted in Partial Fulfillment
of the Requirements
for the Degree of

Doctor of Philosophy

December 1995

UMI Number: 9612774

UMI Microform 9612774

Copyright 1996, by UMI Company. All rights reserved.

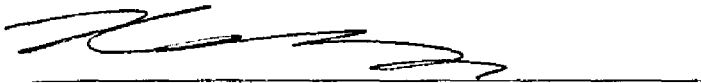
**This microform edition is protected against unauthorized
copying under Title 17, United States Code.**

UMI

**300 North Zeeb Road
Ann Arbor, MI 48103**

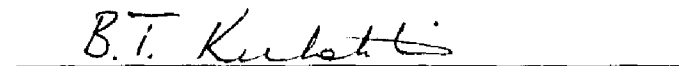
We approve the thesis of Jing-Shiun Lai.

Date of Signature



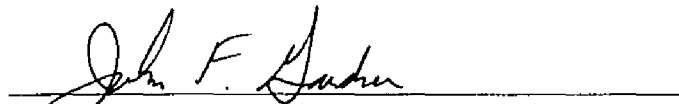
9/11/95

Kon-Well Wang
Associate Professor of Mechanical Engineering
Thesis Advisor
Chair of Committee



9/11/95

Bohdan T. Kulakowski
Professor of Mechanical Engineering



9/11/95

John F. Gardner
Associate Professor of Mechanical Engineering



9/11/95

Jeffrey S. Mayer
Assistant Professor of Electrical Engineering



9-12-95

Richard C. Benson
Professor of Mechanical Engineering
Head of the Department of Mechanical Engineering

ABSTRACT

Most production transmissions today use mechanical devices, such as sprag mechanisms (freewheelers), to achieve acceptable shift quality. These devices are expensive and often complicate the mechanical design. In a recently synthesized class of transmissions, the freewheelers are not present and *clutch-to-clutch* shift [Leising et al., 1990], a non-trivial control problem, is required.

In controlling vehicle transmissions with clutch-to-clutch shifts, there are different types of uncertainties that the controller has to overcome. The most important ones include actuator delay and inconsistency (e.g., clutch fill time), actuator static errors (e.g., clutch frictional characteristics), actuator dynamics, plant modeling errors, unknown external disturbance, and plant structure variations (e.g., torque-to-speed phase change). These important issues are fully addressed in this research. An intelligent robust control system is developed to compensate for these uncertainties and achieve consistent and satisfactory clutch-to-clutch shifts. In this thesis, emphasis is on controlling the upshift operation.

The major achievements of this thesis can be summarized as follows:

1. A unique powertrain model for clutch-to-clutch shifts is developed. A checking logic is designed to examine the lock-up conditions of the clutches, and different sets of state equations are used for different modes of operation.
2. A Hybrid control algorithm consists of a Rule-Based Module and a Sliding Control Module is synthesized for controlling the clutch-to-clutch upshift scenario. The Rule-

Based Module is developed to compensate for the actuator delay and inconsistency in the fill-phase and torque-phase of a shift. The Sliding Control Module is developed to compensate for actuator static errors, actuator dynamics, plant modeling errors, and unknown external disturbance during the speed-phase operation. In this research, two types of output signals are used, namely, output torque and output acceleration (i.e., the acceleration after the final drive). Therefore, a torque-based controller and an acceleration-based controller are developed.

3. Multiple Surface Sliding Control design method is developed to control systems whose control input is not explicitly related to the control output. This scheme is required for speed-phase Sliding Control using output torque signals.
4. To estimate the output torque for the output-torque-based Hybrid algorithm, a Neural Network estimator is developed to identify the transmission input/output torques and the clutch frictional coefficients. Promising results are shown through computer simulation. Limitations of this recurrent network approach are also identified.
5. Since estimating output torque using the Neural Network estimator has limitations, Hybrid control algorithms based on transmission output accelerations are investigated. Two novel acceleration estimation schemes are developed. It is proved that the proposed estimation schemes can improve the performance upon any base-line estimation from available schemes.
6. It is shown that the proposed estimation schemes provide good estimation of acceleration for the Hybrid approach. It is also illustrated that the output-acceleration-

based Hybrid controller can achieve more robust performance compared to two of the most recently developed transmission clutch-to-clutch control schemes.

TABLE OF CONTENTS

LIST OF FIGURES	viii
LIST OF TABLES	xi
NOMENCLATURE	xii
ACKNOWLEDGMENTS	xv
Chapter 1. INTRODUCTION	1
1.1. Background and Problem Statement	1
1.2. Objectives and Approach	2
Chapter 2. POWERTRAIN MODEL	4
2.1. Overview and Assumptions	4
2.2. Clutch Lock-Up Logic	7
2.3. State Equations	7
Chapter 3. CONTROL LAW DEVELOPMENT	12
3.1. Issues and Review of Previous Work	12
3.2. Proposed Method	14
Chapter 4. TORQUE ESTIMATOR DEVELOPMENT	20
4.1. Issues and Problem Statement	20
4.2. Proposed Method	20
4.3. Simulation Results	25
4.4. Discussion	34

Chapter 5.	ACCELERATION ESTIMATION SCHEME DEVELOPMENT	36
	5.1. Issues and Papers Review	36
	5.2. Proposed Methods	40
	5.3. Results and Discussions	47
Chapter 6.	CONTROL SYSTEM SIMULATION RESULTS	64
	6.1. Hybrid Approach Simulation Results	64
	6.2. Comparison Study	64
Chapter 7.	CONCLUSIONS AND DISCUSSIONS	73
	REFERENCES	76
	APPENDIX A. DERIVATION OF NEURAL NETWORK TRAINING ALGORITHM	81
	APPENDIX B. DISCRETE MULTIPLE SURFACE SLIDING CONTROL DESIGN	84
	APPENDIX C. ACCELERATION ESTIMATION SCHEMES	93

LIST OF FIGURES

Figure 2.1	Schematic of the powertrain system model	6
Figure 3.1	Rule-Based control of a 1-2 upshift	16
Figure 3.2	Desired output torque trajectory	17
Figure 3.3	Desired output acceleration trajectory	19
Figure 4.1	Neuron	21
Figure 4.2	Two layer feedforward perceptron	21
Figure 4.3	Schematic of neural network	27
Figure 4.4	Neural Network training flowchart	28
Figure 4.5	Check 1 and Check 2	29
Figure 4.6	Stage 1 training error E , T_s estimation error, and T_i estimation error	30
Figure 4.7	Stage 2 training error E and T_{c2} estimation error	31
Figure 4.8	Stage 3 training error E and T_{c1} estimation error	32
Figure 4.9	Transmission output torque for ideal case and the Hybrid approach combined with Artificial Neural Network estimator	33
Figure 5.1	Schematic of acceleration estimation with feedback controller	39
Figure 5.2	Schematic of acceleration estimation with feedback adaptive filter	39
Figure 5.3	Membership function used for fuzzy rules	43
Figure 5.4	Estimation using Scheme A, base-line estimation, and true acceleration	49
Figure 5.5	Estimation using Scheme B, base-line estimation, and true acceleration	49

Figure 5.6	Engine-Transmission setup and instrumentation used for speed and torque measurement	50
Figure 5.7	A schematic of speed sensor	50
Figure 5.8	Estimation using Scheme A and base-line estimation	55
Figure 5.9	Estimation using Scheme A and estimation using finite difference	55
Figure 5.10	Estimation using Scheme A and base-line estimation	56
Figure 5.11	Estimation using Scheme A and estimation using finite difference	56
Figure 5.12	Estimation using Scheme A and base-line estimation	57
Figure 5.13	Estimation using Scheme A and estimation using finite difference	57
Figure 5.14	Estimation using Scheme B and base-line estimation	58
Figure 5.15	Estimation using Scheme B and base-line estimation	58
Figure 5.16	Estimation using Scheme B and base-line estimation	59
Figure 5.17	Estimation using Scheme A, base-line estimation, and transmission output torque	59
Figure 5.18	Estimation using Scheme A and estimation using finite difference	60
Figure 5.19	Estimation using Scheme A, base-line estimation, and transmission output torque	60
Figure 5.20	Estimation using Scheme A and estimation using finite difference	61
Figure 5.21	Estimation using Scheme B, base-line estimation, and transmission output torque	61
Figure 5.22	Estimation using Scheme B and estimation using finite difference	62
Figure 5.23	Estimation using Scheme B, base-line estimation, and transmission output torque	62
Figure 5.24	Estimation using Scheme B and estimation using finite difference	63

Figure 6.1	Vehicle acceleration during a 1-2 upshift using Hybrid approach with true acceleration and with acceleration estimated using proposed schemes	67
Figure 6.2	Vehicle acceleration during a 1-2 upshift using Hybrid approach with true acceleration and with base-line Estimation of estimation Scheme A	67
Figure 6.3	Vehicle acceleration during a 1-2 upshift using Hybrid approach with true acceleration and with base-line estimation of Estimation Scheme B	68
Figure 6.4	Vehicle acceleration during a 1-2 upshift using Control Scheme I, Control Scheme II, and Hybrid approach with true acceleration(No fill-time uncertainty)	68
Figure 6.5	Vehicle acceleration during a 1-2 upshift using Control Scheme I	69
Figure 6.6	Vehicle Acceleration during a 1-2 upshift using Control Scheme II	69
Figure 6.7	Vehicle acceleration during a 1-2 upshift using Hybrid approach with acceleration estimated using Estimation Scheme A	70
Figure 6.8	Vehicle acceleration during a 1-2 upshift using Hybrid approach with acceleration estimated using Estimation Scheme B	70
Figure 6.9	Clutch pressure commands (P_{d1}, P_{d2}) and actual pressures (P_{c1}, P_{c2}) during a 1-2 upshift using the Hybrid approach with acceleration estimated using Estimation Scheme A	71
Figure 6.10	Clutch pressure commands (P_{d1}, P_{d2}) and actual pressures (P_{c1}, P_{c2}) during a 1-2 upshift using the Hybrid approach with acceleration estimated using Estimation Scheme B	72
Figure A.1	Two layer feedforward Neural Network cascaded with partially known system model	81

LIST OF TABLES

Table 4.1	Variables used in Simulation	26
-----------	------------------------------	----

NOMENCLATURE

A_1	Area * effective radius of clutch 1 (off-going clutch)
A_2	Area * effective radius of clutch 2 (on-coming clutch)
A_o	Transmission output angular acceleration
A_{od}	Desired transmission output angular acceleration
C_1	Clutch 1
C_2	Clutch 2
C_e	Damping between torque converter and transmission
C_t	Damping between transmission and vehicle
F_a	Aerodynamic force
F_f	Tractive/breaking force of front tire
F_r	Tractive/breaking force of rear tire
h_f	Ground to axle height of front wheel
h_r	Ground to axle height of rear wheel
I_1	Equivalent transmission upstream inertia
I_2	Equivalent transmission downstream inertia
I_e	Effective inertia of engine and torque converter pump parts
I_{wf}	Front wheel inertia
I_{wr}	Rear wheel inertia

k_1	Tractive force with respect to slip ratio of front wheel
k_2	Tractive force with respect to slip ratio of rear wheel
k_3	Aerodynamic force coefficient
k_4	Aerodynamic force coefficient
K_{s1}	Transmission input shaft stiffness
K_{s2}	Transmission output shaft stiffness
M_h	Vehicle mass
P_{c1}	Off-going clutch pressure
P_{c2}	On-coming clutch pressure
P_{d1}	Off-going clutch pressure command
P_{d2}	On-coming clutch pressure command
R_1	First gear speed reduction ratio
R_2	Second gear speed reduction ratio
R_d	Final drive speed reduction ratio
T_{c1}	Off-going clutch torque
T_{c1}^0	Transmitted torque of clutch 1 when locked-up
T_{c2}	On-coming clutch torque
T_{c2}^0	Transmitted torque of clutch 2 when locked-up
T_e	Engine indicated torque
T_{fu}	Transmission upstream damping torque

T_{fd}	Transmission downstream damping torque
T_i	Transmission input shaft torque
T_s	Transmission output shaft torque
T_{sd}	Desired transmission output shaft torque
V	Vehicle velocity
τ_{cl}	Effective time constant of off-going clutch
μ_1	Off-going clutch frictional coefficient
μ_2	On-coming clutch frictional coefficient
ω_1	Transmission upstream angular velocity
ω_2	Transmission downstream angular velocity
ω_{2d}	Desired transmission downstream angular velocity
ω_e	Engine angular velocity
ω_n	Natural frequency of hydraulic actuator
ω_{wf}	Front wheel angular velocity
ω_{wr}	Rear wheel angular velocity
ζ	Damping ratio of hydraulic actuator
Δt_{c2}	Hydraulic fill time delay of on-coming clutch
ΔT	Controller loop time

ACKNOWLEDGMENTS

I would like to express my sincere appreciation to my thesis advisor Dr. Kon-Well Wang for his invaluable guidance, patience, encouragement, and financial support throughout the course of this research. I am also very grateful to Dr. Bohdan T. Kulakowski, Dr. John F. Gardner, and Dr. Jeffrey S. Mayer for their serving as my committee members.

I would like to thank Dr. William E. Tobler, Mr. Larry T. Brown, Mr. Marvin P. Kraska, Mr. Dan S. Colvin, Mr. Walt J. Ortmann, and Mr. Pat A. Kaluzny, at the Ford Scientific Research Laboratory for the financial support, valuable discussions, and their assistance in experimental validation.

My deepest gratitude goes to my mother, my wife, and all my family members. Without their continuous support and encouragement, this work would not have been finished. Finally, I would like to share my achievements with my daughter, Cynthia.

1. INTRODUCTION

1.1. Background and Problem Statement

Most production transmissions today use mechanical devices, such as sprag mechanisms (freewheelers), to achieve acceptable shift quality. These devices are expensive and often complicate the mechanical design. In a recently synthesized class of transmissions, the freewheelers are not present and clutch-to-clutch shift, a non-trivial control problem, is required.

In controlling complex mechanical systems such as vehicle transmissions with clutch-to-clutch shifts, there are different types of uncertainties that the controller has to overcome. The most important ones include actuator delay and inconsistency (e.g., clutch fill time), actuator static errors (e.g., clutch frictional characteristics), actuator dynamics, plant modeling errors, unknown external disturbance, and plant structure variations (e.g., torque-to-speed phase change). Any one of these uncertainties will alter the dynamic characteristics of the control system and cause the performance to deviate from its expected behavior. This will normally degrade the shift quality of the vehicle.

Control theories have been developed in the past to compensate for system uncertainties. However, a transmission usually involves a combination of different types of uncertainties, and is too complex to be resolved by applying a single control theory. Therefore, it is important to synthesize an integrated system which consists of the desirable

features of several different control laws. This will lead us to the development of a practical and robust controller for the highly nonlinear and uncertain vehicle transmission system.

1.2. Objectives and Approach

The main objectives of this thesis are to assess and evaluate the current clutch-to-clutch shift algorithms, and to develop an integrated robust control system for vehicle transmissions. Since a 1-2 power-on upshift is the most difficult to do in a clutch-to-clutch shift operation because the gear ratio change is the most significant, we will be focusing on this scenario. The major tasks are identified to be (a) powertrain system modeling, (b) current control law assessment, (c) advanced control law synthesis and analysis, and (d) performance evaluation. The following Chapters 2 through 6 of this thesis will be describing the approach in details.

In Chapter 2, a unique powertrain model for clutch-to-clutch is presented. This model includes the engine, the torque converter, the transmission, the driveline, and the actuators. A checking logic is designed to examine the lock-up conditions of the clutches and different sets of state equations are used for different modes of operation.

In Chapter 3, a Hybrid algorithm consists of a Rule-Based Module and a Sliding Control Module is synthesized. This new approach identifies the fill and torque phases of an upshift scenario through monitoring the transmission output torque signal or transmission output acceleration signal, and uses the Rule-Based Module to control these two phases. The Sliding Control Module is then used to control the speed phase.

In Chapter 4, a Neural Network estimator is developed to identify the transmission input/output torques and the clutch frictional coefficients for the output-torque-based Hybrid algorithm. Computer simulations are performed and limitations for practical application of this recurrent network are identified.

In Chapter 5, two acceleration estimation schemes are developed for the output-acceleration-based algorithm. Both simulation and experimental results are used to examine the estimations and demonstrate their performance.

In Chapter 6, the performance of the Hybrid algorithm is demonstrated and compared with two of the most recently developed transmission clutch-to-clutch control schemes through computer simulations. Finally, conclusions and discussion are included in Chapter 7.

2. POWERTRAIN MODEL

2.1. Overview and Assumptions

Powertrain models with locked-up clutches have been derived by Hrovat and Tobler [1991]. Tugcu et al. [1986] and Cho and Hedrick [1989] have developed powertrain models with slipping clutches. In these previous studies, no scheme was used to identify the locked-up status of the clutch and thus cannot completely represent a true clutch-to-clutch shift situation. In this thesis, a powertrain model with clutch locked-up checking logic for transmission clutch-to-clutch shifts is derived, the following assumptions are made in modeling:

- (a) Torque converter is locked-up during the shift.
- (b) Engine control is not considered.
- (c) A first order transfer function is selected to describe the off-going clutch actuator dynamics. This model is developed based on curve fitting of experimental data obtained in hydraulic actuator tests [Tobler, 1993].
- (d) A second order transfer function is selected to describe the on-coming clutch actuator dynamics. This model is developed based on curve fitting of experimental data obtained in hydraulic actuator tests [Tobler, 1993].
- (e) Only 1-2 upshift is considered.

A schematic of the powertrain model identifying the major components and signals used in this project is shown in Figure 2.1. The variables used in the model are described in the Nomenclature.

The simulation model consists of two control variables: pressure command to the off-going clutch P_{d1} , and the pressure command to the on-coming clutch P_{d2} . The other input is T_e (engine indicated torque). The states are defined to be ω_e (engine angular velocity), ω_1 (transmission upstream angular velocity), ω_2 (transmission downstream angular velocity), ω_{wf} (front wheel angular velocity), ω_{wr} (rear wheel angular velocity), T_i (transmission input shaft torque), T_s (transmission output shaft torque), V (vehicle velocity), P_{c1} (off-going clutch pressure), P_{c2} (on-coming clutch pressure), and \dot{P}_{c2} (rate of on-coming clutch pressure).

There are two major features in this model: (a) it consists of a checking logic to determine the lock-up and slipping conditions of the clutches, and (b) it contains different sets of equations for different phases of the operation. With these characteristics, the model can truly represent a clutch-to-clutch shift scenario. Detailed descriptions of the checking logic and the state equations are presented in the following sections.

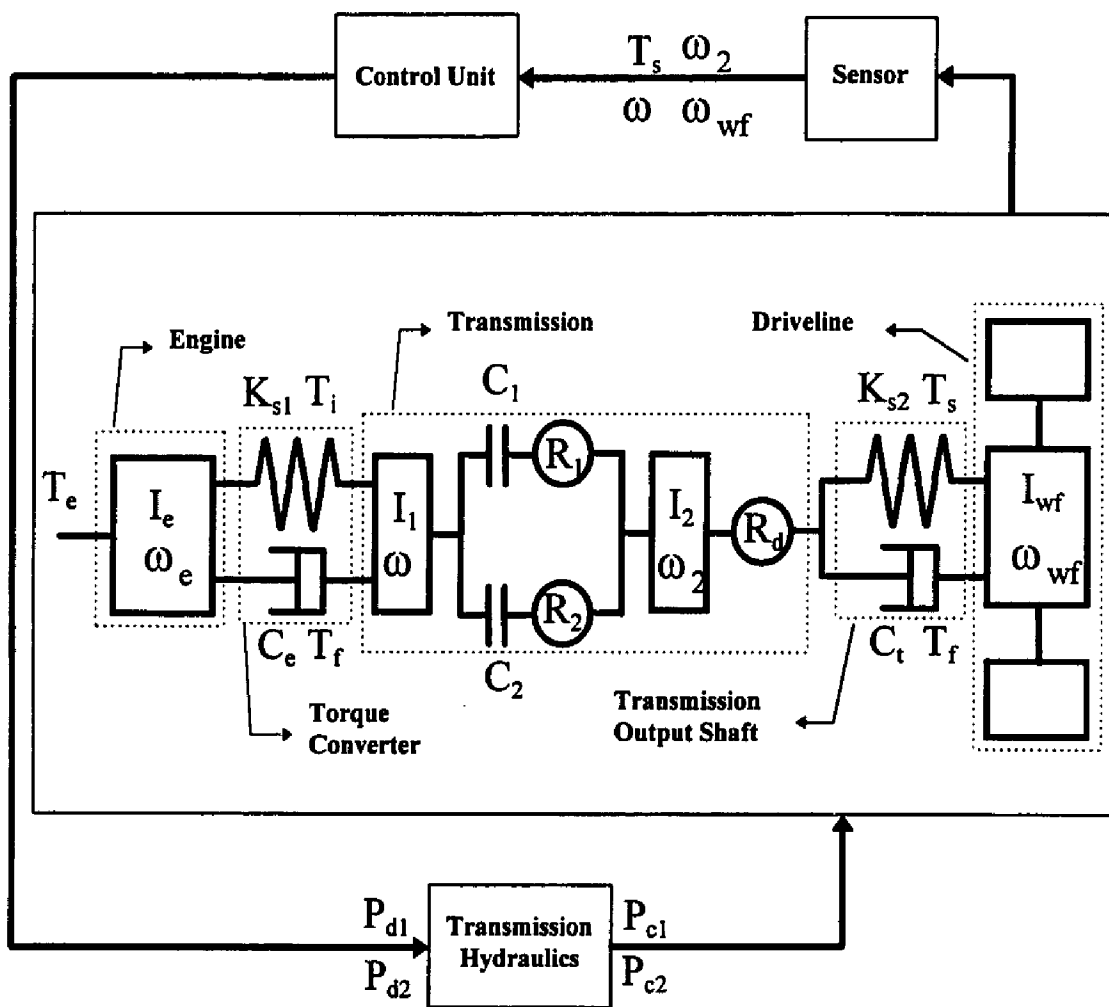


Figure 2.1 Schematic of the powertrain system model

2.2. Clutch Lock-Up Logic

For a given i -th clutch C_i and its corresponding gear ratio R_i ($i=1,2$), the following procedure is used to determining the slipping condition and the torque being transmitted through the clutch.

(a) If $\omega_2 = R_i\omega_1$ and $|T_{ci}| \geq |T_{ci}^0|$, the clutch C_i is locked-up and T_{ci}^0 is being transmitted.

Here, T_{ci}^0 is the torque level across the clutch when it is locked-up (different for different phases of the shift, see section 2.3 for more details), and T_{ci} is the torque created by the applied pressure on a slipping clutch:

$$\begin{aligned} T_{ci} &= P_{ci} A_i \mu_i \operatorname{sgn}(R_i\omega_1 - \omega_2) \\ \operatorname{sgn}(X) &= 1 \quad \text{if } X \geq 0 \\ \operatorname{sgn}(X) &= -1 \quad \text{if } X < 0 \end{aligned} \tag{1}$$

(b) If $\omega_2 = R_i\omega_1$ but $|T_{ci}| < |T_{ci}^0|$, the clutch C_i is not locked-up since the applied pressure is not sufficient to carry the torque transmitted through a locked-up clutch. Here, the torque being transmitted is T_{ci} .

(c) If $\omega_2 \neq R_i\omega_1$, the clutch C_i is slipping and T_{ci} is being transmitted.

2.3. State Equations

The model consists of five major parts: the engine, the torque converter, the transmission, the driveline, and the actuator. The state equations of these individual parts are derived through Newton's Law and are described in the following paragraphs.

2.3.1. Engine / Torque Converter Model

In this thesis, the torque converter is assumed to be locked-up and is modeled as a torsional spring-damper element. The inertia of the torque converter is lumped into the engine inertia I_e and the transmission upstream inertia I_1 .

$$I_e \dot{\omega}_e = T_e - T_i - T_{fd} \quad (2)$$

$$\dot{T}_i = K_{s1}(\omega_e - \omega_1) \quad (3)$$

2.3.2. Transmission Model

The transmission state equations are different at different phases of operation. For a 1-2 upshift, three modules are introduced:

(a) First Gear Operation ($\omega_2 = R_1 \omega_1$, $|T_{c1}| > |T_{c1}^0|$, $T_{c2} = 0$)

$$(I_1 + I_2 R_1^2) \dot{\omega}_1 = T_i - R_1 R_d T_s + T_{fd} - R_1 R_d T_{fd} \quad (4)$$

where,

$$\begin{aligned} T_{c1} &= P_{c1} A_1 \mu_1 \operatorname{sgn}(R_1 \omega_1 - \omega_2) \\ T_{c2} &= P_{c2} A_2 \mu_2 \operatorname{sgn}(R_2 \omega_1 - \omega_2) \\ T_{c1}^0 &= \frac{R_1 R_d T_s I_1 + T_i I_2 R_1^2}{I_2 R_1^2 + I_1} \end{aligned} \quad (5)$$

and

$$\begin{aligned} T_{fd} &= C_e(\omega_e - \omega_1) \\ T_{fd} &= C_f(R_d \omega_2 - \omega_{wf}) \end{aligned} \quad (6)$$

(b) Second Gear Operation ($\omega_2 = R_2 \omega_1$, $|T_{c2}| > |T_{c2}^0|$, $T_{c1} = 0$)

$$(I_1 + I_2 R_2^2) \dot{\omega}_1 = T_i - R_2 R_d T_s + T_{fd} - R_2 R_d T_{fd} \quad (7)$$

where,

$$T_{c2}^0 = \frac{R_2 R_d T_s I_1 + T_i I_2 R_2^2}{I_2 R_2^2 + I_1} \quad (8)$$

(c) 1 - 2 Upshift

In this phase, five possible cases are derived based on the slipping or lock-up condition of the clutches.

Case 1: Off-going clutch locked-up, finite pressure on on-coming clutch

$$(\omega_2 = R_1 \omega_1, |T_{c1}| \geq |T_{c1}^0|, T_{c2} \neq 0).$$

$$(I_1 + I_2 R_1^2) \dot{\omega}_1 = T_i - R_1 R_d T_s - (I_1 - \frac{R_1}{R_2}) T_{c2} + T_{fu} - R_1 R_d T_{fd} \quad (9)$$

Case 2: On-coming clutch locked-up, finite pressure on off-going clutch

$$(\omega_2 = R_2 \omega_1, |T_{c2}| \geq |T_{c2}^0|, T_{c1} \neq 0).$$

$$(I_1 + I_2 R_2^2) \dot{\omega}_1 = T_i - R_2 R_d T_s - (I_1 - \frac{R_2}{R_1}) T_{c1} + T_{fu} - R_2 R_d T_{fd} \quad (10)$$

Case 3: Off-going clutch pressure less than lock-up requirement, finite pressure on

$$\text{on-coming clutch } (\omega_2 = R_1 \omega_1, |T_{c1}| < |T_{c1}^0|, T_{c2} \neq 0).$$

$$\begin{aligned} I_1 \dot{\omega}_1 &= T_i - T_{c1} - T_{c2} + T_{fu} \\ I_2 \dot{\omega}_2 &= \frac{T_{c1}}{R_1} + \frac{T_{c2}}{R_2} - T_s R_d - R_d T_{fd} \end{aligned} \quad (11)$$

Case 4: On-coming clutch pressure less than lock-up requirement, finite pressure on

$$\text{off-going clutch } (\omega_2 = R_2 \omega_1, |T_{c2}| < |T_{c2}^0|, T_{c1} \neq 0).$$

$$\begin{aligned} I_1 \dot{\omega}_1 &= T_i - T_{c1} - T_{c2} + T_{fu} \\ I_2 \dot{\omega}_2 &= \frac{T_{c1}}{R_1} + \frac{T_{c2}}{R_2} - T_s R_d - R_d T_{fd} \end{aligned} \quad (12)$$

Case 5: Both clutches slipping ($\omega_2 \neq R_1 \omega_1$, $\omega_2 \neq R_2 \omega_1$).

$$\begin{aligned} I_1 \dot{\omega}_1 &= T_i - T_{c1} - T_{c2} + T_{fd} \\ I_2 \dot{\omega}_2 &= \frac{T_{c1}}{R_1} + \frac{T_{c2}}{R_2} - T_s R_d - R_d T_{fd} \end{aligned} \quad (13)$$

where,

$$\begin{aligned} T_{c1}^0 &= \frac{(R_1 R_d T_s - \frac{R_1}{R_2} T_{c2}) I_1 + (T_i - T_{c2})(I_2 R_1^2)}{I_2 R_1^2 + I_1} \\ T_{c2}^0 &= \frac{(R_2 R_d T_s - \frac{R_2}{R_1} T_{c1}) I_1 + (T_i - T_{c1})(I_2 R_2^2)}{I_2 R_2^2 + I_1} \end{aligned} \quad (14)$$

2.3.3. Driveline Model

The driveline is modeled as a linear torsional spring-damper element with its inertia lumped into the transmission downstream inertia I_2 and the wheel inertia I_{wf} . Front-wheel drive is assumed.

$$\dot{T}_s = K_{s2}(R_d \omega_2 - \omega_{wf}) \quad (15)$$

$$I_{wf} \dot{\omega}_{wf} = T_s - h_f F_{rf} + T_{fd} \quad (16)$$

$$I_{wr} \dot{\omega}_{wr} = -h_r F_{rr} \quad (17)$$

$$M_h \dot{V} = F_{rf} + F_{rr} - F_a \quad (18)$$

where,

$$\begin{aligned}
F_{ff} &= k_1 \left(1 - \frac{V}{\omega_{wf} h_f} \right) \\
F_{rr} &= k_2 \left(1 - \frac{V}{\omega_{wr} h_r} \right) \\
F_a &= k_3 V^2 + k_4
\end{aligned} \tag{19}$$

2.3.4. Actuator Model

A first order transfer function is selected to describe the off-going clutch actuator dynamics:

$$\tau_{cl} \dot{P}_{cl} + P_{cl} = P_{d1} \tag{20}$$

A second order transfer function is selected to describe the on-coming clutch actuator dynamics:

$$\begin{aligned}
\ddot{P}_{c2} + 2\zeta \omega_n \dot{P}_{c2} + \omega_n^2 P_{c2} &= \omega_n^2 P_{d2}, \text{ if } t \geq \Delta t_{c2} \\
P_{c2} &= 0, \text{ if } t < \Delta t_{c2}
\end{aligned} \tag{21}$$

where Δt_{c2} is the hydraulic fill time.

3. CONTROL LAW DEVELOPMENT

3.1. Issues and Review of Previous Work

The major issues in transmission clutch-to-clutch shift controls are system uncertainties from actuator dynamics, delay and inconsistency (e.g., hydraulic fill time), actuator static modeling errors (e.g., clutch frictional characteristics), plant parameter modeling error, and plant structure variations (e.g., torque phase to speed phase structure change). Recent research work has been focused on developing robust control laws to compensate for these system uncertainties. Therefore, while transmission control in general has been studied by many researchers in the past, we will only be reviewing the most recent advances on robust controls for clutch-to-clutch shifts.

Cho and Hedrick [1989] have developed a Sliding Controller to regulate the transmission output speed through controlling the on-coming clutch pressure in the speed phase. The off-going clutch pressure command is dropped to zero at the beginning of the shift. Based on the Sliding Control Theory, one can design the controller to be robust against system parameter errors, provided that the upper bounds of the errors are known. Glitzenstein and Hedrick [1991] recently proposed an Adaptive Sliding Control algorithm to compensate for the uncertainties in the clutch frictional characteristics (actuator static error), assuming the frictional coefficient is a static parameter. In this approach, they first control the on-coming clutch to maintain zero slip of the off-going clutch until the off-going

clutch pressure is completely released, the Sliding Control is then applied to regulate the transmission output speed during the speed phase.

While these studies have good contributions in illustrating the potential of Sliding Control and Adaptive Control in attacking some of the problems in transmission controls, there are still several critical and practical issues not addressed. Since the fill phase model was not used in the control design, no techniques were developed to identify clutch fill or the fill-to-torque-to-speed phase change. In other words, the fill time uncertainty was not considered in these controller designs, and the on-coming clutch is assumed filled when the control command is applied. Since fill time is a function of many factors (such as temperature, age, hydraulic arrangement, and mechanical design), this assumption is normally not valid. It has been observed in many vehicle road tests that an error in estimating the fill time will seriously degrade the performance of a clutch-to-clutch shift. To consistently maintain good shift quality, a control law that could compensate for the unknown variations in fill time is needed.

Recognizing that the fill time uncertainty being an important problem, Butts, Hebbale, and Wang [1991] proposed a Rule-Based algorithm to identify the fill and torque phases based on the input and output angular acceleration signals of the transmission. While this method is insensitive to the unknown variations in fill time, robustness against plant parameter errors and actuator static modeling errors for the speed phase is not guaranteed. The scheme needs to be modified to ensure robustness throughout the complete shift process.

3.2. Proposed Method

Generally speaking, the transmission output torque and/or acceleration signals are good indicators of shift quality. From reviewing the previous studies in transmission clutch-to-clutch shift controls, it is recognized that a Hybrid Rule-Based Sliding Controller (combining the merits of the Rule-Based approach and that of a robust Sliding Controller) could be effective in compensating the fill time uncertainties, as well as the actuator static modeling errors, plant parameter modeling error, and plant structure variations.

This new algorithm includes two distinct parts, a Ruled-Based Fill/Torque Phase Module, and a Sliding Control Speed Phase Module. The control inputs are P_{d1} , P_{d2} (the on-coming and off-going clutch pressure commands), and the measurement outputs are T_s or A_o (transmission output shaft torque or transmission output acceleration), ω_1 (transmission input angular velocity), ω_2 (transmission output angular velocity), and ω_{wf} (front wheel angular velocity). Depending on the shift quality indicator that we are using, the Sliding Control Speed Phase Module can be either based on output torque (section 3.2.2) or output acceleration (section 3.2.3). The details of the approach are described in the following sections.

3.2.1. Rule-Based Module

Referring to Figure 3.1, transmission output torque or output acceleration will be used as quality indicator, we can outline the rule-based logic for a upshift scenario as follows:

(a) At the beginning of the shift (time t_0 in Figure 3.1), we specify a fill pressure for the on-coming clutch, and start ramping down the off-going clutch pressure.

(b) At the end of the estimated fill time (time t_1), the on-coming clutch pressure command is being ramped up with a given rate. The off-going clutch pressure continues to ramp down with the previously specified rate.

(c) Knowing the quality indicator (output torque or acceleration) level at the beginning of the shift and the gear ratio, a target quality indicator value for the completion of the torque phase can be computed. The initial achievement of the on-coming clutch torque capacity is detected (trigger point #1) when the quality indicator drops by a first specified percentage of the difference between the initial and target values. At such point (time t_2), the reduction of the off-going clutch pressure is intensified, but its slippage is limited to a zero value. The on-coming clutch pressure continues to ramp up with the previously specified rate.

(d) A trigger point #2 is identified when the quality indicator drops by a second specified percentage of the difference between the initial and target quality indicator values. At such point (time t_3), the off-going clutch pressure command is set to zero. The on-coming clutch pressure continues to ramp up with the previously specified rate.

Note that in the above steps (b)-(d), an upper bound of the on-coming clutch pressure command will be pre-assigned. This limit is selected to be the estimated pressure level required to lock up the clutch. Once the pressure command reaches this upper bound, the ramp-up process will stop and the on-coming clutch pressure command will be kept constant.

(e) When slip across the off-going clutch is detected (trigger point #3 at time t_4), the torque phase is considered to be completed, and a Sliding Controller (see next section) is used to regulate the on-coming clutch pressure and control the speed phase.

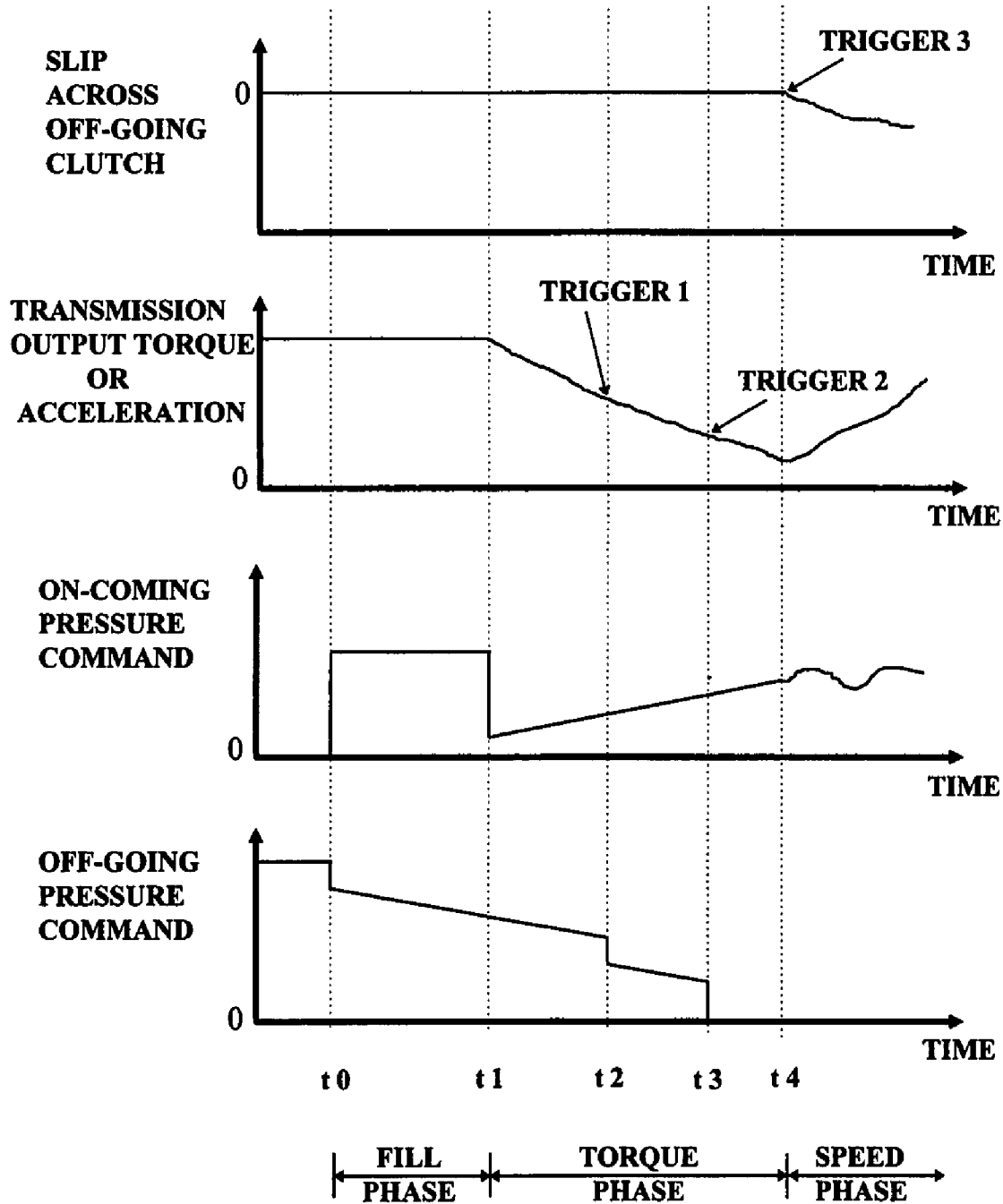


Figure 3.1 Rule-Based control of 1-2 upshift

3.2.2. Sliding Control Module - Transmission Output Torque Based

We will discuss controller design for transmission output torque control in this section. An acceleration-based controller will be discussed in section 3.2.3.

A Sliding Controller is developed for controlling the speed phase of the shift. Given the gear ratio and the transmission output torque at the beginning of the shift, we can estimate the output torque at the end of the shift. With this information and selecting a desired shift time, we can define a desired output torque trajectory T_{sd} (Figure 3.2).

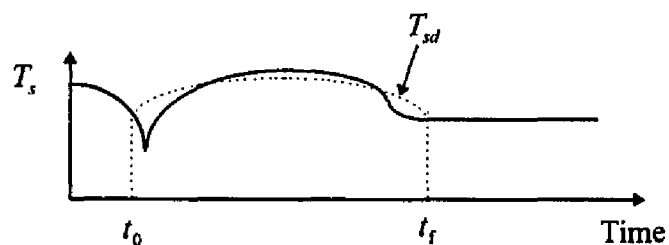


Figure 3.2 Desired output torque trajectory

The principle here is to vary the on-coming clutch pressure and regulate the output torque to follow the desired trajectory. With the state equations shown in Chapter 2, we synthesized the control law to be a two-stage effort with two sliding surfaces because the control objective is not explicitly related to the control [Alleyne, 1994].

We define the first sliding surface to be $S_1 = T_s - T_{sd}$. To satisfy the sliding condition [Slotine and Li, 1991, and Alleyne, 1994],

$$S_1 \dot{S}_1 \leq -\alpha_1 |S_1| \quad (22)$$

We can derive

$$\omega_{2d} = \frac{\dot{T}_{sd} - \alpha_1 \text{sgn}(S_1) + K_{s2} \omega_{wf}}{K_{s2} R_d} \quad (23)$$

That is, a desired transmission output speed trajectory is defined. In order to reduce high frequency chatter, we replace the sign (sgn) function with a saturation function as presented by Slotine and Li [1991].

We then define the second sliding surface to be $S_2 = \omega_2 - \omega_{2d}$. To satisfy the sliding condition:

$$S_2 \dot{S}_2 \leq -\alpha_2 |S_2| \quad (24)$$

We can thus solve for control $T_{c2}(P_{c2})$,

$$T_{c2} = R_2 [R_d T_s + R_d T_{fd} + I_2 \dot{\omega}_{2d} - I_2 \alpha_2 \text{sgn}(S_2) - \frac{T_{c1}}{R_l}] \quad (25)$$

where, α_2 is the estimated upperbound for uncertainties in the system parameters and unknown disturbances. Again, to reduce high frequency chatter, we replace the sign function with a saturation function as presented by Slotine and Li [1991].

Although Multiple Surface Sliding Control has been proposed in [Alleyne, 1994], the controller performance will be degraded and the system can even become unstable when discrete-time control is implemented. A digital Multiple Surface Sliding Control design method and sufficient conditions for the performance of convergence are developed and presented in Appendix B. In this thesis, continuous Multiple Surface Sliding Control law is used. Yet, we have to be aware of the control loop time effect and adopt the digital Multiple Surface Sliding Control law when the loop time is sufficiently large.

3.2.3. Sliding Control Module - Transmission Output Acceleration Based

Given the gear ratio and the transmission output acceleration at the beginning of the shift, we can estimate the transmission output acceleration at the end of the shift. With this information and selecting a desired shift time, we can define a desired acceleration trajectory A_{od} (Figure 3.3).

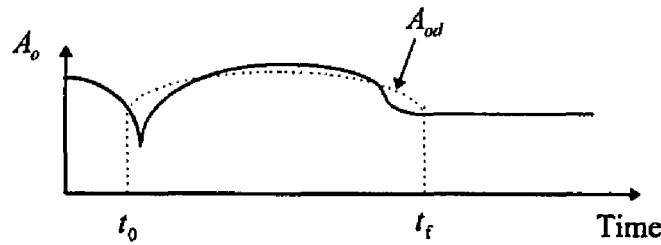


Figure 3.3 Desired output acceleration trajectory

The principle here is to vary the on-coming clutch pressure and regulate the output acceleration to follow the desired trajectory. With the state equations shown in Chapter 2, we define the sliding surface to be $S = A_o - A_{od}$. To satisfy the sliding condition [Slotine and Li, 1991],

$$S \dot{S} \leq -\alpha_3 |S| \quad (26)$$

We can thus solve for control $T_{c2}(P_{c2})$,

$$\dot{T}_{c2} = R_2 [I_2 \ddot{\omega}_{2d} + R_d (A_o - A_{od}) + R_d \dot{T}_{fd} - I_2 \alpha_3 \text{sgn}(S) - \frac{\dot{T}_{c1}}{R_1}] \quad (27)$$

where, α_3 is the estimated upperbound for uncertainties in the system parameters and unknown disturbances. In order to reduce high frequency chatter, we replace the sign (sgn) function with a saturation function as presented by Slotine and Li [1991].

4. TORQUE ESTIMATOR DEVELOPMENT

4.1. Issues and Problem Statement

To implement the output-torque-based controller, it is clear that transmission output torque signals are required. Since direct measurements of torque are expensive, estimation schemes are needed to ensure success in implementing the control law.

While many studies have been done in developing estimation schemes [Misawa and Hedrick, 1989; Luders and Narendra, 1973; Walcott and Zak, 1987] for states and parameters of dynamic systems, most of them require the system model and uncertainties to be completely structured. Some of these methods are also computational intensive. Since the transmission output torque model structure could be quite uncertain and the clutch frictional coefficient could be state-dependent (instead of a slow-varying static parameter), an estimator that requires minimum model information will be more desirable for this specific class of systems that we are interested in.

4.2. Proposed Method

To address the issues mentioned above, an Artificial Neural Network estimator based on partially known models is developed. The method is described in the following sections.

4.2.1. Neural Networks Overview

Neural Networks compose of layers of basic processing elements, the so-called neurons. A schematic of a neuron with a commonly used activation function is illustrated in Fig. 4.1. The output of each neuron is a function of the inputs and bias with adjustable weights W_j . Leshno et al. [1993] have shown that any continuous function defined on a compact set can be approximated to any accuracy by a two layer perceptron (Figure 4.2) with non-polynomial activation functions (such as the one illustrated in Fig. 4.1) and proper weightings W_j and V_{ij} .

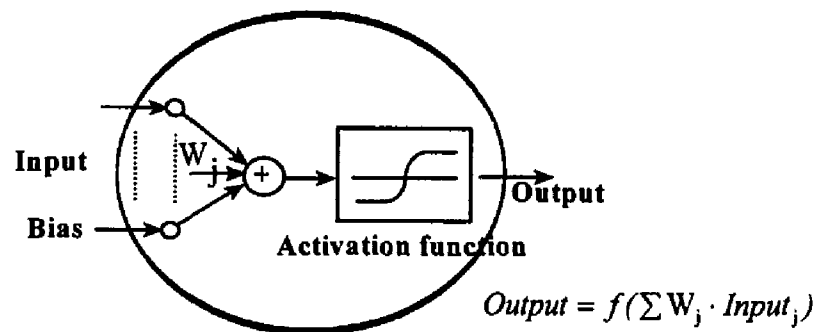


Figure 4.1 Neuron

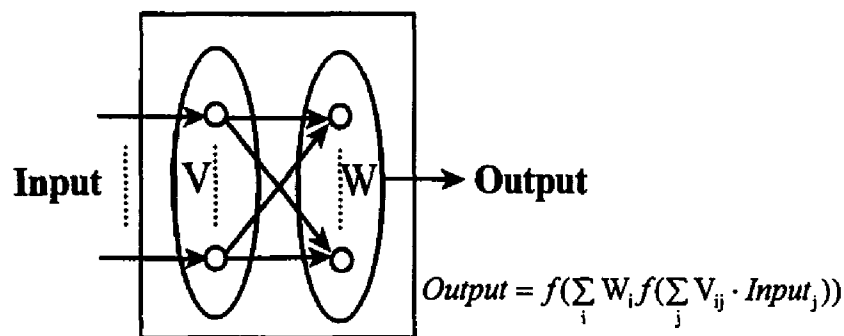


Figure 4.2 Two layer feedforward perceptron

4.2.2. Estimator Network Configuration

The Neural Network structure developed consists of six sub-networks and three modules, representing three different training stages: the first gear stage, the torque phase stage, and the speed phase stage (Fig. 4.3). The networks will be trained to determine the optimal weightings and models. The training procedure is discussed in the next section (section 4.2.3).

During operation, the speed measurements will serve as inputs to the networks.

The functions of these networks are described as follows:

- NN1: Transmission input shaft stiffness estimator
- NN2: Transmission output shaft stiffness estimator
- NN3: Transmission input shaft damping estimator
- NN4: Transmission output shaft damping estimator
- NN5: On-coming clutch frictional coefficient estimator
- NN6: Off-going clutch frictional coefficient estimator

The networks are formulated using the two layer feedforward perceptron structure shown in Fig. 4.2 with weightings W_i and V_{ij} . The activation function shown in Fig. 4.1 is used, which is described mathematically as

$$f(x) = \frac{1}{1 + \exp(-x)} \quad (28)$$

These network outputs (shaft stiffness, damping, and frictional coefficients) will be used to estimate the torque signals through the following equations:

$$\hat{T}_i(k+1) = \hat{T}_i(k) + f_{n1}(\omega_e(k) - \omega_1(k), \omega_e(k)) \cdot \Delta T \cdot (\omega_e(k) - \omega_1(k)) \quad (29)$$

$$\hat{T}_s(k+1) = \hat{T}_s(k) + f_{n2}(R_d\omega_2(k) - \omega_{wf}(k), \omega_{wf}(k)) \cdot \Delta T \cdot (R_d\omega_2(k) - \omega_{wf}(k)) \quad (30)$$

$$\hat{T}_{fu}(k) = f_{n3}(\omega_e(k) - \omega_1(k), \omega_e(k)) \cdot (\omega_e(k) - \omega_1(k)) \quad (31)$$

$$\hat{T}_{fd}(k) = f_{n4}(R_d\omega_2(k) - \omega_{wf}(k), \omega_{wf}(k)) \cdot (R_d\omega_2(k) - \omega_{wf}(k)) \quad (32)$$

$$\hat{T}_{c1}(k) = f_{n6}(\omega_1(k), \omega_2(k), P_{c1}(k)) \cdot P_{c1}(k) \quad (33)$$

$$\hat{T}_{c2}(k) = f_{n5}(\omega_1(k), \omega_2(k), P_{c2}(k)) \cdot P_{c2}(k) \quad (34)$$

Here $f_{ni}(\cdot)$ is the output of the i -th network and ΔT is the computer loop interval. The ^ symbols indicate that the torque signals are *estimated*.

4.2.3. Estimator Training Procedure

To train the estimator initially, test shifts are conducted and the measured speed signals are used as training signals. The network will be retrained after each regular shift while always keeping the optimal set of weightings. The procedure is outlined in the following paragraphs.

There is a total of three training stages. The speed-torque relationships in each of these stages are represented by the following equations:

(a) First Gear Stage (off-going clutch locked-up and on-coming clutch not filled)

$$\hat{\omega}_1(k+1) = \omega_1(k) + (\hat{T}_i(k) - R_1 R_d \hat{T}_s(k) + \hat{T}_{fu}(k) - R_1 R_d \hat{T}_{fd}(k)) \cdot \Delta T / (I_1 + I_2 R_1^2) \quad (35)$$

(b) Torque Phase Stage (off-going clutch locked-up and on-coming clutch filled)

$$\hat{\omega}_1(k+1) = \omega_1(k) + (\hat{T}_i(k) - R_1 R_d (\hat{T}_s(k) + \hat{T}_{fd}(k)) + \hat{T}_{fu}(k) - (1 - \frac{R_1}{R_2}) \hat{T}_{c2}(k)) \cdot \frac{\Delta T}{(I_1 + I_2 R_1^2)} \quad (36)$$

(c) Speed Phase Stage (both clutches slipping)

$$\hat{\omega}_1(k+1) = \omega_1(k) + (\hat{T}_i(k) + \hat{T}_{fu}(k) - \hat{T}_{c1}(k) - \hat{T}_{c2}(k)) \cdot \Delta T / I_1 \quad (37)$$

$$\hat{\omega}_2(k+1) = \omega_2(k) + (\frac{1}{R_1} \hat{T}_{c1}(k) + \frac{1}{R_2} \hat{T}_{c2}(k) - R_d \hat{T}_s(k) - R_d \hat{T}_{fd}(k)) \cdot \Delta T / I_2 \quad (38)$$

The relationships of these stage equations and the six networks are illustrated in Figure 4.3. Figure 4.4 presents the overall flowchart of the training process.

During the first stage training process, the vehicle is in first gear. The angular velocity training signals are input into NN1 through NN4 to estimate shaft stiffness and damping functions. The torque signals are then estimated using equations (29)-(34). Through the first stage equation (35), the transmission input velocity $\hat{\omega}_1$ is estimated. A training method based on Delta learning rule [Zurada, 1992] is then employed to tune the weightings in the networks NN1 through NN4 to minimize the differences between ω_1 and $\hat{\omega}_1$. A summary of how the Delta rule is used is illustrated in the Appendix A.

After NN1 through NN4 are trained, we will continue to use the first gear model equation (35) to estimate the transmission upstream angular velocity until we see the difference between the estimated and measured velocity starts to increase and exceeds a preset value (Check 1 in Fig. 4.4 and Fig. 4.5). This indicates a significant change of the model has occurred. In other words, the torque phase model equation (36) should be used,

and the second training stage begins. A similar process with the Delta learning rule is carried out to tune the weightings and train NN5.

The last stage is triggered when the off-going clutch starts to slip (Check 2 in Fig.4.4 and Fig. 4.5). In this stage, the speed phase equations (37)-(38) will be used to derive the estimated velocities from the estimated torque. Again, a similar process with the Delta learning rule is used to tune the weightings and train NN6.

4.3. Simulation Results

To examine the performance of the estimator, computer simulations are carried out on the model described in Chapter 2. The parameters used in the analysis are shown in Table 4.1.

The training error E , transmission output torque T_s , estimation error, and transmission input torque T_i , estimation error for the stage 1 training are illustrated in Figure 4.6. The training error E , and on-coming clutch torque T_{c2} estimation error for the stage 2 training are illustrated in Figure 4.7. The training error E , and off-going clutch torque T_{c1} estimation error for the stage 3 training are illustrated in Figure 4.8. It is shown in these figures that the training error decreases as training cycles increase at the beginning and reaches a minimal point.

A shift conducted by the Hybrid approach controller combined with the Artificial Neural Network estimator after training is simulated. The transmission output torque for the ideal case (know torque signals exactly) and the shift conducted by the Hybrid approach controller combined with Artificial Neural Network estimator are illustrated in

Figure 4.9. It is shown that the performance is close to the ideal case with perfect knowledge of the torque signals.

Table 4.1 Variables Used in Simulation

A_1	6.045 m^3	K_{s1}	1399 Nm/rad
A_2	6.045 m^3	K_{s2}	6221 Nm/rad
C_e	$41.97 \text{ Nm/(rad/sec)}$	M_h	1644 Kg
C_t	$186.63 \text{ Nm/(rad/sec)}$	R_1	0.3609
h_f	0.31 m	R_2	0.6481
h_r	0.315 m	R_d	0.288
I_1	0.05623 Kg m^2	T_e	102.721 Nm
I_2	0.03668 Kg m^2	μ_1	$0.17 + 0.00001(w_1 - w_2/R_1)$
I_e	0.1995 Kg m^2	μ_2	$0.17 + 0.00001(w_1 - w_2/R_2)$
I_{wf}	0.8822 Kg m^2	τ_{c1}	0.025 sec
I_{wr}	0.8822 Kg m^2	w_n	8 Hz
k_1	178000 N	ζ	0.7
k_2	178000 N	Δt_{c2}	0.3 sec
k_3	$0.38079 \text{ N/(m/sec)}^2$	ΔT	0.016 sec
k_4	110.5825 N		

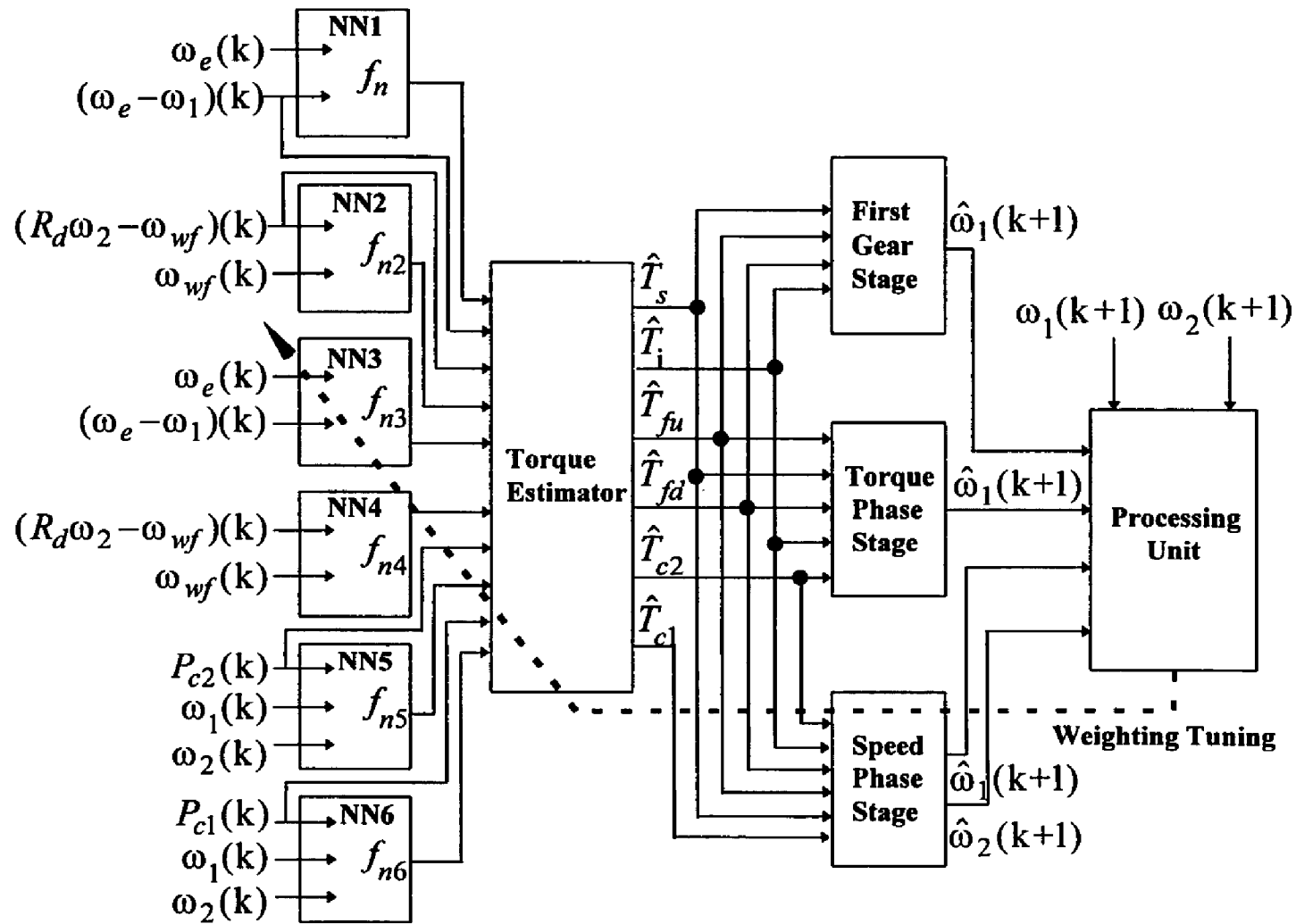


Figure 4.3 Schematic of Neural Network

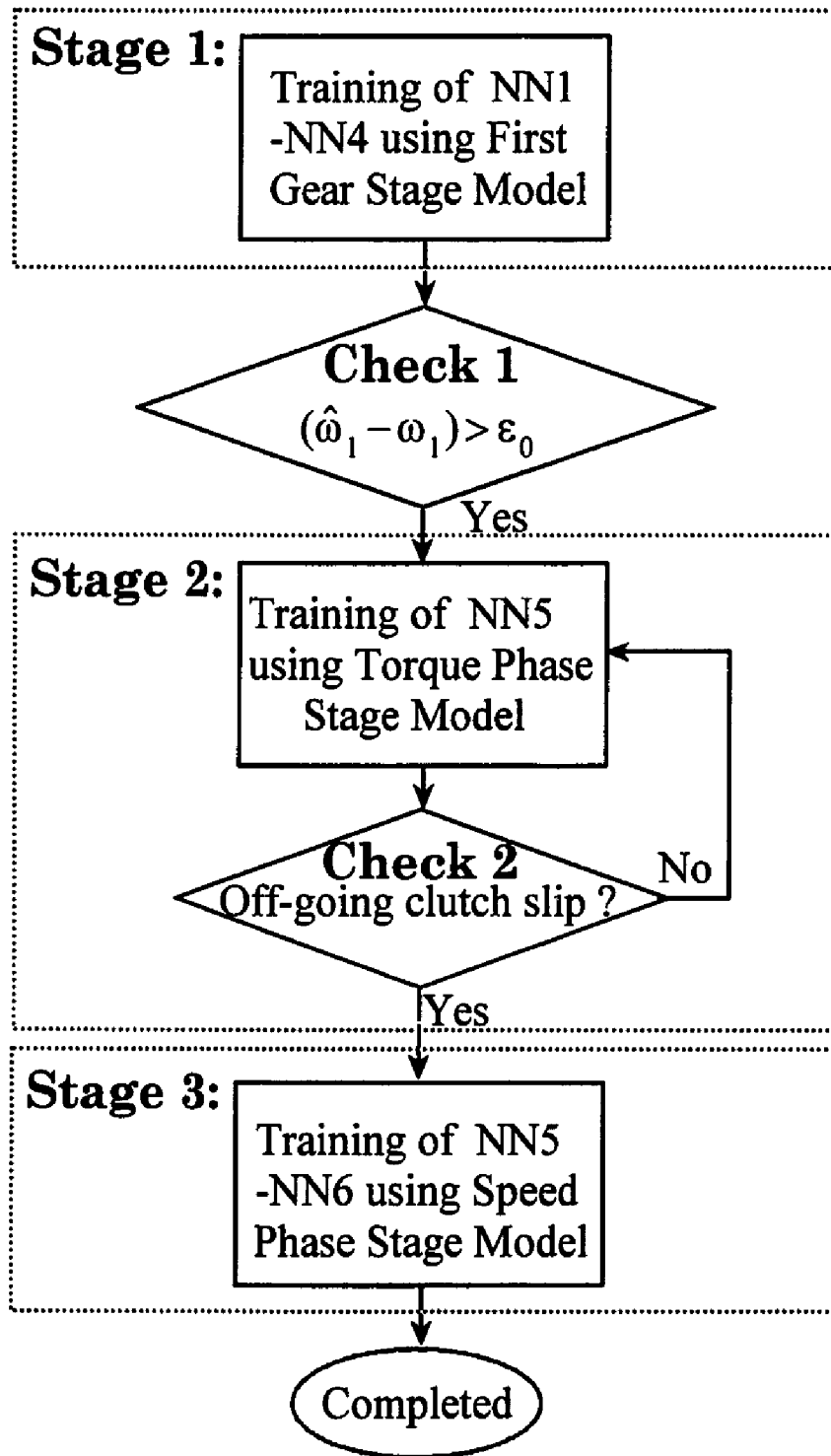


Figure 4.4 Neural Network training flowchart

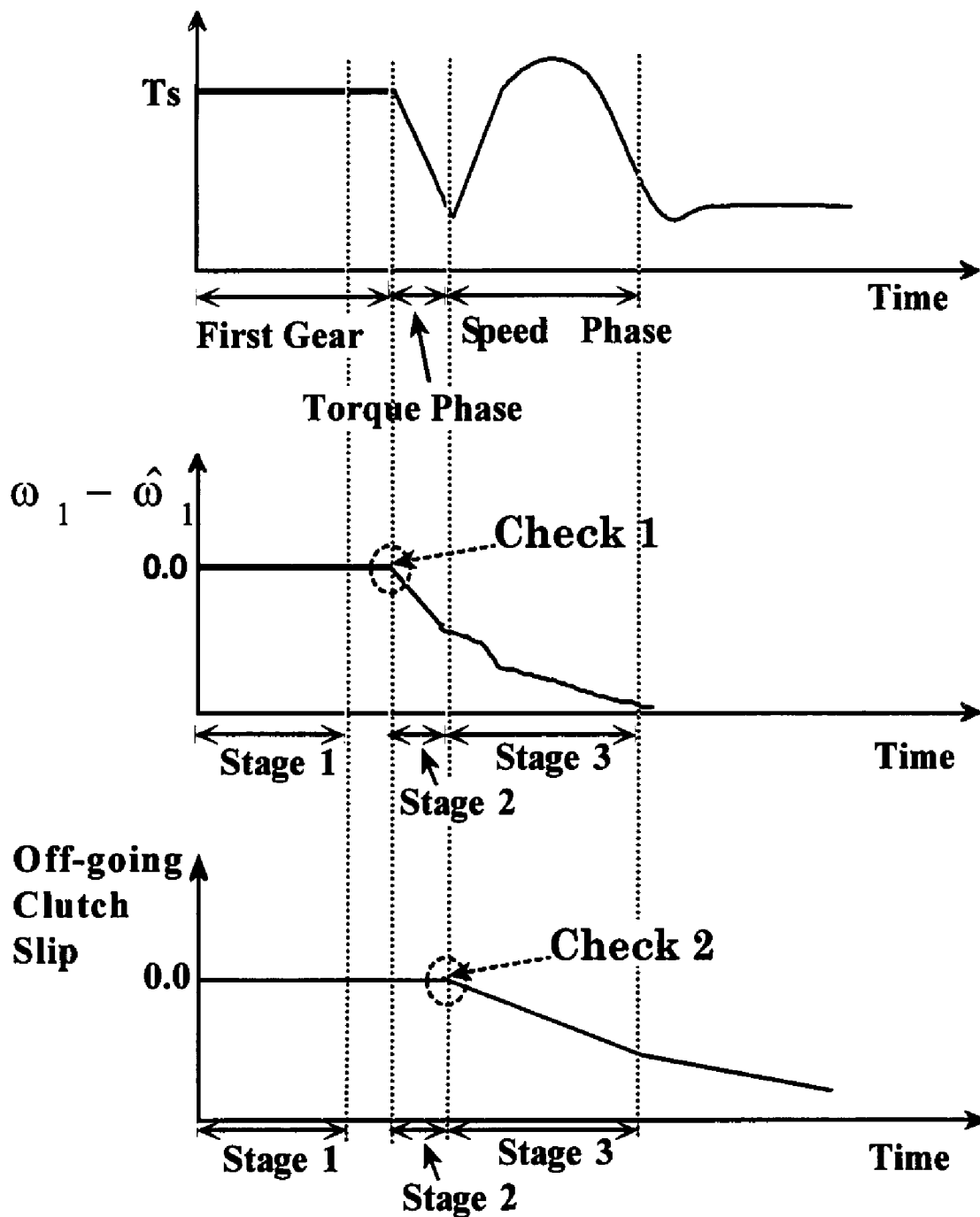


Figure 4.5 Check 1 and Check 2

Stage 1 Training

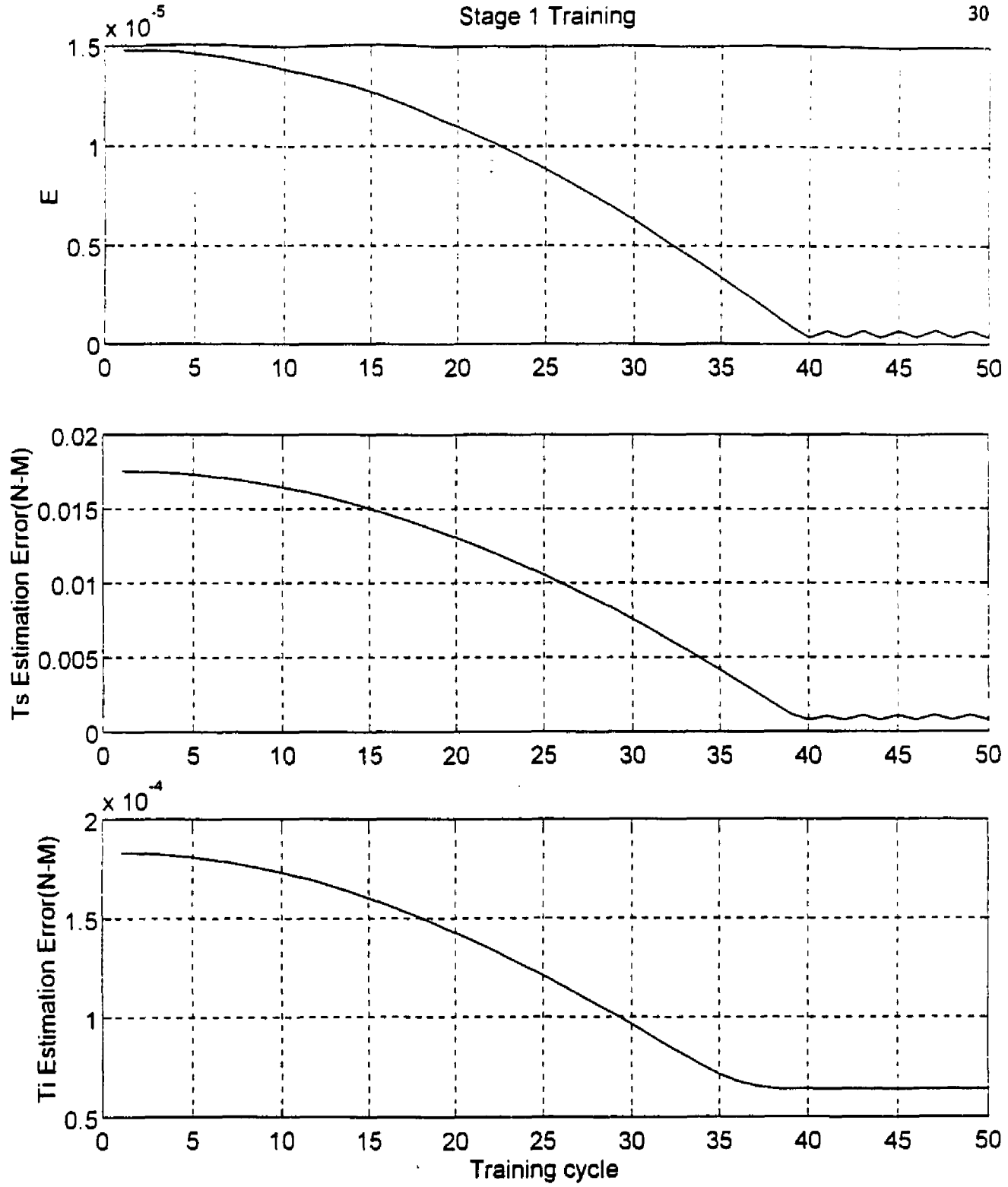


Figure 4.6 Stage 1 Training Error E, T_s Estimation Error, and T_i Estimation Error

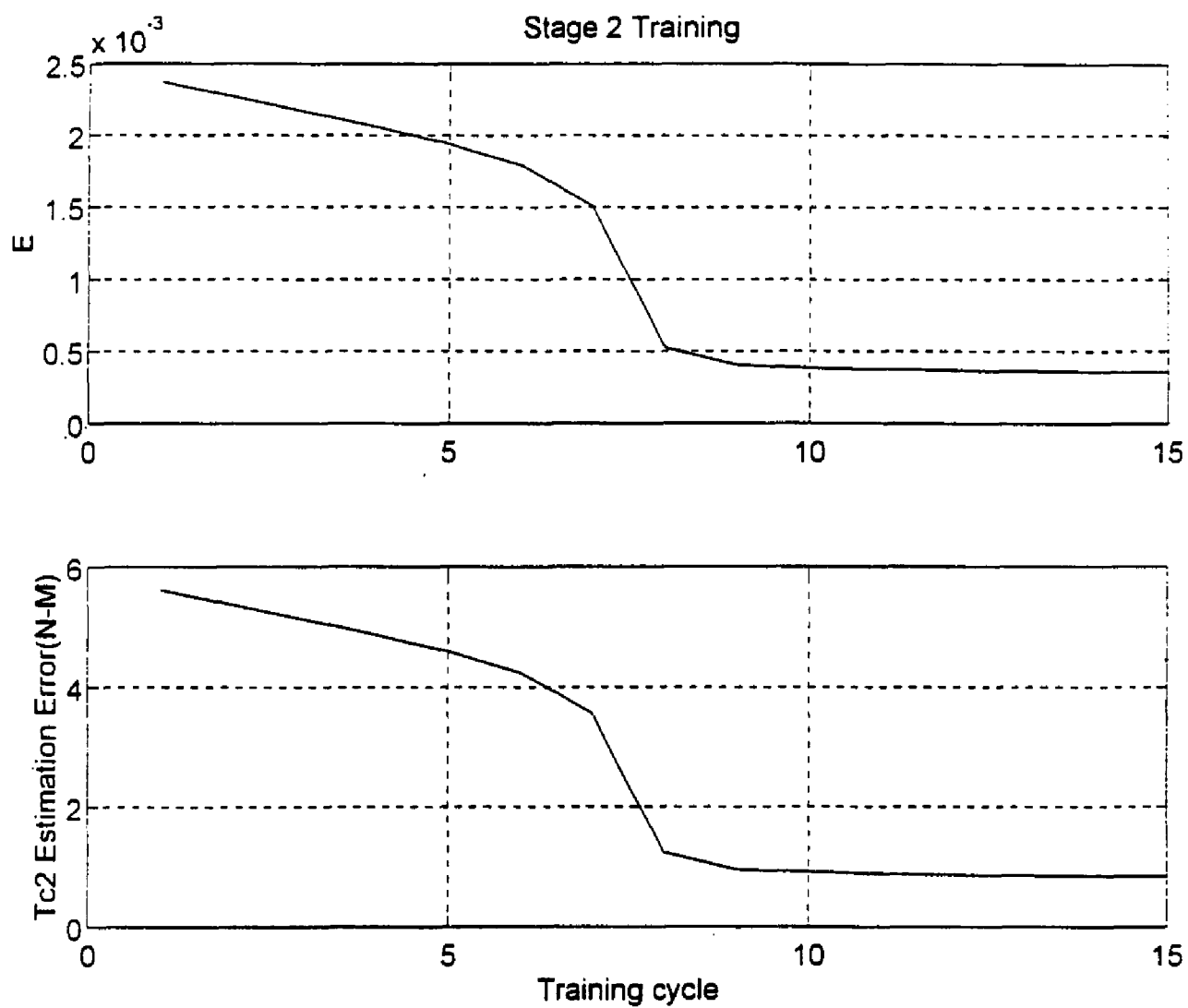


Figure 4.7 Stage 2 Training Error E and Tc2 Estimation Error

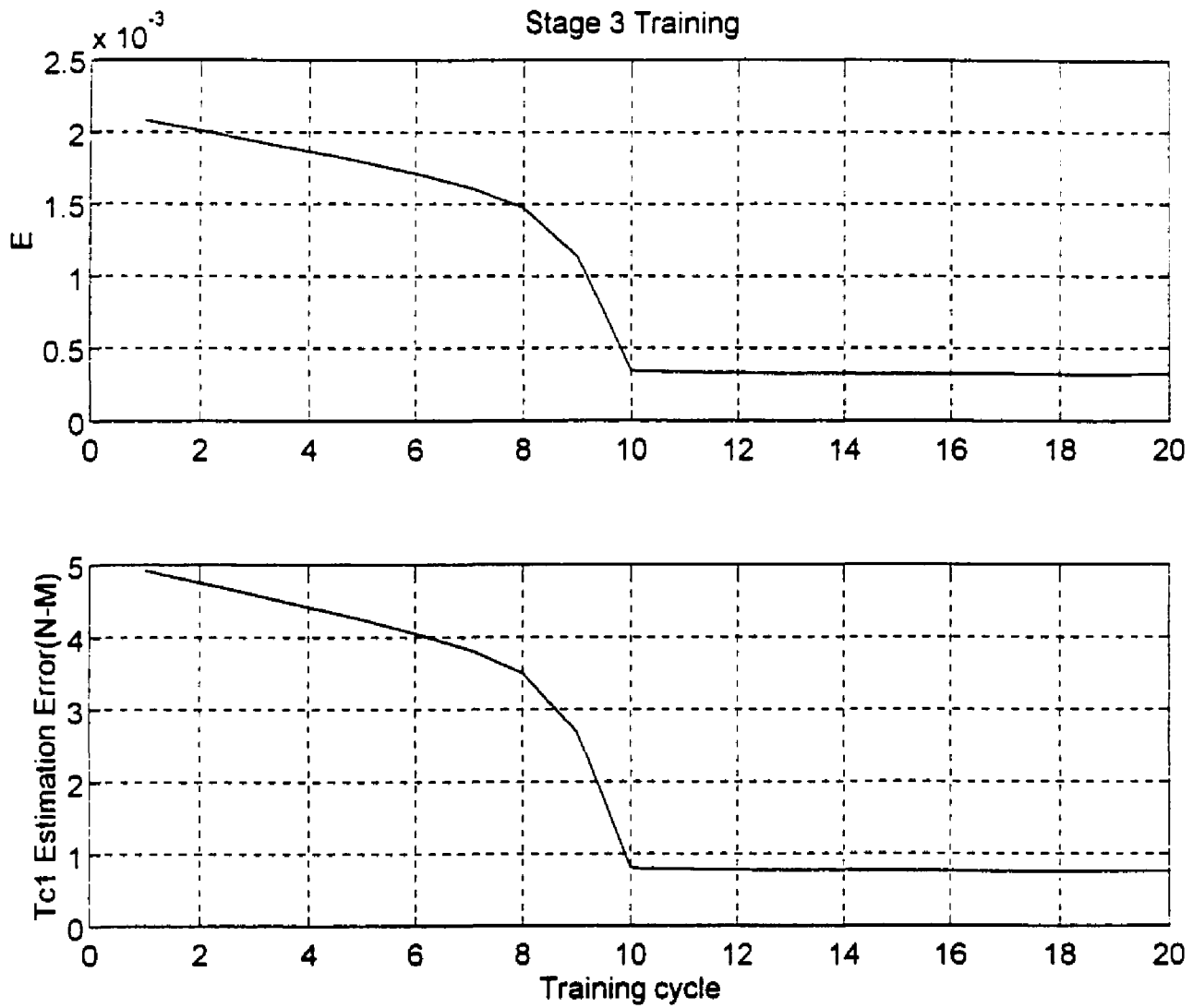


Figure 4.8 Stage 3 Training Error E and Tc1 Estimation Error

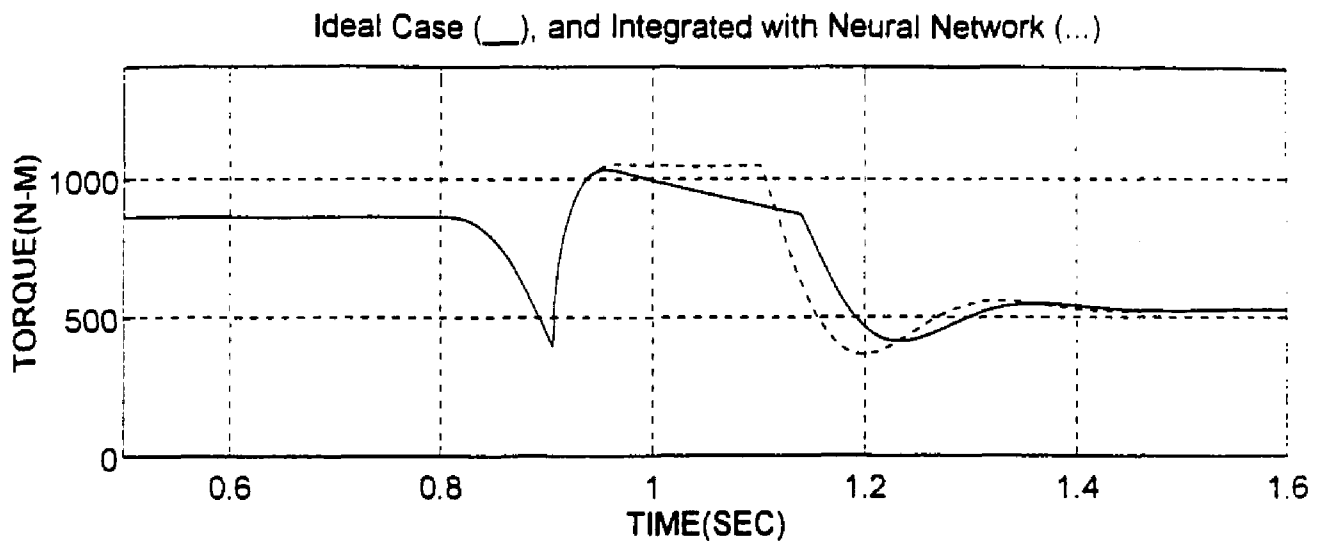


Figure 4.9 Transmission Output Torque for Ideal Case and the Hybrid Approach Combined with Artificial Neural Network Estimator

4.4. Discussion

With the simulation result shown in Figure 4.9, Neural Network appears to be a promising approach for transmission clutch-to-clutch shift control. However, practical applications of the Artificial Neural Network estimator are limited by the following issues:

- (a) Partial system dynamics must be known for the training. Since the estimator incorporates with partial system dynamics (see section 4.2.2), the performance will be degraded if the partial system dynamics incorporated are not correct.
- (b) Three stage training degrades the performance. The estimator must be trained through three different stages to model the transmission dynamics during the 1-2 shift. This will degrade the performance since the modeling error will propagate through the training stages.
- (c) High sampling rate of signal is required to use discrete-time Neural Network to model continuous system. The transmission system is modeled as a discrete system using zero order hold. If the sampling rate of the data is not high enough, the identified discrete-time model based on the minimization of the training error will be quite different from the real system [Sinha and Rao, 1991].
- (d) High precision speed sensors are needed. The sensitivity of the sensors will affect the performance of Check 1 and Check 2 (see section 4.2.3), which are used to identify the structure changes (first gear stage and torque phase, torque phase and speed phase). Fault detections of the phases will result in mistakes in the training process.

(e) High computation power is needed for the training of recurrent network [Bengio, Simard, and Frasconi, 1994]. Since the Artificial Neural Network estimator is a nonlinear system, the tuning of the weightings may be trapped in local minima, especially for a multi-input-multi-output system. Random optimization technique is needed to train the network and this requires a great deal of computation power.

From the above discussions, we recognize that applying Artificial Neural Network in an automotive transmission system environment is not practical due to its limitations. Therefore, another approach using transmission output acceleration as the quality indicator is investigated and presented in Chapter 5 and Chapter 6.

5. ACCELERATION ESTIMATION SCHEME DEVELOPMENT

5.1. Issues and Review of Previous Work

To implement the acceleration-based controller, the transmission output angular acceleration signals are required. Since direct measurement of such signals is not feasible and measurements of the vehicle longitudinal acceleration are usually severely contaminated by noise, schemes are needed to estimate the acceleration with measurable angular velocity signals. In other words, we want to estimate the derivatives of a measured signal.

Previous research on this subject can be summarized into four major areas: curve fitting method, frequency domain approach, adaptive tuning approach, and Kalman filter approach.

In the curve fitting approach, a cost based on assumed functions of the measured signal (such as velocity) is defined and minimized, then the derivative (such as acceleration) is calculated analytically from the assumed functions. Orthogonal Chebyshev polynomial was studied by Zernicke et al. [1976] and Pezzack et al. [1977]. Cubic spline has been used by Zernicke et al. [1976], Hutchinson and Hoog [1985], Soudan and Dierckx [1979]. Quintic spline has been used by Wood and Jennings [1979]. There is a trade-off between the infidelity to the data and the roughness of the estimated solution for this approach. It has been reported by Lanhammar [1982a, b], Graven and

Wahba [1979], Golub et al. [1979], Wahba [1985], Ansley and Kohn [1987], and Kohn and Ansley [1987] that the choice of the functions can be very critical.

In the frequency domain approach, measured data is first filtered and finite difference method is then used to estimate the derivative. Low pass IIR filter has been studied by Pezzack et al. [1977], low pass FIR filter has been used by Lesh et al. [1979], and central finite difference method was adopted by Harrison and McMahon [1993]. The main drawback of this approach is that it is impossible to reduce noise without distorting the signal.

In the adaptive tuning approach, adaptive filter is used to cancel the noise or to restore the signal. Adaptive restoring method has been used by Zeidler et al. [1978], Bershada and Feintuch [1980], Widrow and Stearns [1985], Friedlander [1982], and Heinonen et al. [1984], where only signals from AR, IIR, or FIR filters can be used. Adaptive noise cancellation has been studied by Abutaleb [1988], and Widrow and Stearns [1985]. A reference signal which is uncorrelated with the signal but is correlated with the noise is needed for adaptive noise cancellation. For real-time clutch-to-clutch shift control, it is not possible to generate such a reference signal.

Kalman filter designed based on augmented state equations has been presented by Ramachandra [1987], Belanger [1992], Speyer and Crues [1987], Fioretti and Jetto [1989], Fioretti and Jetto [1986], Jetto [1985], Jetto [1987], Palival and Basn [1987], Gibson et al. [1988], Gibson et al. [1991], Tugnait [1985], and Hebbale and Ghoneim [1991]. An off-line fixed-lag Kalman smoother was studied by Fioretti and Jetto [1994].

High order dynamics of the system are neglected, and treated as white noise uncertainties.

Therefore, the optimality of the estimation cannot be rigorously guaranteed.

Form the above review, it is recognized that all the current schemes are either not applicable to real-time transmission control systems or the estimator performance cannot be guaranteed. Since consistent good acceleration signals are critical to the success of clutch-to-clutch shift controls, more studies and better methods are needed. The major content of this Chapter is to present two new schemes that do not have the shortcomings of the previous methods, can guarantee performance, and can be easily implemented for transmission controls. The proposed methods can also be used as schemes to improve upon results from any existing estimation algorithm (such as the filtered finite difference approach or the Kalman filter estimator).

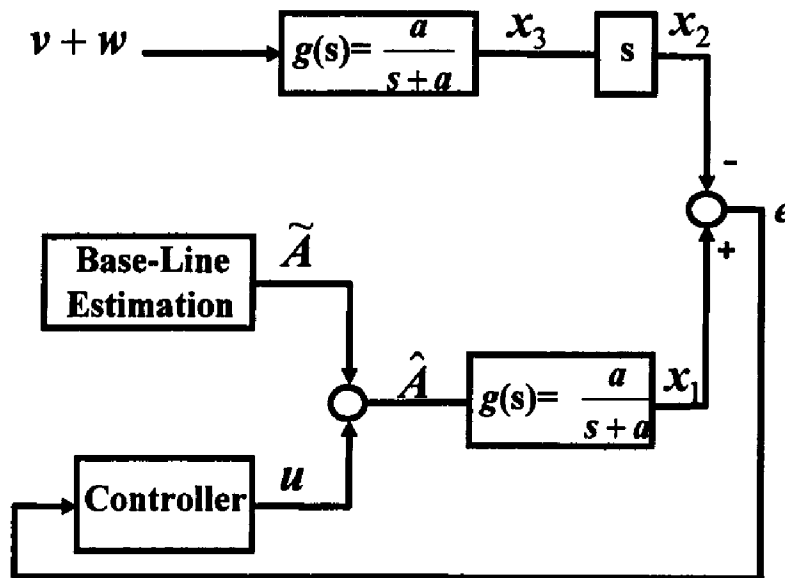


Figure 5.1. Schematic of acceleration estimation with feedback controller

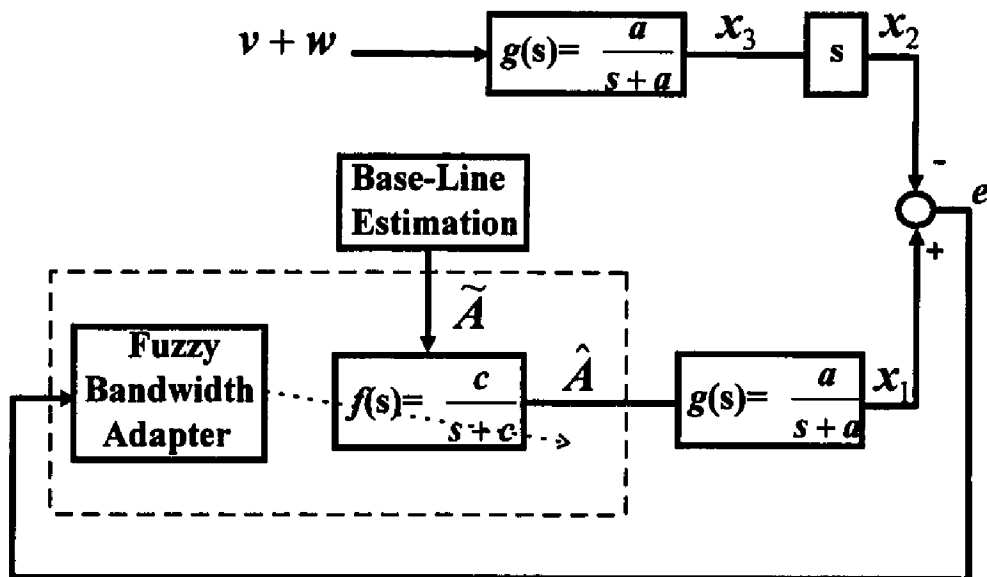


Figure 5.2. Schematic of acceleration estimation with feedback adaptive filter

5.2. Proposed Methods

Two acceleration estimation schemes with feedback action are developed. As shown in Figure 5.1 and Figure 5.2, $v+w$ is the measured angular velocity signal (v is the true velocity, w is noise). $\tilde{A}(t)$ is a base-line acceleration estimation using any available estimation schemes (or simply just use x_2), g is an augmented first order low pass filter. $\hat{A}(t)$ is the estimated acceleration, and $e(t)$ is the augmented error. For Estimation Scheme A (refer to Figure 5.1), the controller is used to design control signal u to compensate for the distortion of the base-line estimation. For Estimation Scheme B (refer to Figure 5.2), $f(c)$ is a low pass filter with bandwidth c . The fuzzy bandwidth adapter is used to tune the bandwidth c of the filter f based on feedback.

Since the first scheme is to compensate for signal distortion and recover the signal, it is usually adopted when the base-line signal noise level is acceptable but the distortion is significant. On the other hand, the second scheme is to adapt the filter bandwidth such that the noise of the estimated signal is reduced and the distortion is acceptable. Scheme B is thus adopted when the base-line signal distortion is acceptable but the noise level is significant. The true acceleration signal, the noise, the base-line estimation signal, and the control signal are assumed to be band-limited and bounded. The design procedures will be described in section 5.2.1 for Estimation Scheme A and in section 5.2.2 for Estimation Scheme B.

5.2.1. Estimation Scheme A

The general idea of this scheme (see Figure 5.1) is to improve upon the base-line estimation through feedback control action. In this thesis, the controller is designed to be a fuzzy controller with constant proportional gain. The fuzzy logic is used to create a feedback signal $fuzzy(e)$ such that the control signal is *smooth* (see Theorem C.2 in Appendix C). The proportional controller is designed to drive $fuzzy(e)$ to zero by satisfying some design criterion (see Theorem C.3 in Appendix C). When $fuzzy(e)$ approaches zero, $e(t)$ will be bounded by some upper bound and the acceleration estimation error will be bounded. The design procedure is outlined as follows:

- (a) Given the measurement of true angular velocity v with high frequency noise w , signal x_2 is created through the standard filtered finite difference method with a low pass filter g . The bandwidth of the filter should be designed such that x_2 is sufficiently smooth.
- (b) With base-line acceleration estimation $\tilde{A}(t)$ and control u , \hat{A} and x_1 are derived. Since the controller is not designed to cancel the signal noise, the noise level of the base-line estimation should be acceptable.
- (c) With $e = x_1 - x_2$, set up $fuzzy(e)$ to be the feedback signal and control objective. The $fuzzy(e)$ is defined using fuzzy logic by considering the level of the filtered high frequency noise such that u is smooth.
- (d) With the smooth but distorted base-line estimation, use $fuzzy(e)$ as feedback signal to calculate the control signal u . Use the control signal to compensate for the distortion

and recover the signal \dot{v} . It can be shown that $\hat{A} \rightarrow \dot{v}$ when $fuzzy(e)$ approaches zero (see Theorem C.3 in Appendix C).

Before we discuss the controller design in detail, we will describe the logic behind this scheme. Some properties of low pass filters are introduced first.

Remark 5.1. From Lemma C.4 (see Appendix C), we can see that (1) For wide bandwidth (filter bandwidth vs. input signal frequency band) first order low pass filters, large output implies that input signal is large, and (2) For narrow bandwidth first order low filters, output will be small even when the input signal is large.

It is well known that feedback control is a widely used technique for robustness and performance improvement [Horowitz, 1963 and Cruz, 1972]. However, a measurable feedback signal is required and it must be related to the control objective such that the control action can be determined from it. In order to apply feedback control to estimate acceleration, we need to define a control objective and measurable feedback signal. From Remark 5.1, we developed a feedback signal $e(t)$ via the two augmented low pass filters g . The augmented error, $e(t)$, is large only when the estimation error, $|\dot{v}(t) - \hat{A}|$, is large. By using this approach, we are able to design a feedback controller to improve the acceleration estimation.

Controller design is an important factor in ensuring performance of the estimator. Since the true acceleration is assumed to be low frequency signal, high frequency control signal will degrade the estimation. In order to design a controller with smooth control signal, a feedback signal, $fuzzy(e)$, is defined using fuzzy logic.

Next, we will describe the proportional fuzzy controller design. The membership function for fuzzy rules with input S_i is shown in Figure 5.3.

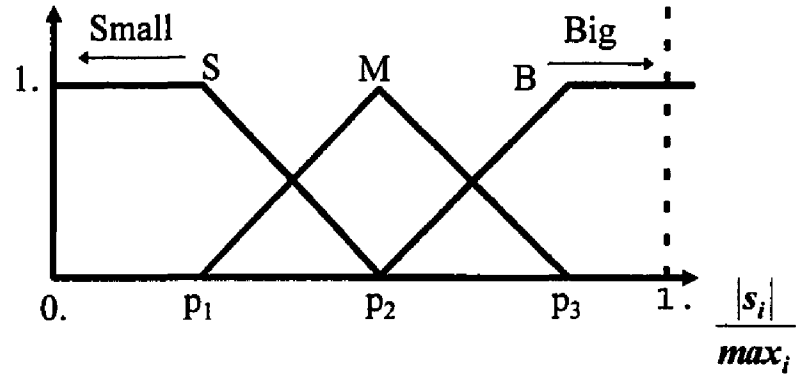


Figure 5.3. Membership function used for fuzzy rules

The fuzzy rules for $fuzzy(e)$ are described as follows:

$$\begin{aligned} \frac{|e|}{max_e} \text{ is Small}(S) &\Rightarrow \text{weighting} = \text{small weighting} \\ \frac{|e|}{max_e} \text{ is Medium}(M) &\Rightarrow \text{weighting} = \text{medium weighting} \\ \frac{|e|}{max_e} \text{ is Big}(B) &\Rightarrow \text{weighting} = \text{big weighting} \end{aligned} \quad (39)$$

Thus,

$$Fuzzy(e) = (B \cdot \text{big weighting} + M \cdot \text{medium weighting} + S \cdot \text{small weighting}) \cdot e \quad (40)$$

The feedback proportional control output is therefore expressed by:

$$u = K_p \cdot Fuzzy(e) \quad (41)$$

With the feedback controller described above, if the low pass filter g is design to satisfy equation (C.40) (see Appendix C), the acceleration estimated using this scheme will improve upon the base-line estimation, in the sense that the maximum estimation error is reduced.

Remark 5.2. To implement the control $u(t) = -K_p \cdot \text{fuzzy}(e(t))$ using discrete system, a modified control can be used to compensate for the control loop time delay Δt

$$u(t) = -K_p \cdot \text{fuzzy}(e(t - \Delta t)) - K_d \cdot \frac{d[\text{fuzzy}(e(t - \Delta t))]}{dt} \quad (42)$$

where $\frac{d[\text{fuzzy}(e(t - \Delta t))]}{dt}$ is evaluated via finite difference.

Remark 5.3. In this proposed estimation scheme, a smooth base-line estimation is used. The extreme case is to use zero signal as the base-line estimation, then a great deal of control effort will be needed and the convergent rate of the performance will be slow.

5.2.2. Estimation Scheme B

The general idea of this scheme (see Figure 5.2) is to estimate the acceleration through adaptively tuning the bandwidth of the filter f . The fuzzy bandwidth adapter is designed using fuzzy logic with $\text{fuzzy}(e)$ as input. The $\text{fuzzy}(e)$ is set up to be the feedback signal using fuzzy logic with input $e(t)$. The design procedure is outlined as follows:

- (a) Given the measurement of velocity v and noise w , signal x_2 is calculated through the standard filtered finite difference method with the g filter. Design the bandwidth a of the low pass filter g such that x_2 is smooth.

- (b) With the base-line estimation $\tilde{A}(t)$, derive \hat{A} and x_l . Since the bandwidth adapter is not designed to recover the signal distortion, the distortion of the base-line estimation should be acceptable.
- (c) Set up $fuzzy(e)$ to be the tuning signal from $e(t)$ and set up a fuzzy logic to tune the bandwidth of the low pass filter f by using $fuzzy(e)$ as input. The $fuzzy(e)$ is defined using fuzzy logic by considering the level of the filtered high frequency noise. The fuzzy logic for tuning the bandwidth of the low pass filter f is designed such that (1) the signal distortion and the noise level are acceptable, and (2) when $fuzzy(e)$ is zero, the bandwidth is a constant. The constant bandwidth is designed such that the level of the filtered high frequency noise is acceptable.

Before we discuss the detailed design, we will describe the logic behind this scheme.

In order to apply feedback adaptive actions to estimate acceleration, we need to define a control objective and measurable feedback signal. As discussed in section 5.2.1, $e(t)$ is used as the feedback signal. By using this approach, we are able to design a feedback bandwidth adapter to improve the acceleration estimation.

The bandwidth of the low pass filter f is first designed to be a constant such that the noise level of the filtered signal is acceptable. The fuzzy bandwidth adapter is then used to tune the bandwidth to obtain an estimation with acceptable noise level and distortion. In this thesis, it is shown that a better estimation (better than that without

bandwidth adapter, see Theorem C.4 in Appendix C) can always be achieved using the adapter if certain conditions are satisfied.

To implement the adaptive action, noise characteristics have to be known (see equation (C.44) and (C.45) in Appendix C). It is usually difficult or even impossible to determine these values. It has been proved that fuzzy functions can approximate any continuous function [Ying, 1994; Zeng and Singh, 1995]. It is also known that fuzzy controller is more robust against parameter errors. In order to implement the adapter without knowing the characteristics of the noise, the adaptive action is designed through fuzzy logic such that the bandwidth is wide when $fuzzy(e)$ is big and narrow when $fuzzy(e)$ is small.

Next, we will describe the fuzzy bandwidth adapter design. The membership function for fuzzy rules with input S_i is shown in Figure 5.3. The defining of $fuzzy(e)$ is the same as that described in section 5.2.1. The fuzzy rules for fuzzy bandwidth adapter are described as follows:

$$\begin{aligned} \frac{|fuzzy(e)|}{max_{fuz}} \text{ is } Small(S) &\Rightarrow Bandwidth = small\ band \\ \frac{|fuzzy(e)|}{max_{fuz}} \text{ is } Medium(M) &\Rightarrow Bandwidth = medium\ band \\ \frac{|fuzzy(e)|}{max_{fuz}} \text{ is } Big(B) &\Rightarrow Bandwidth = big\ band \end{aligned} \quad (43)$$

Therefore, the bandwidth b of the filter $h(s)$ is therefore expressed by:

$$Bandwidth\ b = B \cdot big\ band + M \cdot medium\ band + S \cdot small\ band \quad (44)$$

With the bandwidth adapter as described above, if the conditions in Theorem C.4 are satisfied, the acceleration estimated using this scheme will always have better performance than that without the bandwidth adapter (see Appendix C).

5.3. Results and Discussions

Next, we will examine some examples to illustrate the estimation design. Both simulation data and experimental results are used.

5.3.1 Acceleration estimation using speed data from simulation

Example 5.1:

Transmission output speed and acceleration signals generated through simulation on the powertrain model described in Chapter 2 are used. A white noise with covariance 0.22 is added to the transmission output angular velocity signal and used to simulate measurement noise. Both schemes will be applied and the true acceleration from simulation is used for comparison.

Case 1: Scheme A estimation

A low pass filter with bandwidth 5.0 rad/sec is used to filter the speed signal, then finite difference is used to estimate the acceleration and the result is used as baseline.

The g filter is designed to be:

$$g(s) = 5.0 / (s + 5.0)$$

The parameters of the fuzzy rules for $fuzzy(e)$ and the proportional controller are:

$$\begin{aligned}
 p_1 &= 0.2, p_2 = 0.5, p_3 = 0.8, \max_e = 2.0 \\
 \text{small weighting} &= 0.0, \text{medium weighting} = 0.5, \text{big weighting} = 1.0 \\
 K_p &= 5.0
 \end{aligned}$$

The results are shown in Figure 5.4. Acceleration estimated using Scheme A is compared with the baseline and the true acceleration. As shown in the figure, the proposed scheme can derive smooth acceleration signals with much less distortion (comparing to baseline).

Case 2: Scheme B estimation

A low pass filter with bandwidth 80.0 rad/sec is used to filter the speed signal, then finite difference is used to estimate the acceleration and the result is used as baseline.

The g filter is designed to be:

$$g(s) = 10.0 / (s + 10.0)$$

The parameters of the fuzzy rules for $fuzzy(e)$ are:

$$\begin{aligned}
 p_1 &= 0.2, p_2 = 0.5, p_3 = 0.8, \max_e = 2.0 \\
 \text{small weighting} &= 0.0, \text{medium weighting} = 0.5, \text{big weighting} = 1.0
 \end{aligned}$$

The parameters of the fuzzy rules for the fuzzy bandwidth adapter are:

$$\begin{aligned}
 p_1 &= 0.3, p_2 = 0.5, p_3 = 0.9, \max_e = 4.0 \\
 \text{small band} &= 10.0, \text{medium band} = 40.0, \text{big band} = 200.0
 \end{aligned}$$

The result are shown in Figure 5.5. Acceleration estimated using Scheme B is compared with the baseline and the true acceleration. As shown in the figure, the proposed scheme can derive smooth acceleration signals (comparing to baseline) with little distortion.

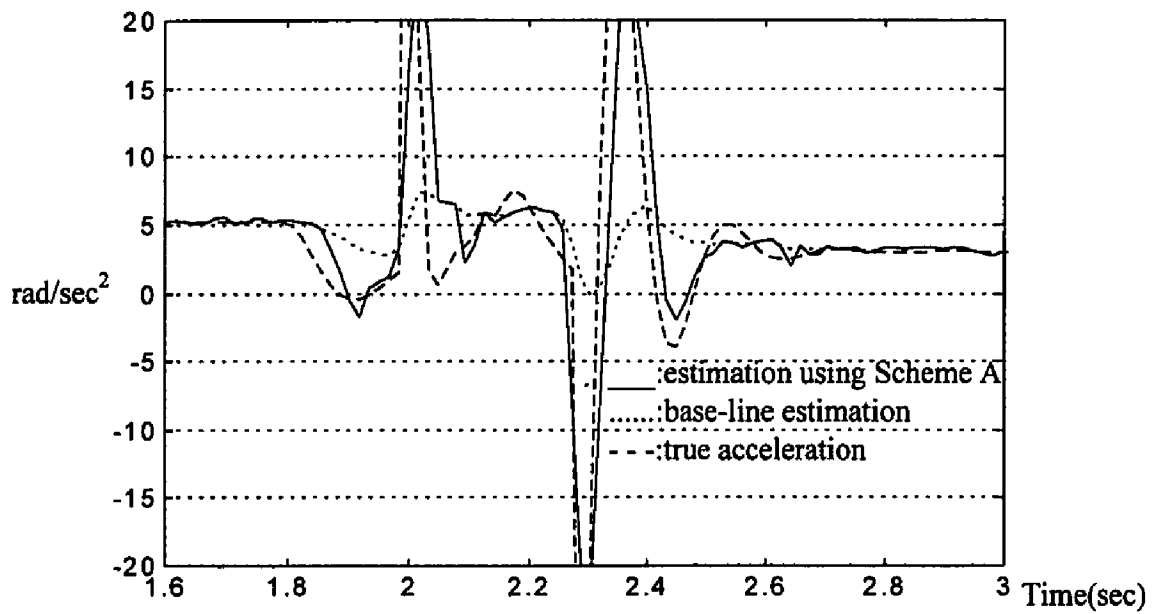


Figure 5.4 Estimation using Scheme A, base-line estimation, and true acceleration

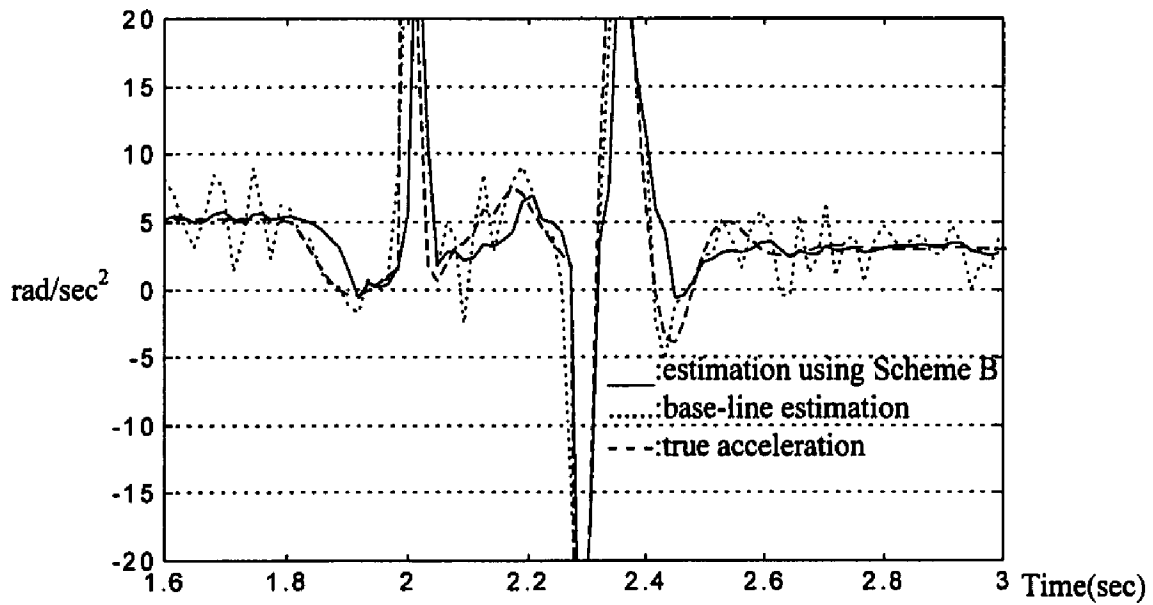


Figure 5.5 Estimation using Scheme B, base-line estimation, and true acceleration

5.3.2 Acceleration estimation using experimental data

To evaluate the estimation algorithm with actually measured data, experimental effort is performed. A schematic of the experimental setup is shown in Figure 5.6. The test stand consists of four major parts: the engine, the torque converter, the transmission, and the flywheel with dynamic loading. Two computers are used for engine control, transmission control, and data acquisition. The flywheel is used to simulate the vehicle load. Transmission output speed and output torque are measured.

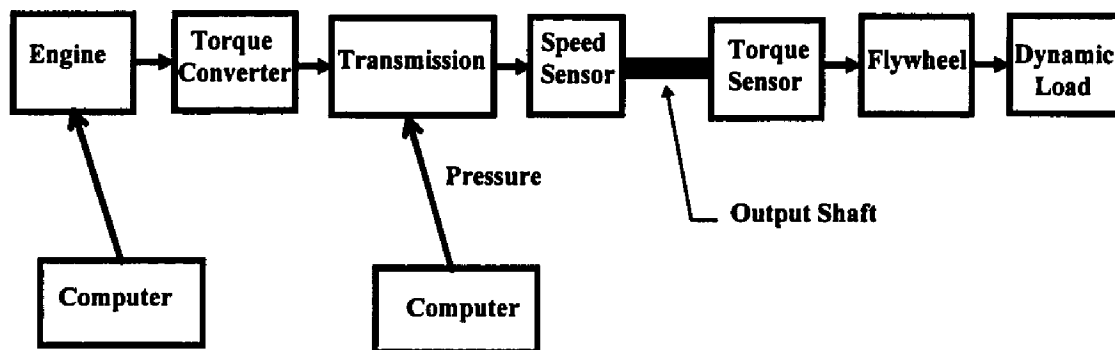


Figure 5.6 Engine-Transmission setup and instrumentation used for speed and torque measurement in the test cell

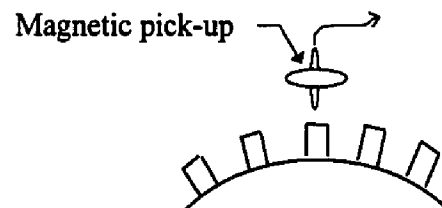


Figure 5.7 A schematic of speed sensor

For the experimental data used in the thesis, speed signals are measured using a magnetic pick-up. Refer to Figure 5.7, the pick-up contains a magnet and is mounted on a nonrotating frame such that the tip of the sensor is close to the teeth. As a tooth enters and leaves the magnetic field in the neighborhood of the pick-up, a change in the magnetic flux is sensed by a coil in the pick-up. These alternating changes in the flux field produce pulses in the output voltage of the sensor. The number of pulses observed in a period is the average speed of the shaft during the period. The speed can be calculated by dividing the number of pulses per unit time by the number of teeth on the wheel.

Both schemes are used to estimate the acceleration and the results are compared with the baseline and the estimation using direct finite difference on the measured speed signal. In example 5.3, the results will also be compared with the transmission output torque.

Example 5.2:

In this example, the transmission output speed sensor has a 16 teeth/revolution resolution and the sampling time is 16 ms. The speed ranges from 50 RPM to 420 RPM.

Case 1: Scheme A estimation

The smooth acceleration signal estimated using finite-difference with a narrow bandwidth (below 1 Hz) low pass filter is used as baseline.

The g filter is designed to be:

$$g(s) = 5.0 / (s + 5.0)$$

The parameters of the fuzzy rules for $fuzzy(e)$ and the proportional controller are:

$$\begin{aligned}
 p_1 &= 0.3, p_2 = 0.5, p_3 = 0.9, \max_e = 20.0 \\
 \text{small weighting} &= 0.0, \text{medium weighting} = 0.5, \text{big weighting} = 1.0 \\
 K_p &= 2.0
 \end{aligned}$$

The results are shown in Figure 5.8 - Figure 5.13. Acceleration estimated using Scheme A is compared with the baseline (smooth estimation) and the estimation using a direct finite difference (without filter). As shown in these figures, the proposed scheme can derive smooth (comparing to the estimation using direct finite difference) acceleration signals with much less distortion (comparing to the baseline).

Case 2: Scheme B estimation

The estimation using direct finite difference without filter is used as the baseline.

The g filter is designed to be:

$$g(s) = 5.0 / (s + 5.0)$$

The parameters of the fuzzy rules for $fuzzy(e)$ are:

$$\begin{aligned}
 p_1 &= 0.3, p_2 = 0.5, p_3 = 0.9, \max_e = 20.0 \\
 \text{small weighting} &= 0.0, \text{medium weighting} = 0.5, \text{big weighting} = 1.0
 \end{aligned}$$

The parameters of the fuzzy rules for the fuzzy bandwidth adapter are:

$$\begin{aligned}
 p_1 &= 0.3, p_2 = 0.5, p_3 = 0.9, \max_e = 10.0 \\
 \text{small band} &= 10.0, \text{medium band} = 15.0, \text{big band} = 50.0
 \end{aligned}$$

The results are shown in Figure 5.14 - Figure 5.16. Acceleration estimated using Scheme B is compared with the baseline. As shown in these figures, the proposed scheme can derive smooth acceleration signals with little distortion.

Example 5.3:

In this case, the transmission output speed sensor has 69 teeth/revolution resolution and the sampling time is 16 ms. The speed ranges from 160 RPM to 760 RPM.

Case 1: Scheme A estimation

The base-line signal is derived using finite difference with a low pass filter of bandwidth 5.0 rad/sec.

The g filter is designed to be:

$$g(s) = 5.0 / (s + 5.0)$$

The parameters of the fuzzy rules for $fuzzy(e)$ and the PD controller are:

$$p_1 = 0.3, p_2 = 0.5, p_3 = 0.9, \max_e = 50.0$$

$$small\ weighting = 0.1, medium\ weighting = 0.5, big\ weighting = 1.0$$

$$K_p = 5.0, K_D = 0.08$$

The results are shown in Figure 5.17 - Figure 5.20. Acceleration estimated using Scheme A is compared with the base-line acceleration estimation and the transmission output torque measurement in Figure 5.17 and Figure 5.19. Acceleration estimated using Scheme A is compared with the estimation using the direct finite difference method (without filter) in Figure 5.18 and Figure 5.20. As shown in these figures, the proposed scheme can derive smooth (comparing to the estimation using the finite difference method) acceleration signals with much less distortion (comparing to the baseline).

Case 2: Scheme B estimation

The base-line signal is estimated using a filtered finite difference approach with a low pass filter of bandwidth 80.0 rad/sec.

The g filter is designed to be:

$$g(s) = 10.0 / (s + 10.0)$$

The parameters of the fuzzy rules for $fuzzy(e)$ are:

$$p_1 = 0.2, p_2 = 0.5, p_3 = 0.8, \max_e = 100.0$$

$$small\ weighting = 0.1, medium\ weighting = 0.5, big\ weighting = 1.0$$

The parameters of the fuzzy rules for the fuzzy bandwidth adapter are:

$$p_1 = 0.3, p_2 = 0.5, p_3 = 0.9, \max_e = 10.0$$

$$small\ band = 10.0, medium\ band = 50.0, big\ band = 100.0$$

The results are shown in Figure 5.21 - Figure 5.24. Acceleration estimated using Scheme B is compared with the baseline and the transmission output torque measurement in Figure 5.21 and Figure 5.24. Acceleration estimated using Scheme B is compared with the estimation using the direct finite difference method (without filter) in Figure 5.22 and Figure 5.24. As shown in these figures, the proposed scheme can derive smooth (comparing to the estimation using the direct finite difference method) acceleration signals with little distortion.

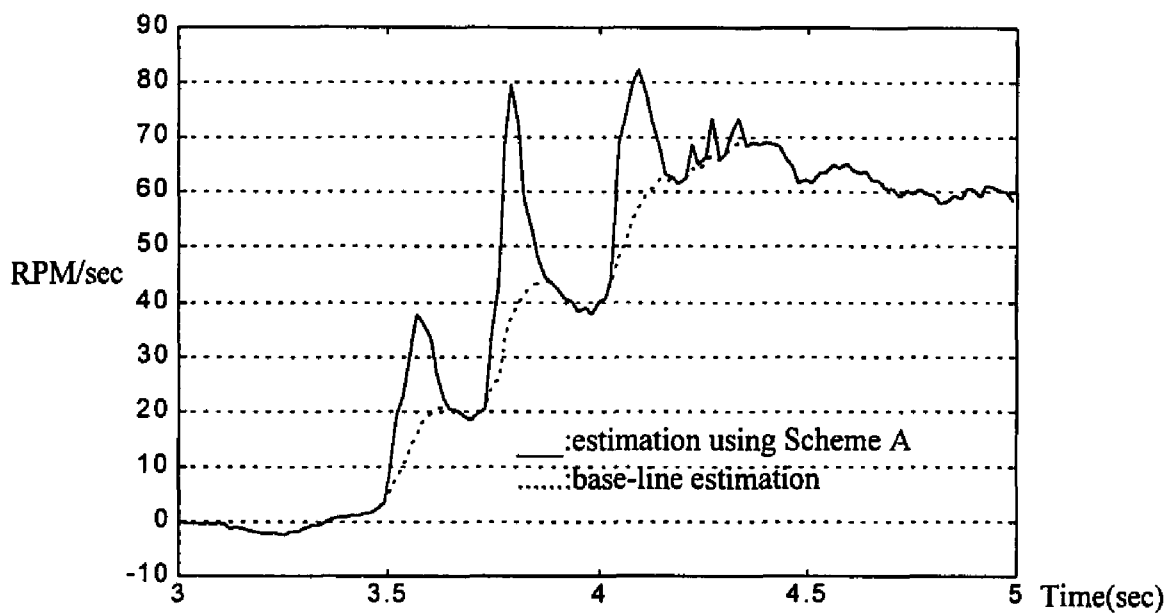


Figure 5.8 Estimation using Scheme A and base-line estimation

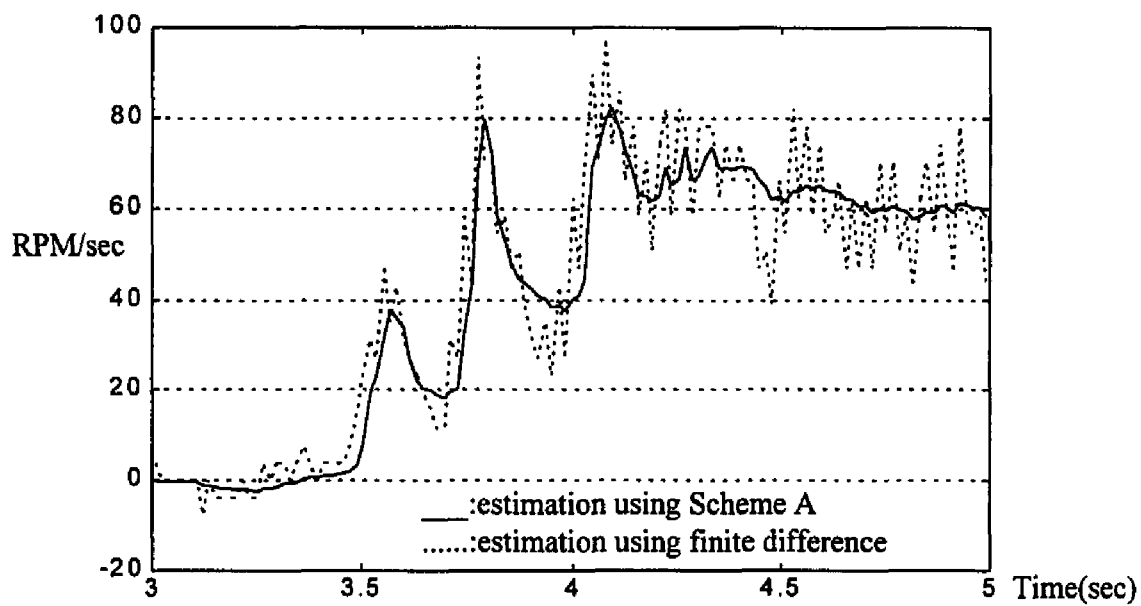


Figure 5.9 Estimation using Scheme A and estimation using finite difference

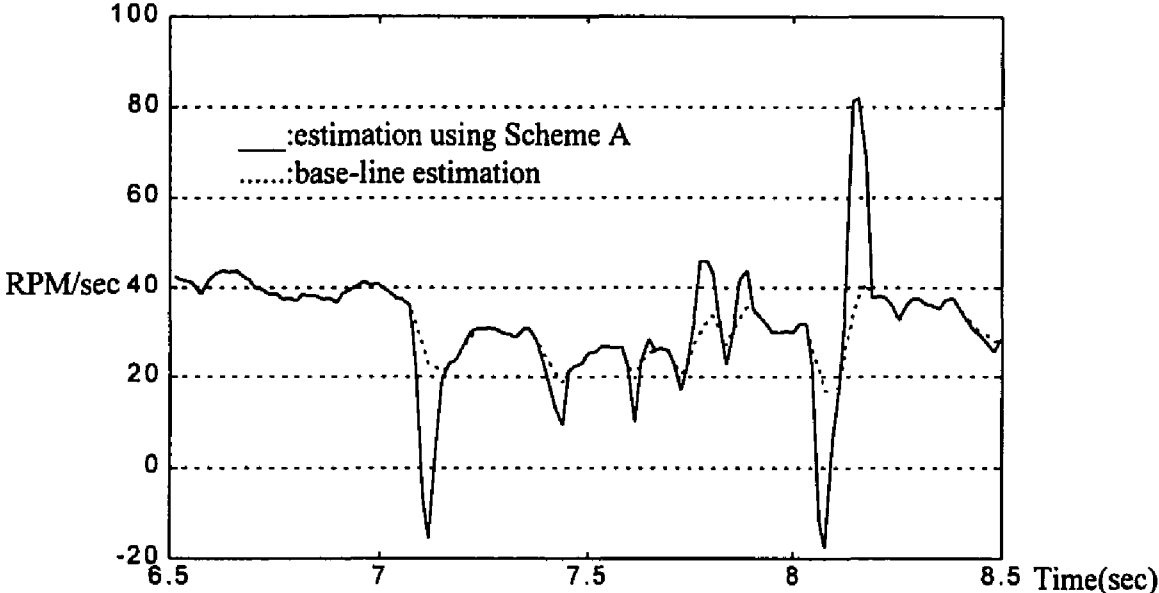


Figure 5.10 Estimation using Scheme A and base-line estimation

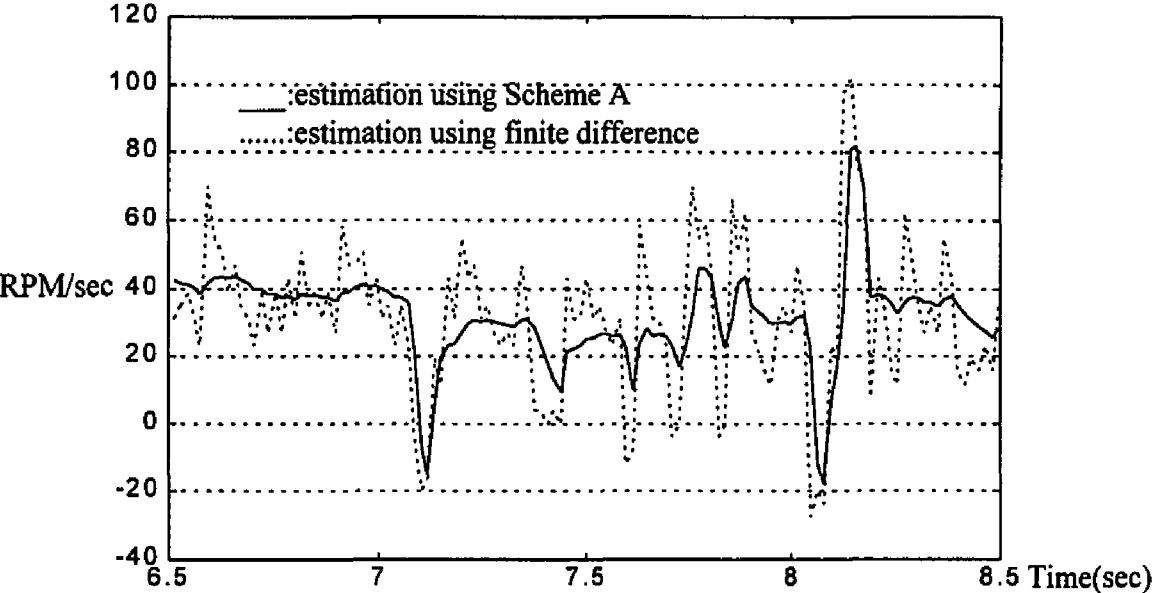


Figure 5.11 Estimation using Scheme A and estimation using finite difference

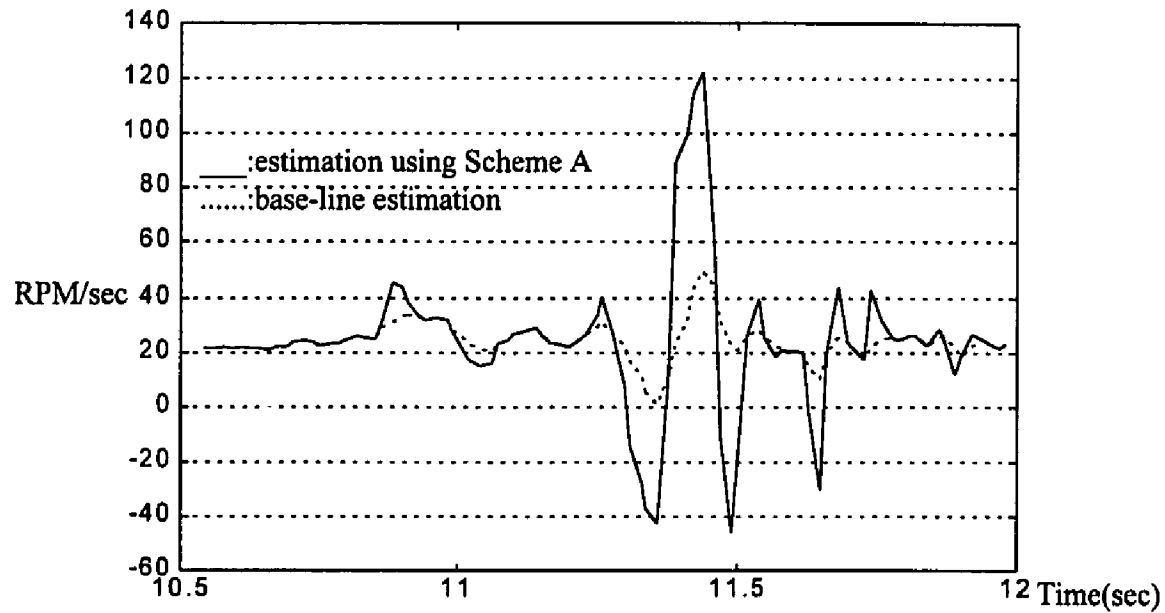


Figure 5.12 Estimation using Scheme A and base-line estimation

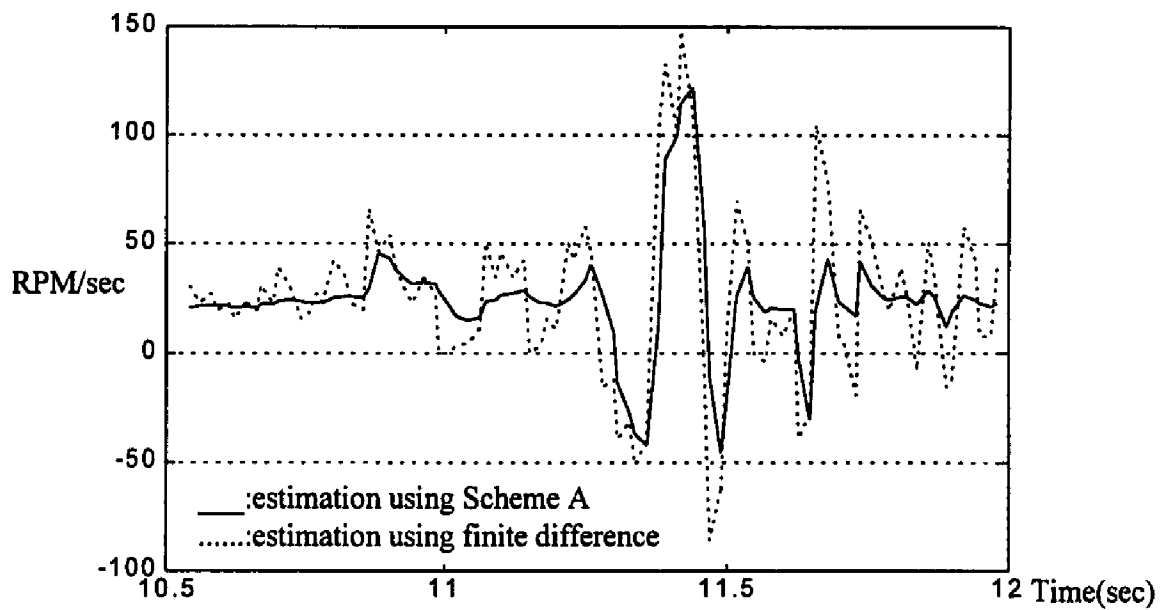


Figure 5.13 Estimation using Scheme A and estimation using finite difference

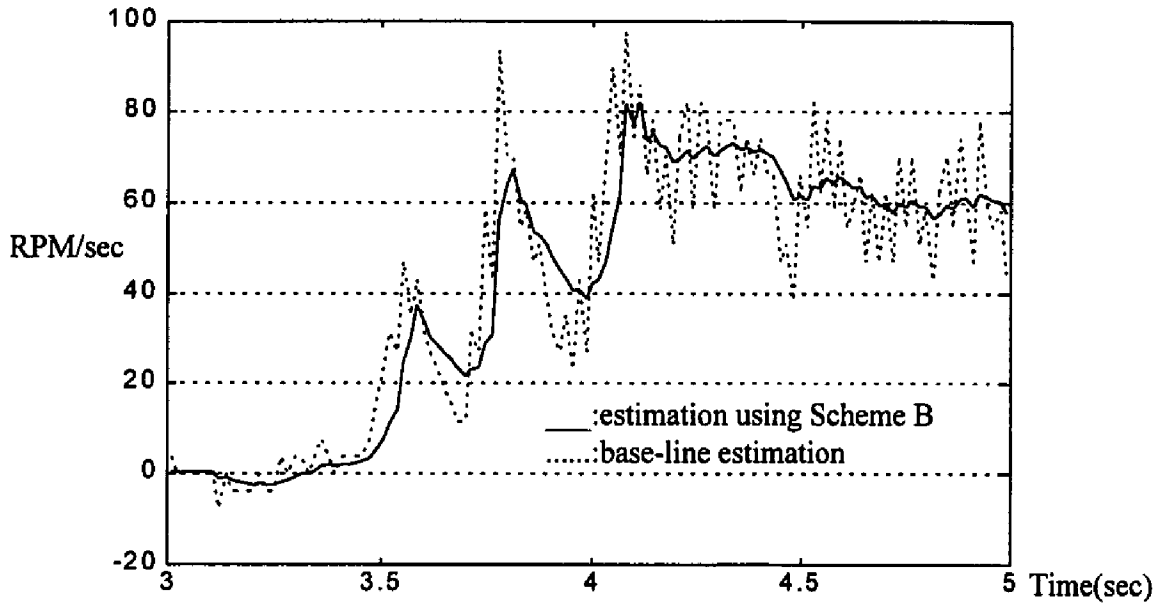


Figure 5.14 Estimation using Scheme B and base-line estimation

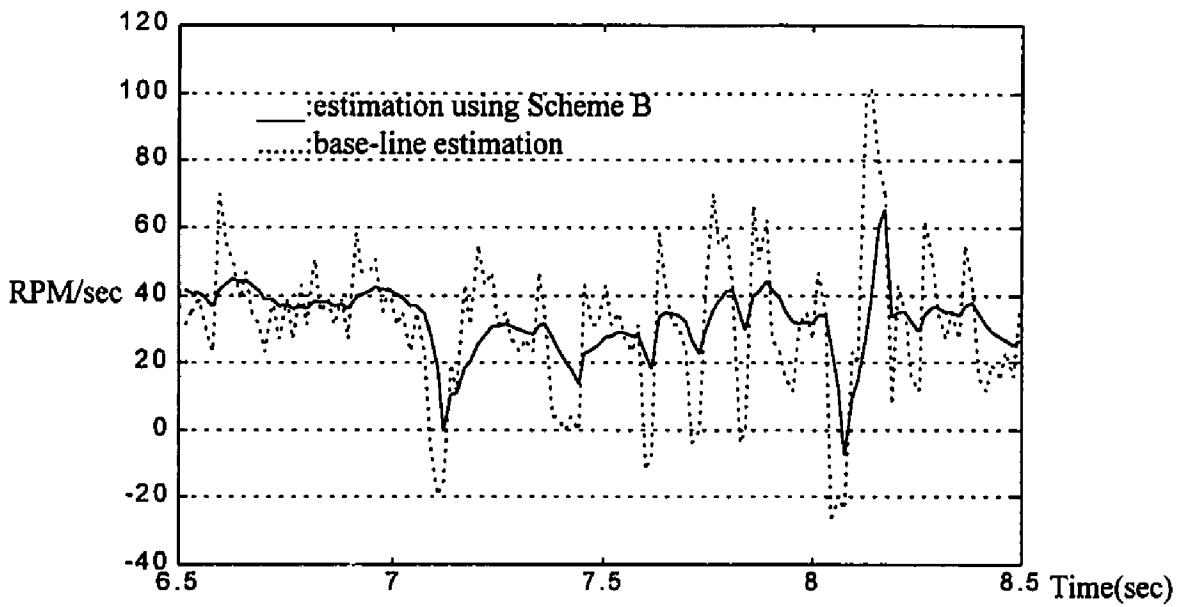


Figure 5.15 Estimation using Scheme B and base-line estimation

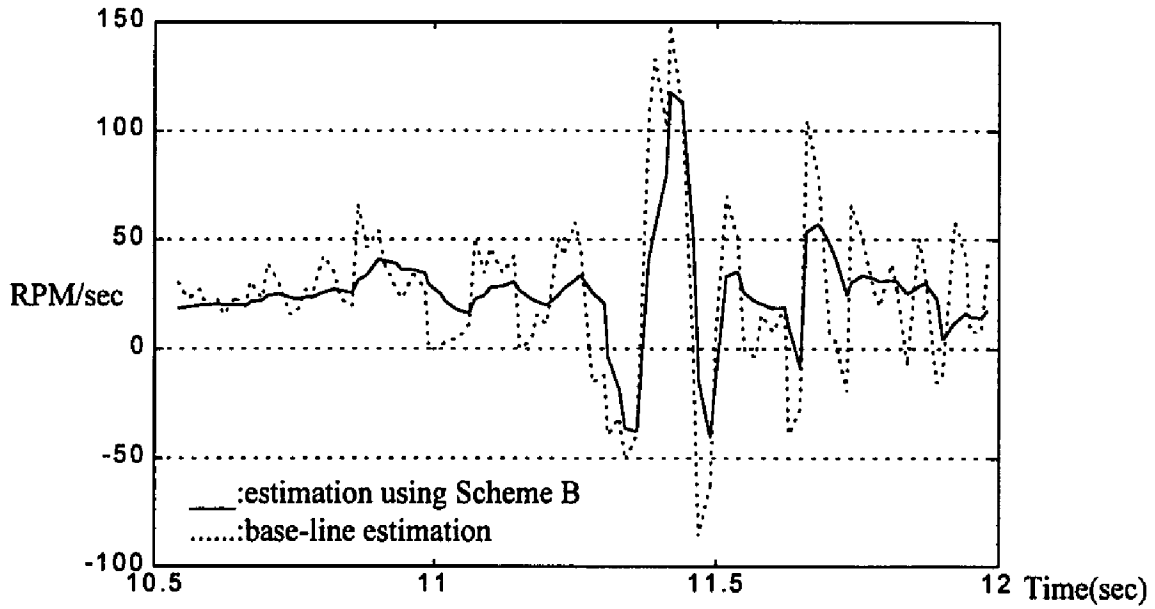


Figure 5.16 Estimation using Scheme B and base-line estimation

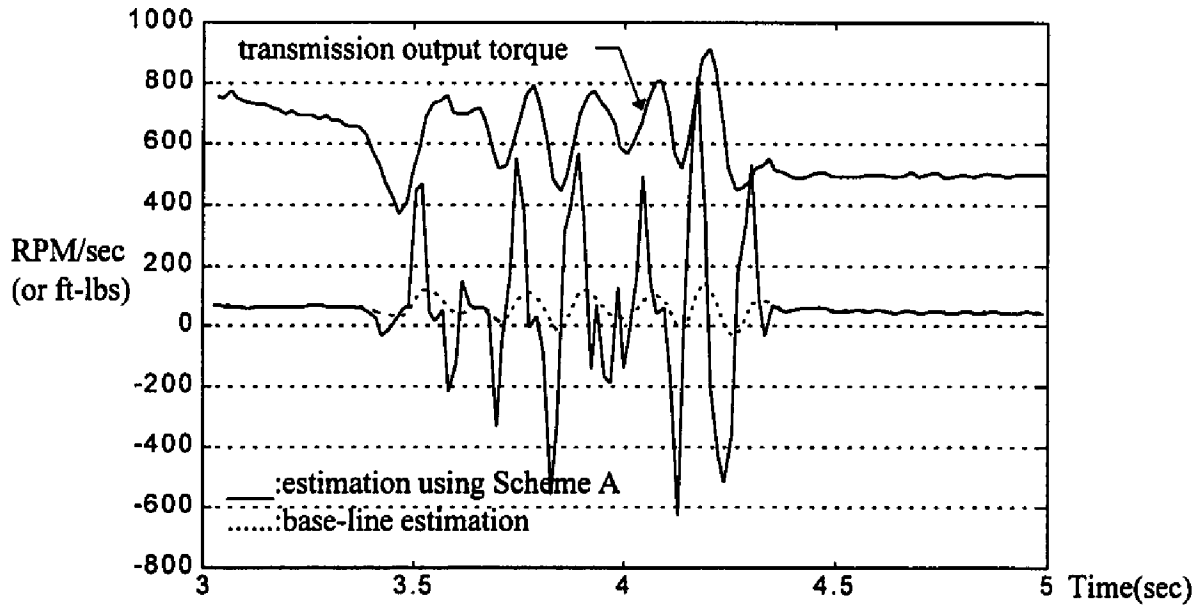


Figure 5.17 Estimation using Scheme A, base-line estimation, and transmission output torque

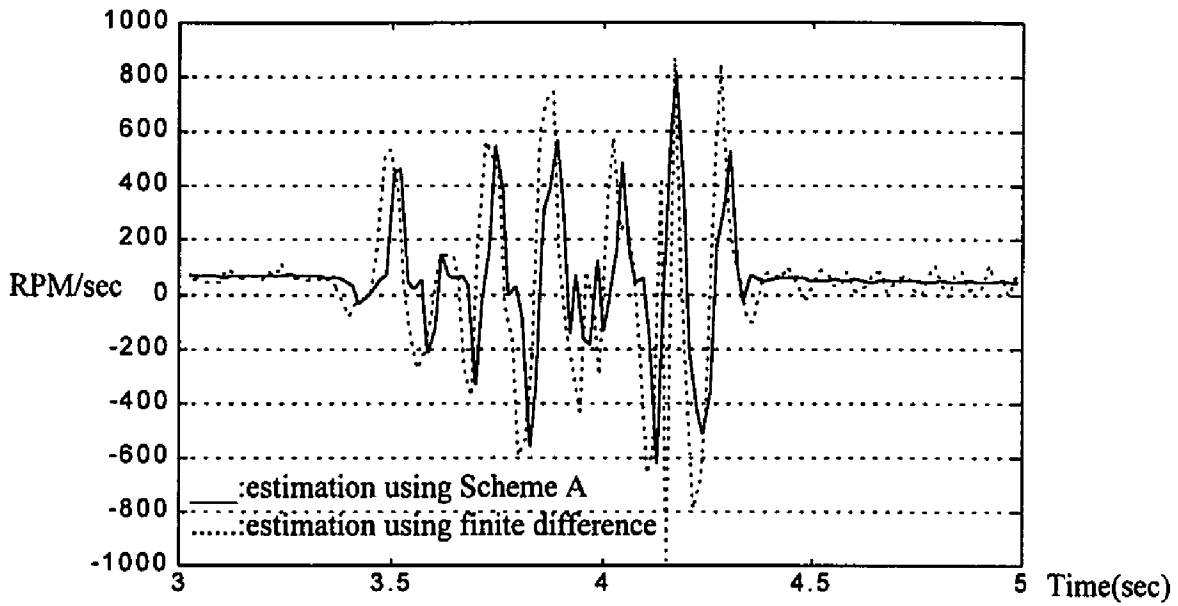


Figure 5.18 Estimation using Scheme A and estimation using finite difference

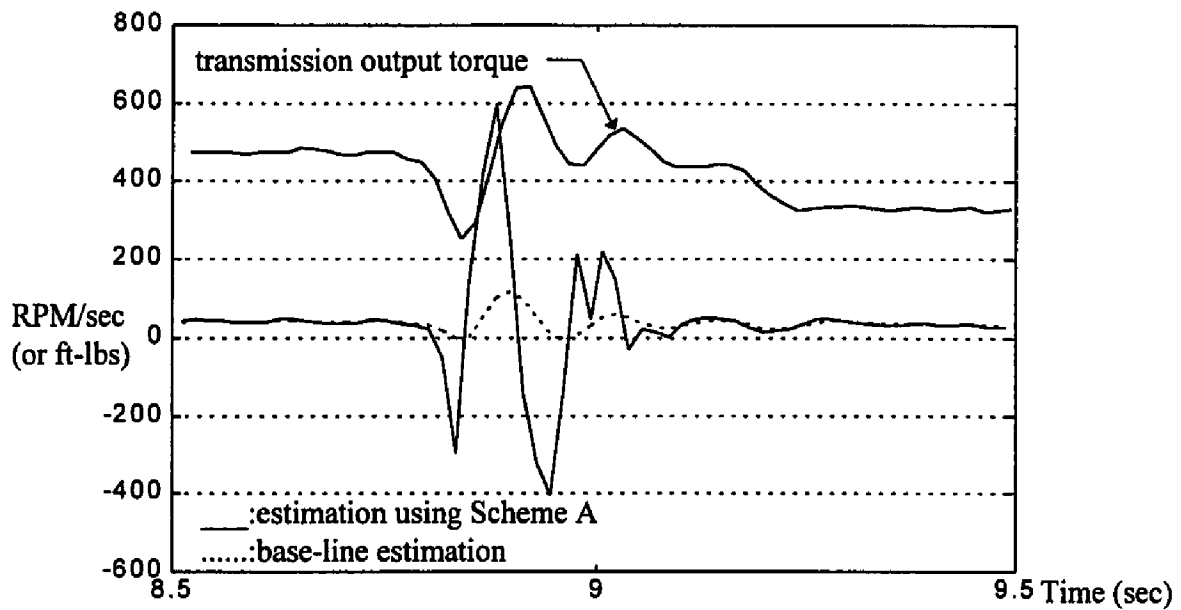


Figure 5.19 Estimation using Scheme A, base-line estimation, and transmission output torque

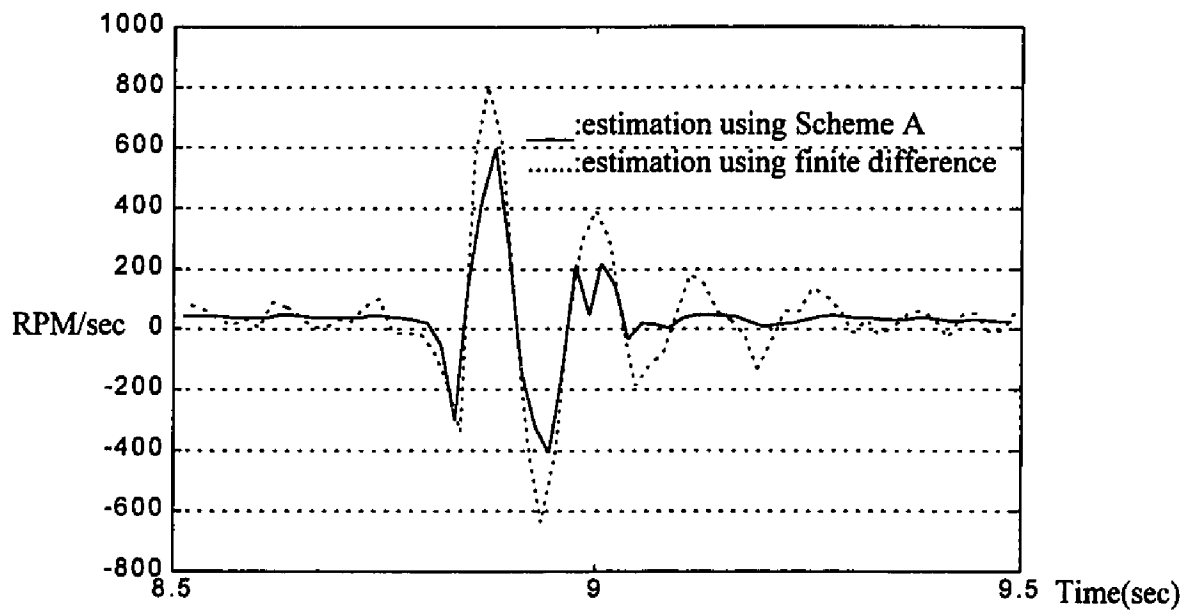


Figure 5.20 Estimation using Scheme A and estimation using finite difference

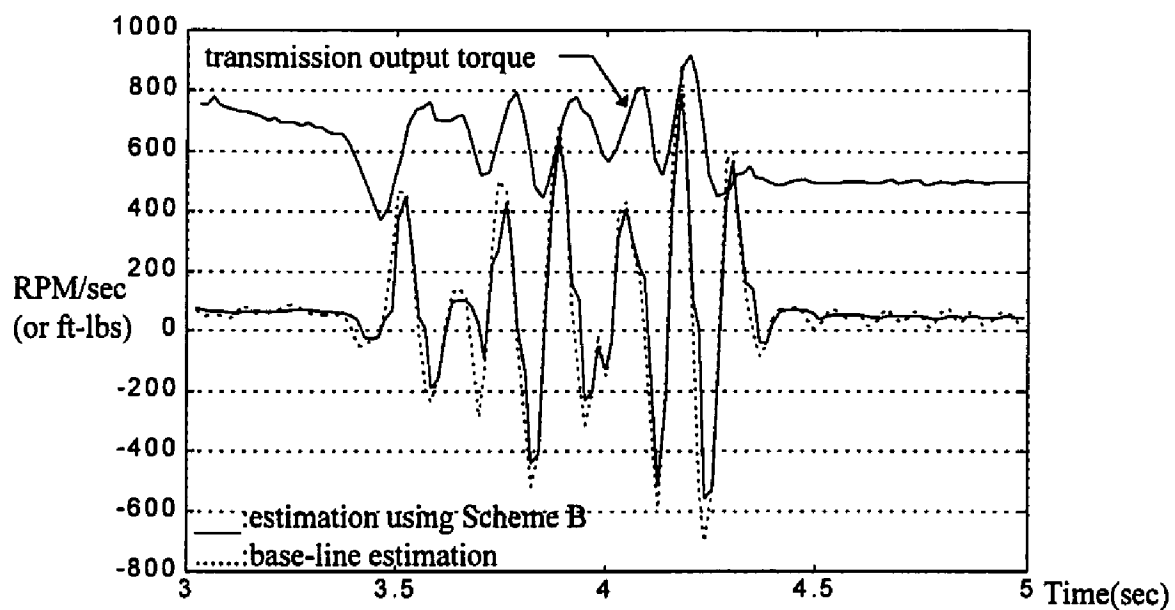


Figure 5.21 Estimation using Scheme B, base-line estimation, and transmission output torque

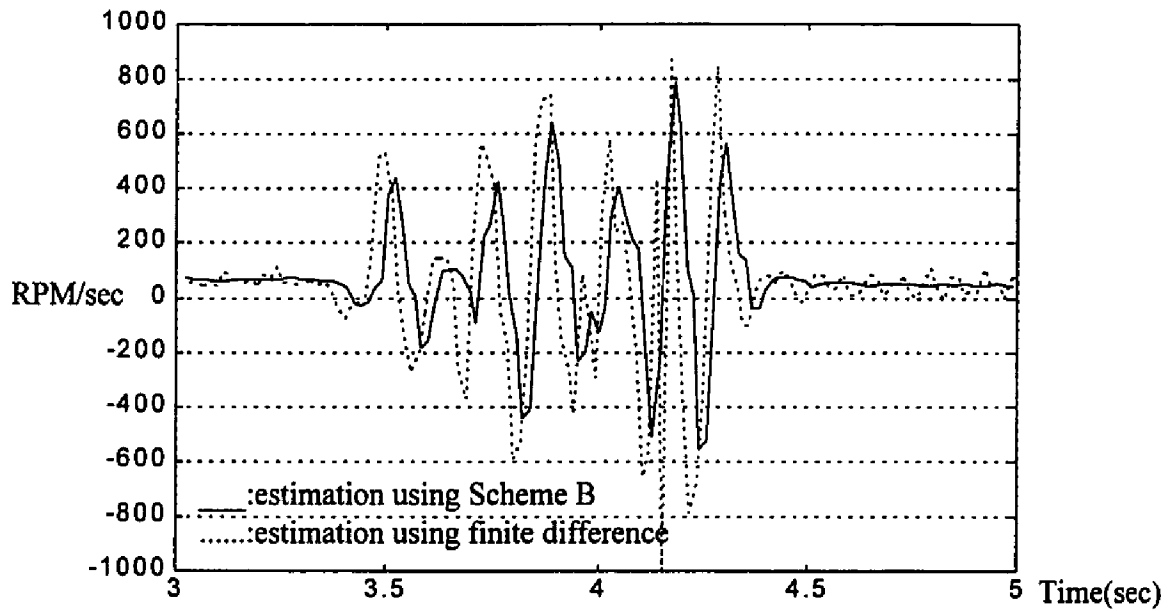


Figure 5.22 Estimation using Scheme B and estimation using finite difference

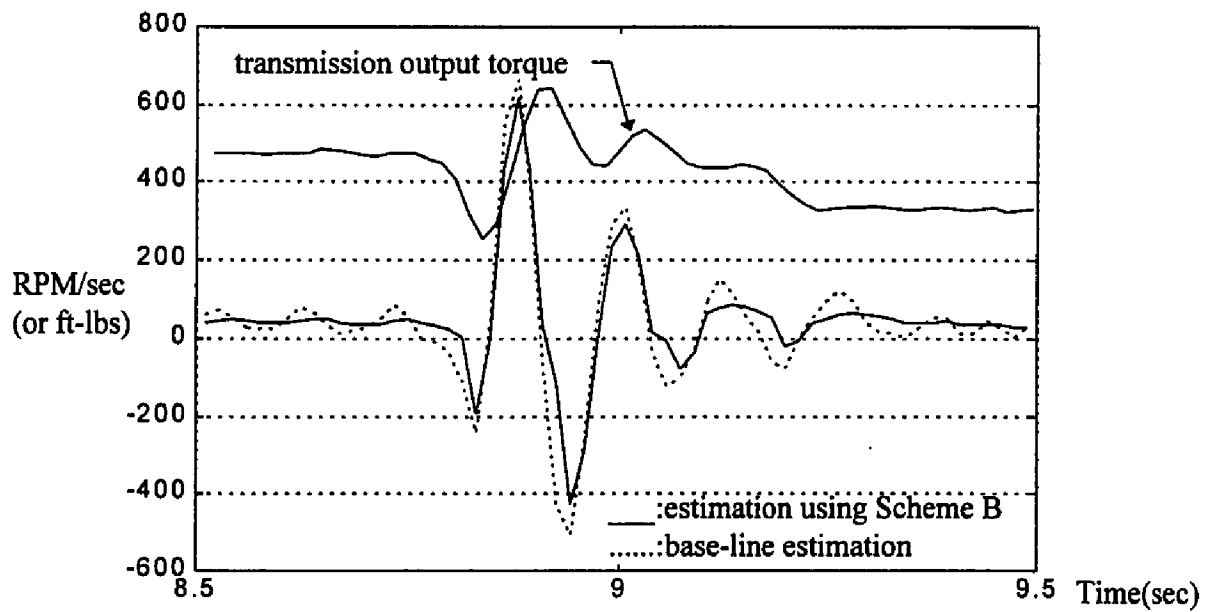


Figure 5.23 Estimation using Scheme B, base-line estimation, and transmission output torque

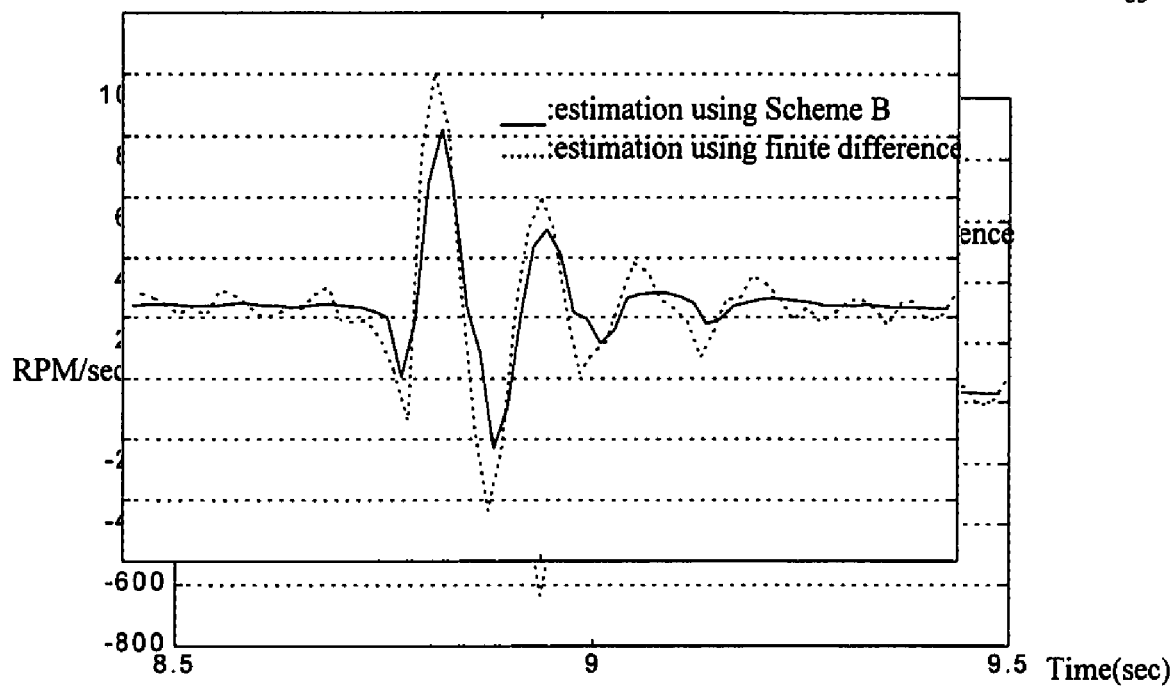


Figure 5.24 Estimation using Scheme B and estimation using finite difference

6. CONTROL SYSTEM SIMULATION RESULTS

To examine the performance of the controllers, computer simulations are carried out on the model described in Chapter 2. The parameters used in the analysis are shown in Table 4.1 unless stated otherwise.

6.1. Hybrid Approach Using Estimated Acceleration

The acceleration-based Hybrid Rule-Based Sliding controller is examined in a 1-2 upshift scenario. Results from using Scheme A and B are compared with an ideal case (known true transmission output acceleration signal). The vehicle accelerations for these three cases are illustrated in Figure 6.1. It is shown that the performance of the Hybrid controller using estimated transmission output acceleration are very close to that using the true transmission output acceleration signals. To further understand the merits of using these two estimation schemes, shift controls are performed using the base-line estimation in Example 5.1. As shown in Figure 6.2 and Figure 6.3, the performance degrade significantly when these base-line signals are used.

6.2. Comparison Study with Other Control Approaches

The Hybrid Approach is compared with two other control methods through computer simulation in this section, namely Control Schemes I and II as described in the following paragraphs.

Control Scheme I is similar to the strategy proposed by Cho and Hedrick [1989] without the engine control. The off-going clutch pressure will be dropped immediately at the beginning of the shift, and the on-coming clutch pressure is used to regulate the transmission output velocity through Sliding Control.

Control Scheme II is similar to the method proposed by Glitzenstein and Hedrick [1991], but without the engine control and the adaptive action. The off-going clutch pressure is dropped with a specific rate at the beginning of the shift, and the on-coming clutch pressure is used to maintain zero slip of the off-going clutch until the off-going clutch pressure command is zero. The on-coming clutch is then used to regulate the transmission output velocity through Sliding Control.

Without fill time uncertainties (ideal case), the vehicle accelerations resulted from the different algorithms are illustrated in Figure 6.4. It is shown that the torque phase drop and the speed phase overshoot (indication of shift quality) are similar for all control laws. As shown in Figure 6.4, the vehicle accelerations drop to almost the same level of that after the shift during the torque phase.

To investigate the effect of fill time uncertainties, the ideal cases are compared with the underfilled and overfilled (± 0.1 second error in fill time) scenarios (Figures 6.5 - 6.8). Under these conditions, the system performance is obviously degraded when Control Scheme I or Control Scheme II is used (Figures 6.5, 6.6). As shown in Figure 6.5 and 6.6, the vehicle accelerations drop to a level of less than 50% of that after the shift during the torque phase. However, the Hybrid Rule-Based Sliding Control still produces consistent and acceptable shift quality (Figure 6.7, 6.8). The pressure commands (P_{d1} ,

P_{d2}) and the actual pressures (P_{c1} , P_{c2}) for the overfilled, underfilled, and ideal cases are illustrated for the Hybrid approach in Figure 6.8, 6.9. It is shown in these figures that the rule-based trigger mechanism is effective in detecting the fill and torque phases, and the Hybrid approach is therefore much less sensitive to the fill time variations than the other two schemes.

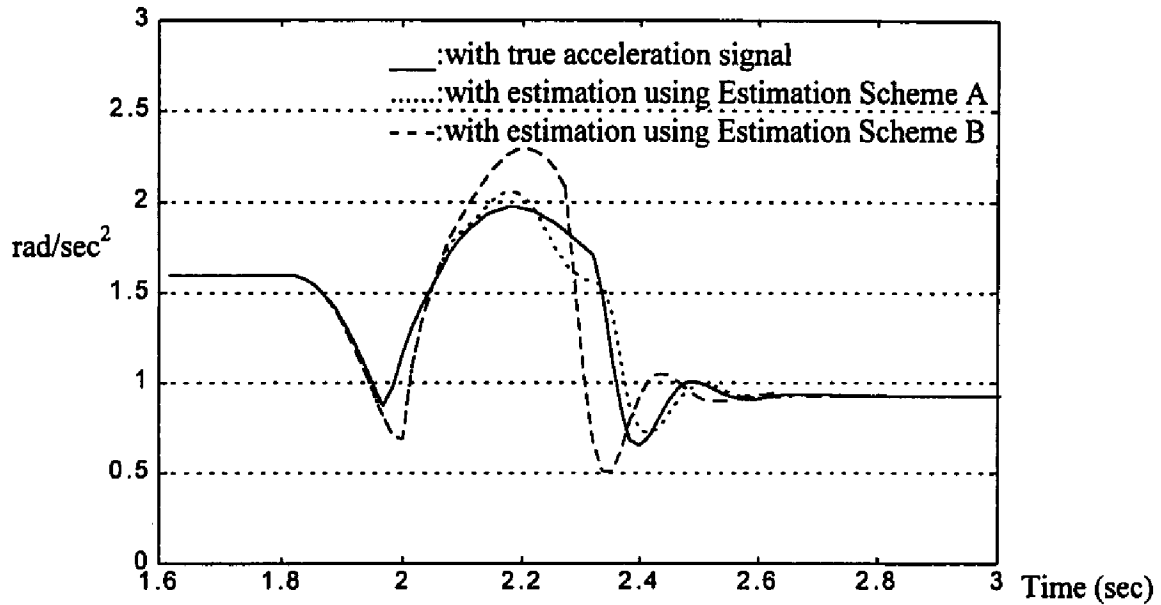


Figure 6.1 Vehicle acceleration during a 1-2 upshift using Hybrid approach with true acceleration and with acceleration estimated using the proposed schemes

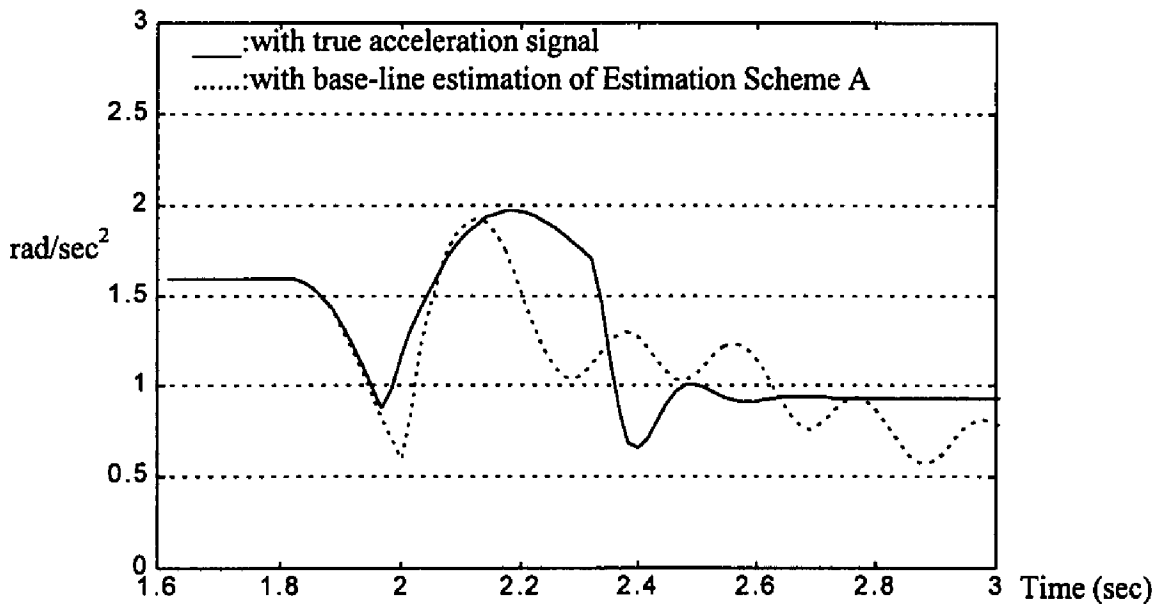


Figure 6.2 Vehicle acceleration during a 1-2 upshift using Hybrid approach with true acceleration and with the base-line estimation of Estimation Scheme A in Example 5.1

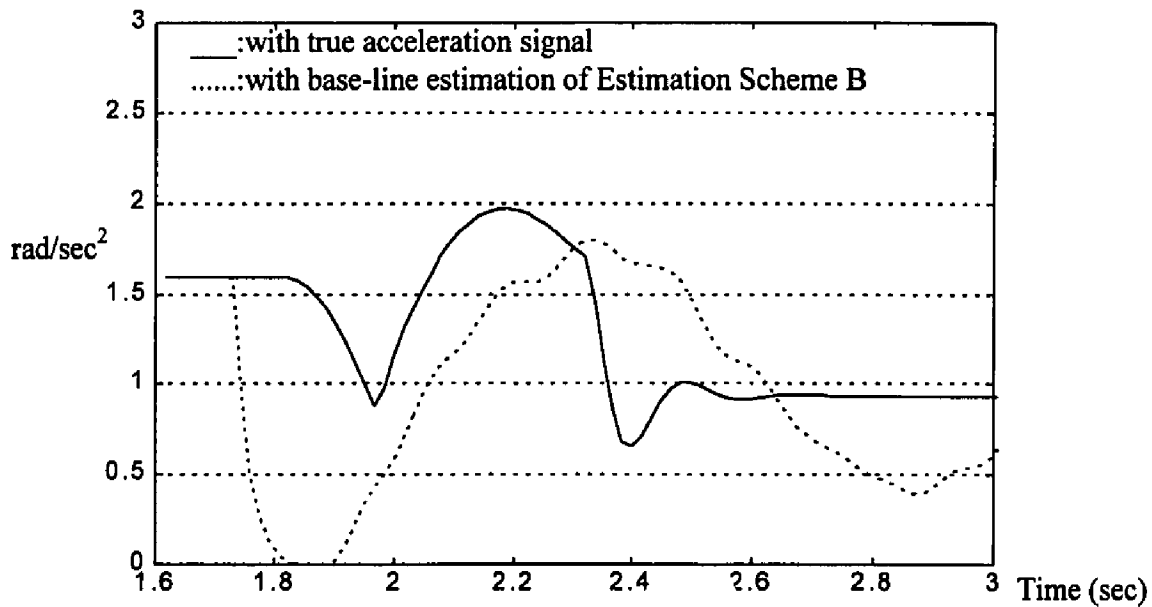


Figure 6.3 Vehicle acceleration during a 1-2 upshift using Hybrid approach with true acceleration and with the base-line estimation of Estimation Scheme B in Example 5.1

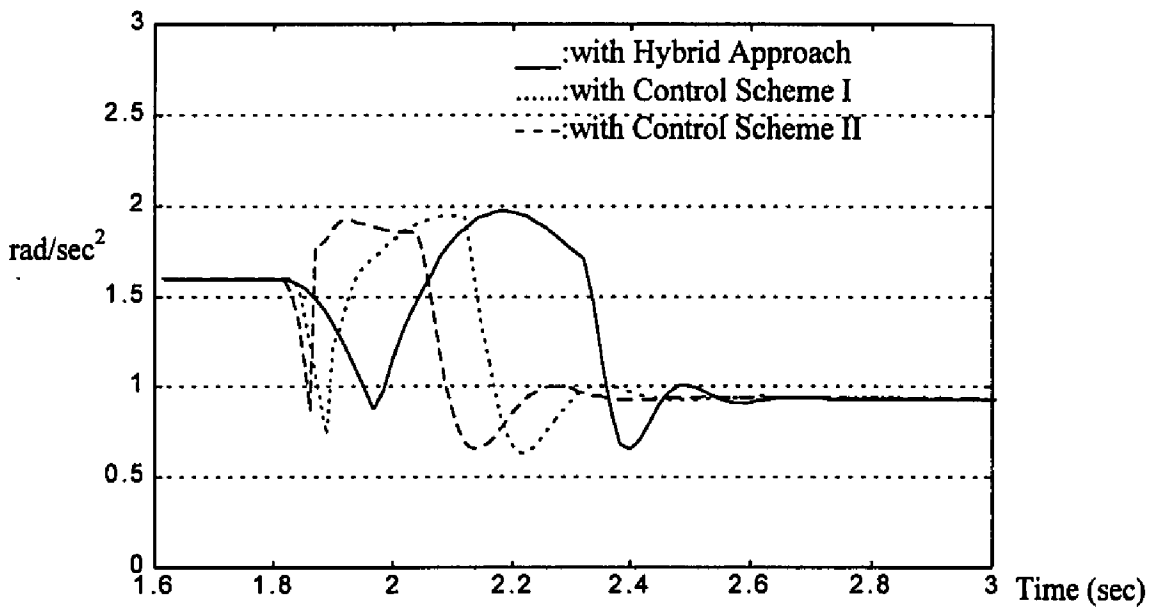


Figure 6.4 Vehicle acceleration during a 1-2 upshift using Control Scheme I, Control Scheme II, and Hybrid approach with true acceleration (No fill-time uncertainty)

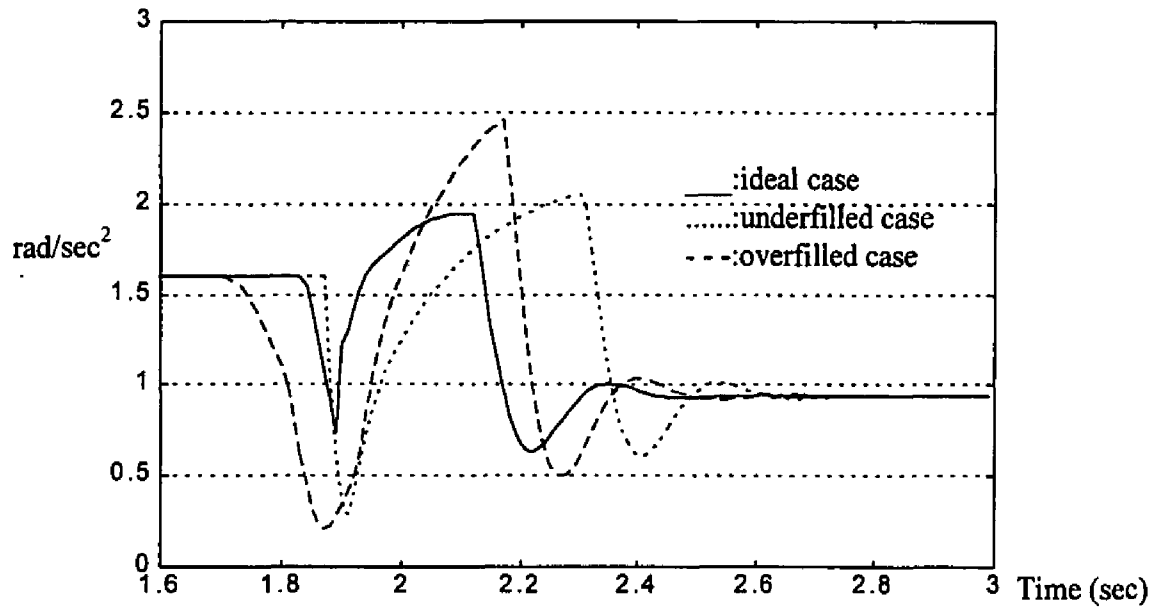


Figure 6.5 Vehicle acceleration during a 1-2 upshift using Control Scheme I

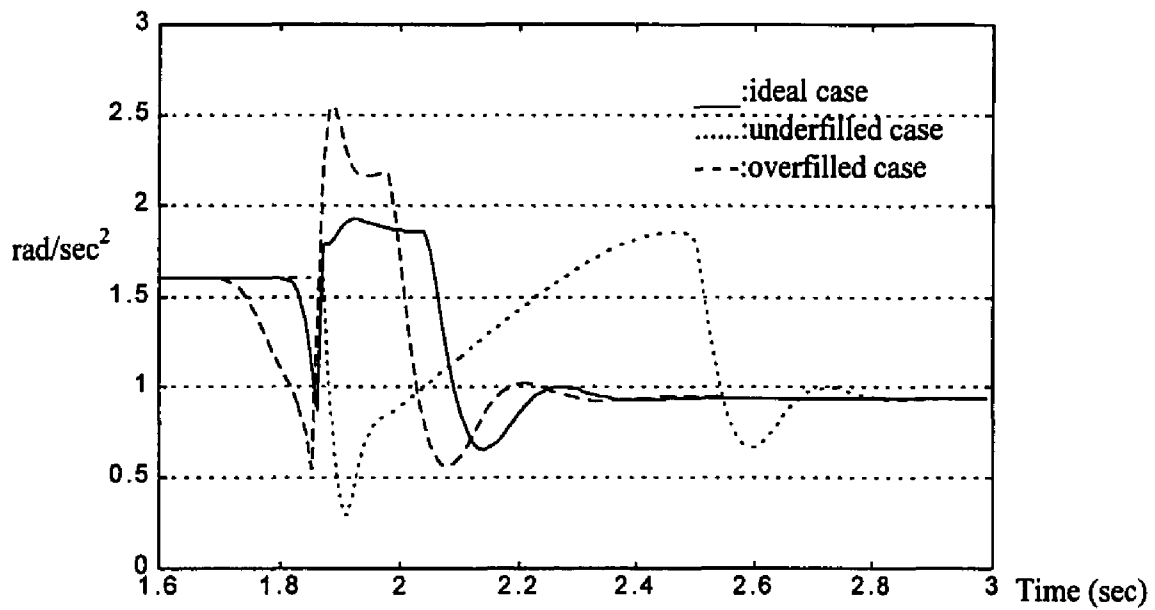


Figure 6.6 Vehicle acceleration during a 1-2 upshift using Control Scheme II

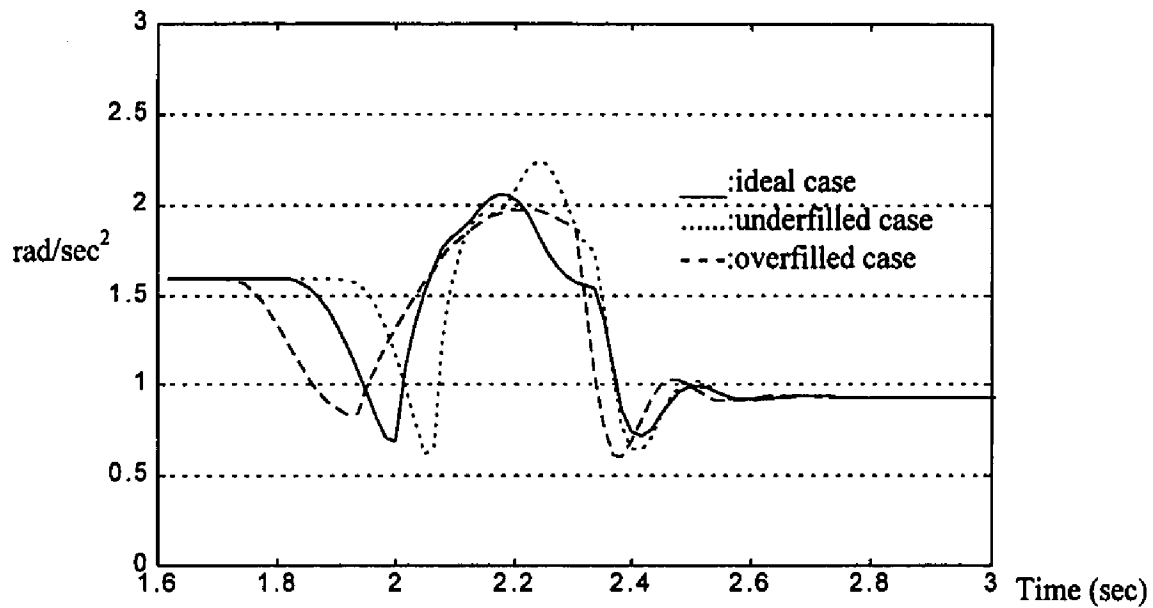


Figure 6.7 Vehicle acceleration during a 1-2 upshift using Hybrid approach with acceleration estimated using Estimation Scheme A

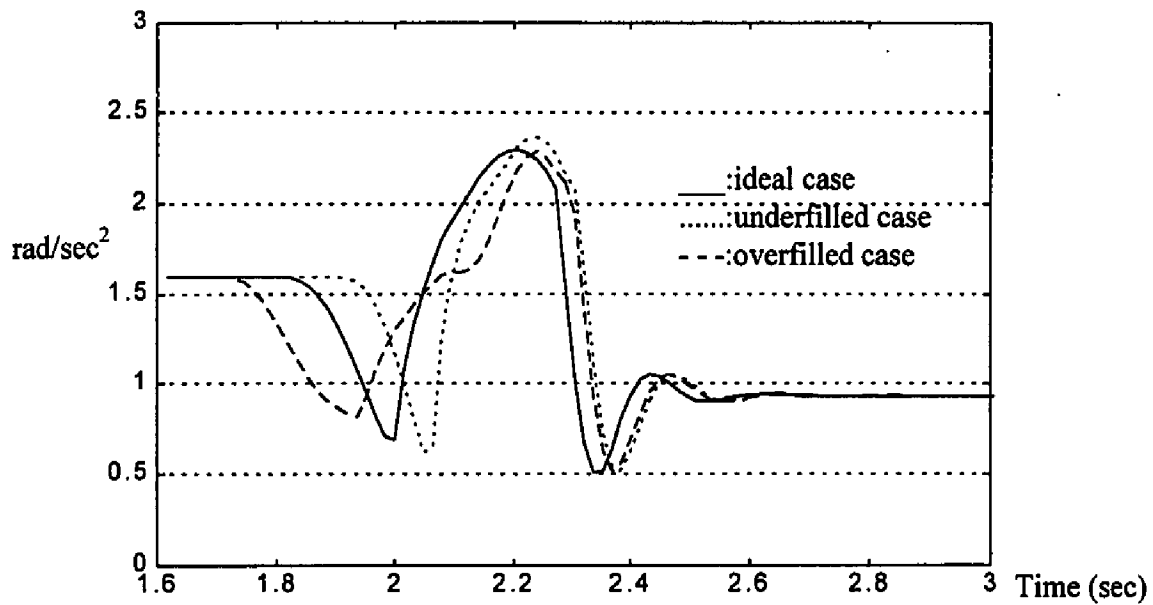


Figure 6.8 Vehicle acceleration during a 1-2 upshift using Hybrid approach with acceleration estimated using Estimation Scheme B

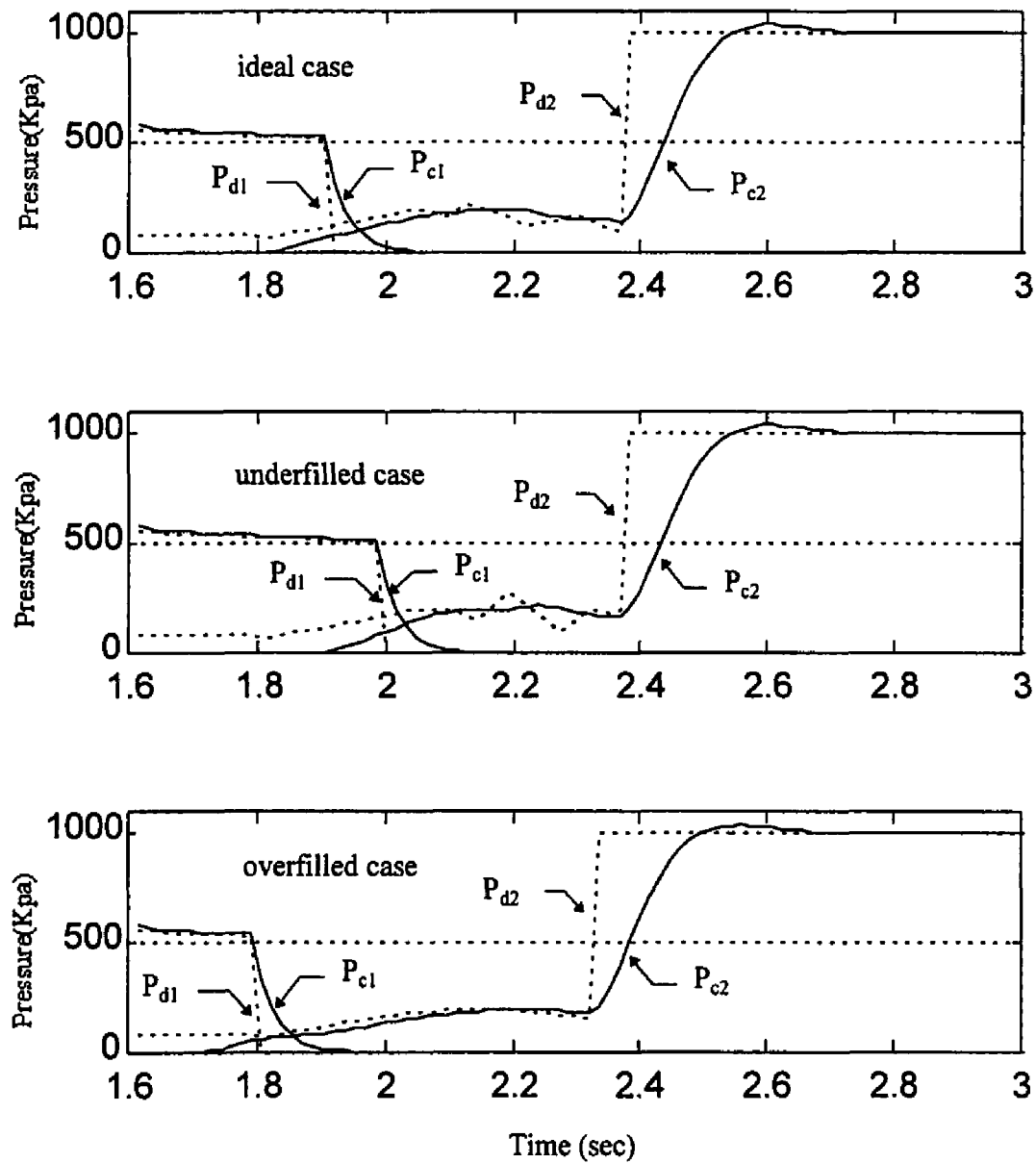


Figure 6.9 Clutch pressure commands (P_{d1} , P_{d2}) and actual pressures (P_{c1} , P_{c2}) during a 1-2 upshift using the Hybrid approach with acceleration estimated using Estimation Scheme A

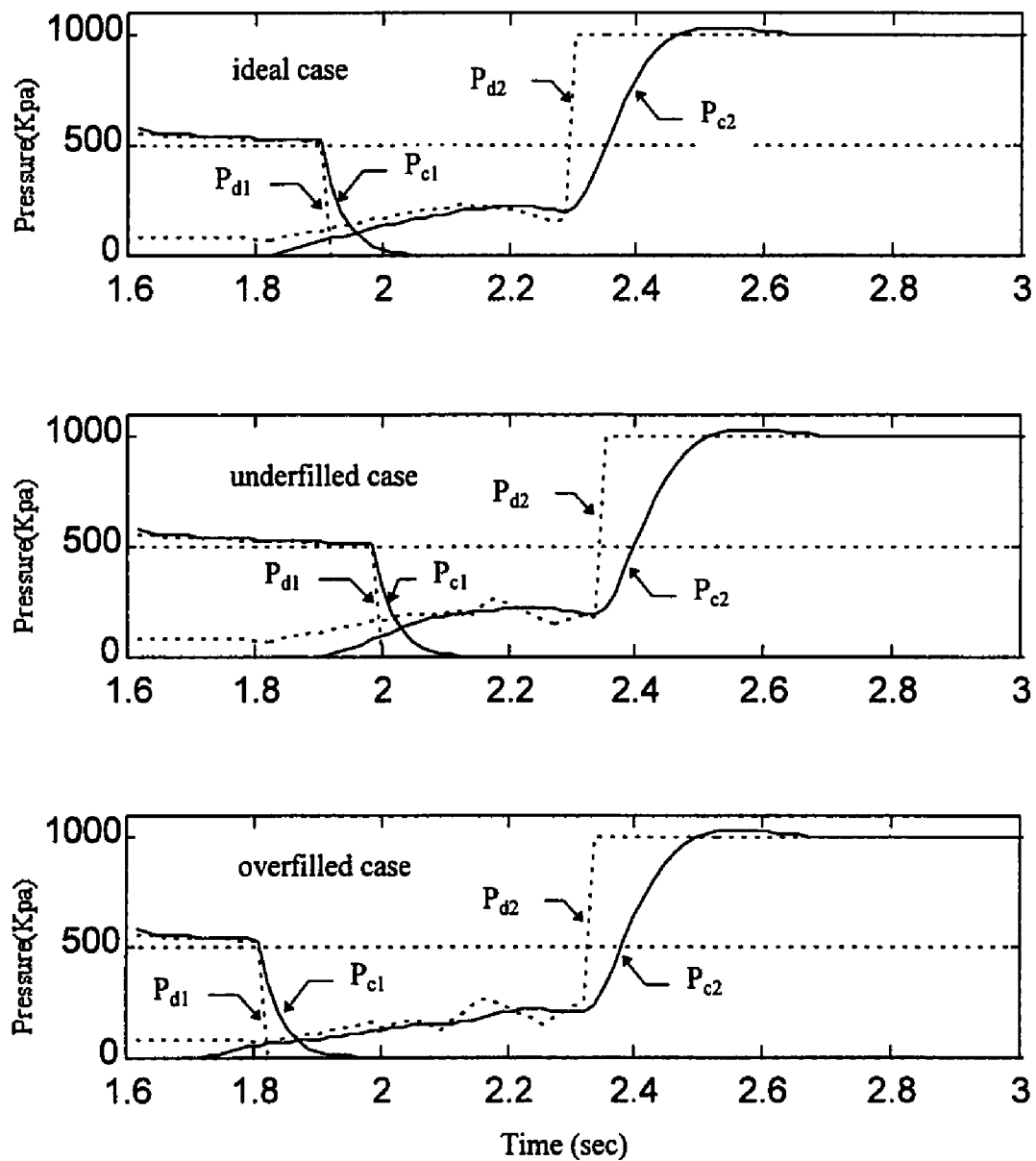


Figure 6.10 Clutch pressure commands (P_{d1} , P_{d2}) and actual pressures (P_{c1} , P_{c2}) during a 1-2 upshift using the Hybrid approach with acceleration estimated using Estimation Scheme B

7. CONCLUSIONS AND DISCUSSIONS

The achievements of this research can be summarized as follows:

1. A unique powertrain model for clutch-to-clutch shift is developed. This model includes the engine, the torque converter, the transmission, the driveline, and the actuators. A checking logic is designed to examine the lock-up conditions of the clutches and different sets of state equations are used for different modes of operation. This model can truly represent a clutch-to-clutch shift scenario.
2. A Hybrid controller combining the merits of a Rule-Based controller and a Robust Sliding Controller is developed for the transmission clutch-to-clutch shift control. The Rule-Based Module is used in the fill and torque phases to compensate for the actuator delay and inconsistency, and plant structure variations. The Sliding Mode Control Module is used in the speed phase to compensate for system modeling errors and external disturbances.
3. For the output-torque-based Sliding Control Module, Multiple Surface Sliding Control is used. Discrete-time implementation becomes an important issue when the control loop frequency is small relative to the system response frequency. A discrete-time Multiple Surface Sliding Control design method is developed for this kind of systems.
4. A Neural Network estimator is developed to identify the transmission input/output torques and the clutch frictional coefficients with speed signals as inputs. Promising results are shown through computer simulations. Limitations for practical application of this recurrent network are also identified.

5. Two acceleration estimation schemes are developed. It is proved that the proposed schemes can improve upon any base-line estimations and the lowest upper bound of the estimation error can be guaranteed. It is shown that these two schemes are very effective through the analysis of experimental data.
6. It is shown that (a) the proposed estimation schemes provided the Hybrid approach with good estimation of acceleration, (b) the acceleration-based Hybrid controller can achieve more robust performance comparing to two of the most recently developed transmission clutch-to-clutch control schemes.

Although this research presents good achievements, there are several issues worth studying further:

1. While the simulation results of the proposed Hybrid approach for the transmission clutch-to-clutch shift control are very promising, experimental validation of this approach will be valuable.
2. In the proposed acceleration estimation schemes, augmented first order low pass filters are used. The feasibility of using higher order or other types of low pass filters to enhance the performance should be studied.
3. In the developed acceleration estimation schemes, off-line tuning is used to choose the parameters for the fuzzy rules and controller. To advance the technology, learning methods [Chang, 1994; Wang et al., 1995] can be developed to on-line tune the parameters adaptively.

4. In the current Rule-Based Module, the trigger points are tuned off-line. Learning rules that can adjust trigger points adaptively should be explored to further enhance the robustness of the controller.

REFERENCES

Abutaleb, A. S., "An Adaptive Filter for Noise Canceling," *IEEE Trans. Cir. Syst., CAS-35*, pp. 1201-1209, 1988.

Alleyne, A., "Multiply Surface Sliding Control," *ASME Dynamic Systems and Control*, Vol. 1, pp. 93-99, 1994.

Ansley, C. F. and R. Kohn, "Efficient Generalized Cross-Validation for State-Space Methods," *Biometrika*, No. 74, pp. 139-148, 1987.

Belanger, P. R., "Estimation of Angular Velocity and Acceleration from Shaft Encoder Measurements," *Proc. of the 1992 IEEE Int. Conf. on Robotics and Automation*, pp. 585-592.

Bengio, Y., P. Simard, and P. Frasconi, "Learning Long-Term Dependencies with Gradient Descent is Difficult," *IEEE Transactions on Neural Networks*, pp 157-166, 1994.

Bershad, N. and P. Feintuch, "The Recursive Adaptive LMS filter - a line enhancer application and analytical model for mean weight behavior," *IEEE Trans. Acoustic, Speech, and Signal Processing.*, ASSP-28, pp. 652-660, 1980.

Butts, K. R., K. V. Hebbale, and K. W. Wang, *Acceleration-Based Control of Power-On Clutch-to-Clutch Upshifting in an Automatic Transmission*, US Patent 5,046,383, 1991.

Chang, S. H., *Adaptive Nonlinear Control Using Fuzzy Logic and Neural Network*, Ph.D. Dissertation, Department of Mechanical and Industrial Engineering, New Jersey Institute of Technology, 1994.

Cho, D. and J. K. Hedrick, "Sliding Mode Control of Automotive Powertrains with Uncertain Actuator Models," *Proc. of American Controls Conference*, pp. 1046-1052, 1989.

Cho, D. and J. K. Hedrick, "Automotive Powertrain Modeling for Control," *ASME Journal of Dynamic Systems, Measurement and Control*, Vol. 111, pp. 568-576, 1989.

Cruz, J. B. Jr.(Edit), *Feedback Systems*, McGraw-Hill Book Company, 1972.

Filev, D. P. and R. R. Yager, "Sliding Mode Design of Fuzzy Logic Controller," *ASME DSC-Vol. 55-1, Dynamic Systems and Control*, Vol. 1, 1994.

Fioretto, S. and L. Jetto, "Accurate Derivative Estimation from Noisy Data: a State Space Approach," *International Journal of System Science*, Vol. 20, No. 1, pp. 33-53, 1989.

Fioretto, S. and L. Jetto, "Low A Priori Statistical Information Model for Optimal Smoothing and Differentiation of Noisy Signals," *International Journal of Adaptive Control and Signal Processing*, Vol. 8, pp. 305-320, 1994.

Fioretti, S. and L. Jetto, "A Kalman Smoother for Numerical Differentiation," *Proc. Eight Ann. Conf. IEEE/Engineering in Medicine and Biology Society*, Fort Worth, TX, pp. 723-726, 1986.

Friedlander, B., "System Identification for Adaptive Noise Cancellation," *IEEE Trans. Acoustic, Speech, and Signal Processing.*, ASSP-30, pp. 699-708, 1982.

Gibson, J. D., T. R. Fisher, and B. Koo, "Estimation and Vector Quantization of Noisy Speech," *Proc. IEEE Int. Conf. on Acoustics, Speech, and Signal Processing*, New York, pp. 541-544, 1988.

Gibson, J. D., B. Koo, and S. D. Gray, "Filtering of Colored Noise for Speech Enhancement and Coding," *IEEE Trans. Signal Process.*, Sp-39, pp. 1732-1742, 1991.

Glitzenstein, K. and J. K. Hedrick, "Adaptive Control of Automotive Transmissions," *Proc. of American Controls Conference*, pp. 1849-1855, 1991.

Golub, G. M., M. Heath, and G. Wahba, "Generalized-cross Validation as a Method for Choosing a Good Ridge Parameter," *Technometrics*, No. 21, pp. 215-223, 1979.

Graven, P. and G. Wahba, "Smoothing Noisy Data with Spline Functions: Estimating the Correct Degree of Smoothing by the Method of Generalized Cross-Validation," *Numer. Math.*, No. 31, pp. 377-403, 1979.

Harrison, A. J. and C. A. McMahon, "Estimation of Acceleration from Data with Quantization Error Using Central Finite-Difference Methods," *Proc. of the Institute of Mechanical Engineers*, Vol. 207, pp. 77-86, 1993.

Hebbale, K. V., "A Mathematical Model of the Speed Measurement Process For Control System Simulation," pp. 517-524, DE-Vol. 40, *Advanced Automotive Technologies*, ASME 1991.

Hebbale, K. V. and Y. A. Ghoneim, "A Speed and Acceleration Estimation Algorithm for Powertrain Control," *Proc. of American Control Conference*, pp. 415-420, 1991.

Heinonen, P., T. Sarmaki, J. Malmivno, and Y. Neuvo, "Periodic Interference Rejection using Coherent Sampling and Waveform Estimation," *IEEE Trans. Cir. Syst., CAS-31*, pp. 438-446, 1984.

Horowitz, I. M., *Synthesis of Feedback Systems*, Academic Press, 1963.

Hrovat, D. and W. E. Tobler, "Bond Graph Modeling of Automotive Power Trains," *Journal of The Franklin Institute*, Vol. 328, No. 5, pp 623-662, 1991.

Hutchinson, M. F. and F. R. de Hoog, "Smoothing Noisy Data with Spline Functions," *Numer. Math.*, No. 1, pp. 47, 1985.

Hwang, Y. R. and M. Tomizuka, "Fuzzy Smoothing Algorithms for Variable Structure Systems," *IEEE Trans. Fuzzy Systems*, Vol. 2, no. 4, pp. 277-284, 1994.

Jetto, L., "Small Computer Procedure for Optimal Filtering of Haemodynamic Data," *Med. Bio. Eng. Comput.*, No. 23, pp. 203-208, 1985.

Jetto, L., "An Adaptive Kalman Filter for Haemodynamic Signals," *Proc. Digital Signal Processing - 87*, Firenze, 1987, pp. 568-572, Elsevier Science Pub. B. V., North-Holland, Amsterdam.

Kohn, R. and C. F. Ansley, "A New Algorithm for Spline Smoothing Based on a Stochastic Process," *SIAM J. Sci. Stat. Comput.*, No. 78, pp. 33-48, 1987.

Lanhammar, H., "On Practical Evaluation of Differentiation Techniques for Human Gait Analysis," *J. Biomech.*, No. 15, pp. 99-105, 1982a.

Lanhammar, H., "On Precision Limits for Derivatives Numerically Calculated from Noisy Data," *J. Biomech.*, No. 15, pp. 459-470, 1982b.

Leising, M. B., G. L. Holbrook, and H. L. Benford, "Adaptive Control Strategies for Clutch-to-Clutch Shifting," SAE Paper No. 905048, 1990.

Lesh, M. D., J. M. Mansour, and S. R. Simon, *Journal of Biomech. Engingeers*, pp. 10, 1979.

Leshno, M., V. Y. Lin, A. Pinkus, and S. Schocken, "Multilayer Feedforward Networks With a Nonpolynomial Activation Function Can Approximate Any Function," *Neural Networks*, Vol. 6, pp 861-867, 1993.

Luders, G. and K. S. Narendra, "An Adaptive Observer and Identifier for a Linear System," *IEEE Transactions on Automatic Control*, pp 496-499, 1973.

Malki, H. A., H. Li, and G. Chen, "New Design and Stability Analysis of Fuzzy Proportional-Derivative Control Systems," *IEEE Trans. on Fuzzy Systems*, Vol. 2, No. 4, pp. 245-254, 1994.

Meyer, J. E., S. E. Burke, and J. E. Hubbard, "Fuzzy-Sliding Mode Control for Vibration Damping of Flexible Structures," *SPIE Mathematics in Smart Structures*, Vol. 1919, pp. 182-193, 1993.

Misawa, E. A. and J. K. Hedrick, "Nonlinear Observers-A State-of-the-Art Survey," *ASME Journal of Dynamic Systems, Measurement, and Control*, Vol. 111, pp.344-352, 1989.

Palm, R., "Robust Control by Fuzzy Sliding Mode," *Automatica*, Vol. 30, No. 9, pp. 1429-1437, 1994.

Palival, K. K. and A. Basu, "A Speech Enhancement Method Based On Kalman Filtering," *Proc. IEEE Int. Conf. on Acoustics, Speech, and Signal Processing*, Dallas, TX, pp. 177-180, 1987.

Pezzack, J. C., R. W. Norman, and D. A. Winter, "An Assessment of Derivative determining techniques used for motion analysis," *J. Biomech.*, No. 10, pp. 377-382, 1977.

Ramachandra, K. V., "Optimum Steady State Position, Velocity, and Acceleration Estimation Using Noisy Sampled Position Data," *IEEE Trans. Aeros. Elec. Syst.*, pp. 705-708, 1987.

Sinha, N. K. and Rao, G.P. (edit), *Identification of Continuous-Time Systems*, Kluwer Academic Publishers, 1991.

Slotine, J-J. E. and W. Li, *Applied Nonlinear Control*, Prentice Hall, 1991.

Soudan, K. and P. Dierckx, "Calculation of Derivatives and Fourier Coefficients of human Motion Data, While Using Spline Functions," *J. Biomech.*, No. 12, pp. 21-26, 1979.

Speyer, J. L. and E. Z. Crues, "On-Line Aircraft State and Stability Derivative Estimation Using the Modified-Gain Extended Kalman Filter," *J. of Guidance, Control, and Dynamics*, Vol. 10, No. 3, pp. 262-268, 1987.

Tobler, W. E., *personal communication*.

Tugnait, J. K., "Constrained Signal Restoration via Iterated Kalman Filtering," *IEEE Trans. Acoust., Speech, and Signal Process.*, ASSP-33, pp. 472-475, 1985.

Tugcu, A. K., K. V. Hebbale, A. A. Alexandridis, and A. M. Karmel, "Modeling and Simulation of The Powertrain Dynamics of Vehicles Equipped with Automatic Transmission," *Symposium on Simulation and Control of Ground Vehicles and Transportation Systems*, pp. 39-61, 1986.

Utkin, V. I., *Sliding Modes in Control Optimization*, Springer-Verlag, 1992.

Wahba, G., "A Comparison of GCV and GML for Choosing the Smoothing Parameter in the Generalized Spline Smoothing Problem," *Ann. Stat.*, No. 13, pp. 1378-1402, 1985.

Walcott, B. L. and S. H. Zak, "State Observation of Nonlinear Uncertain Dynamical Systems," *IEEE Transactions on Automatic Control*, Vol. AC-32, No.2, pp 166-170, 1987.

Wang, C. H., W. Y. Wang, T. T. Lee, and P. S. Tseng, "Fuzzy B-Spline Membership Function (BMF) and Its Applications in Fuzzy-Neural Control," *IEEE Trans. Syst., Man, and Cyber.*, Vol. 25, No. 5, pp. 841-851, 1995.

Widrow, B. and S. D. Stearns, *Adaptive Signal Processing*, Englewood Cliffs, NJ, Prentice-Hall, 1985.

Wood, G. A. and L. S. Jennings, "On the Use of Spline Functions for Data Smoothing," *J. Biomech.*, pp. 477-479, 1979.

Xu, J. X., H. Hashimoto, J. J. E. Slotine, Y. Arai, and F. Harashima, "Implementation of VSS Control to Robotic Manipulators - Smoothing Modification," *IEEE Trans. Indus. Elec.*, Vol. 36, no. 3, pp. 321-329, 1989.

Ying, H., "Sufficient Conditions on General Fuzzy Systems as Function Approximators," *Automatica*, Vol. 30, No. 3, pp. 521-525, 1994.

Zeng, X. J. and M. G. Singh, "Approximation Theory of Fuzzy Systems-MIMI Case," *IEEE Trans. on Fuzzy Systems*, Vol. 3, No. 2, pp. 219-235, 1995.

Zeidler, J. R., E. H. Satorius, D. M. Chabries, and H.T. Wexler, "Adaptive enhancement of multiply sinusoids in uncorrelated noise," *IEEE Trans. Acoustic, Speech, and Signal Processing.*, ASSP-26, pp. 240-254, 1978.

Zernicke, R. F., G. Caldwell, and E. M. Roberts, "Fitting Biomechanical Data with cubic spline functions," *Res. Q.*, No. 47, pp. 9-19, 1976.

Zurada, J. M., *Introduction to Artificial Neural Systems*, West Publishing Company, pp. 133, 1992.

APPENDIX A. DERIVATION OF NEURAL NETWORK TRAINING

ALGORITHM

To illustrate the learning rule for training the network and determining the optimal weightings, a two layer feedforward network cascaded with a partially known system model (Fig. A.1) is used.

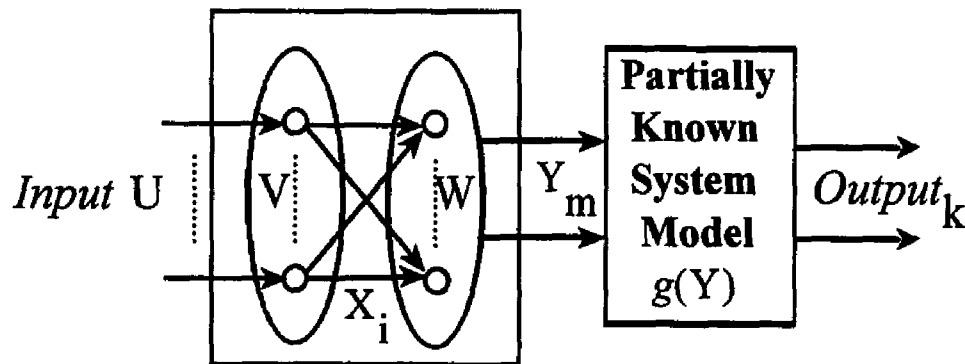


Figure A.1 Two layer feedforward Neural Network cascaded with partially known system model

Refer to Figure A.1, given N pairs of training input / training output for the network, the weightings V and W are tuned such that the sum of the weighted square difference (error) between the output and the training output is minimized. The output are computed from the stage equations (35)-(38). The equations are described as follows:

$$X_i(p) = f(\sum_j V_{ij} U_j(p))$$

$$Y_m(p) = f(\sum_i W_{mi} X_i(p))$$

$$Output_k(p) = g_k(Y(p))$$

where $p = 1 \dots N$ and the activation function $f(net)$ is described by

$$f(net) = \frac{1}{1 + \exp(-net)}$$

and

$$f'(net) = \frac{1}{2} f(net)(1 - f(net))$$

The error function is defined to be

$$E = \sum_{p=1}^N \sum_{k=1}^K \lambda(p) \cdot (Output_k(p) - Training Output_k(p))^2$$

where $\lambda(p) = \frac{1}{1 + 0.02 \times p}$ is the weighting function.

The objective again is to minimize E by tuning W and V.

By using the Gradient Descent method [Zurada, 1992], we can derive

$$\begin{aligned} \frac{\partial E}{\partial W_{mi}} &= \sum_{p=1}^N \sum_{k=1}^K \lambda(p) \cdot (Output_k(p) - Training Output_k(p)) \cdot \frac{\partial g_k(Y(p))}{\partial W_{mi}} \\ &= \sum_{p=1}^N \sum_{k=1}^K \lambda(p) \cdot (Output_k(p) - Training Output_k(p)) \cdot \sum_m \frac{\partial g_k(Y(p))}{\partial Y_m(p)} \frac{\partial Y_m(p)}{\partial W_{mi}} \\ &= \sum_{p=1}^N \sum_{k=1}^K \frac{\lambda(p)}{2} \cdot (Output_k(p) - Training Output_k(p)) \cdot \sum_m \frac{\partial g_k(Y(p))}{\partial Y_m(p)} Y_m(p)(1 - Y_m(p)) X_i \\ \frac{\partial E}{\partial V_{ij}} &= \sum_{p=1}^N \sum_{k=1}^K \lambda(p) \cdot (Output_k(p) - Training Output_k(p)) \cdot \frac{\partial g_k(Y(p))}{\partial V_{ij}} \\ &= \sum_{p=1}^N \sum_{k=1}^K \lambda(p) \cdot (Output_k(p) - Training Output_k(p)) \cdot \sum_m \frac{\partial g_k(Y(p))}{\partial Y_m(p)} \frac{\partial Y_m(p)}{\partial X_i} \frac{\partial X_i}{\partial V_{ij}} \end{aligned}$$

$$= \sum_{p=1}^N \sum_{k=1}^K \lambda(p) \cdot (\text{Output}_k(p) - \text{Training Output}_k(p)) \cdot \sum_m \frac{\partial g_k(Y(p))}{\partial Y_m(p)} W_{mi} X_i (1 - X_i) U_j$$

The updating of weighting can therefore be derived as follows

$$V_{ij, \text{new}} = V_{ij, \text{old}} - \alpha \cdot \frac{\partial E}{\partial V_{ij}}$$

$$W_{mi, \text{new}} = W_{mi, \text{old}} - \alpha \cdot \frac{\partial E}{\partial W_{mi}}$$

APPENDIX B. DISCRETE MULTIPLE SURFACE SLIDING CONTROL

B.1. Introduction and Problem Statement

Most of the researches on Sliding Control are on the design methods with only one sliding surface. The order of the surface depends on the relative degree of the systems where the relative degree is defined to be the order of the differentiation of the output required to obtain an explicit relationship between the output and the control input [Alleyne, 1994]. To control systems with high relative degree, such as in the transmission torque control example, high order derivatives of the output are needed.

In this Appendix, we will consider a class of systems with relative degrees greater than one

$$\begin{aligned}
 \dot{x}_1 &= f_1(x_1, x_{m+1}, \dots, x_n) + g_1(x_1, x_{m+1}, \dots, x_n)x_2 + \varepsilon_1 h_1(x_1, \dots, x_n) \\
 &\vdots \\
 \dot{x}_i &= f_i(x_1, \dots, x_i, x_{m+1}, \dots, x_n) + g_i(x_1, \dots, x_i, x_{m+1}, \dots, x_n)x_{i+1} + \varepsilon_i h_i(x_1, \dots, x_n) \quad (\text{B.1}) \\
 &\vdots \\
 \dot{x}_m &= f_m(x_1, \dots, x_m, x_{m+1}, \dots, x_n) + g_m(x_1, \dots, x_m, x_{m+1}, \dots, x_n)u \\
 \dot{X}_N &= F(X_N) + G(X_N) \cdot r \quad (\text{B.2})
 \end{aligned}$$

where $X_N = [x_{m+1}, \dots, x_n]^T$ and $X_m = [x_1, \dots, x_m]^T$ are the state vectors, r is the plant input, F , G , f_i 's, and g_i 's are nonlinear functions of states, and h_i 's represent the system

uncertainties. The goal is to design a control u such that x_1 will track a desired output trajectory x_{1d} .

In this Appendix, we consider a system composed of a continuous plant and a discrete-time controller. A design method for the digital controller using the Multiple Surface Sliding Control approach is developed. Sufficient conditions for implementing the proposed method and sufficient conditions for convergence of the tracking error are derived.

B.2. Discrete-Time Multiple Surface Sliding Control Design

Traditional sliding mode control design for systems with relative degree m greater than one usually requires a sliding surface with $(m-1)th$ derivatives of the control output and desired trajectory. This will need estimations of the $(m-1)th$ derivatives of the control output and desired trajectory. It is usually not easy or even possible to measure high order derivatives of output. Estimation of that using observable data is not accurate because the observed data is usually corrupted by noise. Multiple Surface Sliding Control design is another approach to achieve the control objective by satisfying m sliding conditions. For continuous system, many research results have been reported on this topic. However, discrete-time control for systems with relative degrees greater than one is still an issue to be investigated. In this section, we will design sliding surfaces and discrete-time control law based on the Bounded-Input-Bounded-Output (BIBO) criterion.

First, let us introduce the concept of δ - regulation.

Definition B.1 (Freeman and Kokotovic, 1993). For a given $\delta > 0$, if the trajectories of the states in equations (B.1) and (B.2) are globally uniformly ultimately bounded with respect to a compact residual set $\Omega \in R^n$ satisfying $x \in \Omega \Rightarrow |x_i| \leq \delta$, then the system is call δ - regulated.

We introduce the following assumptions for the system in the form of equations (B.1) and (B.2)

a) The estimated system dynamics $\hat{g}_i \neq 0$ and $\left| \frac{\Delta g_i}{\hat{g}_i} \right| \leq C_i < 1, \forall i = 1 \dots m$, where

$\Delta g_i = g_i - \hat{g}_i$ and C_i 's are positive constants.

b) The subsystem (B.2) is BIBO and input r is bounded.

c) \dot{x}_i is piecewise continuous.

It is worth noting that the above statement (a) means that the control direction is known and statement (c) means that the desired trajectory doesn't have jump discontinuity.

Before we introduce the design method, we will establish the condition for δ - regulation and the results will be used for the controller design.

Lemma B.1: If $S(t)$ satisfies the following conditions [Wang et al., 1994]

$$(a) S(t_k) \left(\int_{t_k}^t \dot{S}_i(t) dt \right) < \frac{-1}{2} \left(\int_{t_k}^t \dot{S}_i(t) dt \right)^2, \forall S(t_k) > \delta, t_{k+1} \geq t \geq t_k.$$

$$(b) -S(t_k) - \delta \leq \int_{t_k}^t \dot{S}_i(t) dt \leq -S(t_k) + \delta, \forall S(t_k) \leq \delta, t_{k+1} \geq t \geq t_k.$$

then there exists some t_p such that $|S(t)| \leq \delta, \forall t \geq t_p$.

Next, we will describe the discrete-time controller design procedure. With the desired output trajectory, the desired regulation bound, and the control loop time, we need to design $(m-1)$ desired trajectories for some of the states to form m sliding surfaces. The saturation function, the boundary layer, and the control gain are designed such that once the j -th tracking error is within the boundary layer, the $(j-1)$ th sliding condition will be satisfied. Finally, the control input is designed to satisfy the m -th sliding condition.

Discrete-Time Multiple Surface Sliding Control design procedure

Given a desired trajectory x_{1d} and desired upper bound δ_1 of the output tracking error, the goal is to design the control u such that x_1 will track x_{1d} . The first sliding surface is directly set up as $S_1 = x_1 - x_{1d}$.

Next, we will describe the procedure to set up $(m-1)$ sliding surfaces $S_i = x_i - x_{id}$ and desired trajectory x_{id} for $i = 2 \dots m$. We will also design sliding control gain k_i , boundary layer δ_i , and saturation function σ_i , for $i = 1 \dots m$. The following m -iteration five steps design procedure is used to synthesize the robust discrete-time control:

Step 1. Choose non-decreasing saturation functions σ_i satisfying $\sigma_i(0) = 0$. These functions should be smooth such that chatter of the response and control signal can be avoided.

Step 2. Estimate derivative of the i -th desired trajectory \hat{x}_{id} and the upper bound of the change of the rate of the desired trajectory, B_{1i} , such that $|\hat{x}_{id}^k - \hat{x}_{id}| < B_{1i}$, $t_{k+1} \geq t \geq t_k$.

Step 3. Estimate the upper bound of the change of the rate of the trajectory, B_{2i} , such that

$$|\dot{x}_i - \dot{x}_i^k| < B_{2i}, \quad t_{k+1} \geq t \geq t_k.$$

Step 4. Estimate the upper bound of the system dynamics uncertainties and external

noise, B_{3i} , such that $\left| \Delta f_i^k + \varepsilon_i h_i^k + \frac{\Delta g_i^k}{\hat{g}_i^k} (\hat{x}_{i,d}^k - f_i^k) \right| < B_{3i}$, where $\Delta f_i = f_i - \hat{f}_i$.

Step 5. Determine the boundary layer for $(i+1)th$ sliding surface, δ_{i+1} , such that

$$\begin{cases} \frac{\delta_i}{\Delta t} > \frac{1}{(1-C_i)} (B_{1i} + B_{2i} + B_{3i} + |g_i^k \delta_{i+1}|) & \forall i = 1 \dots m-1 \\ \frac{\delta_i}{\Delta t} > \frac{1}{(1-C_i)} (B_{1i} + B_{2i} + B_{3i}) & \forall i = m \end{cases} \quad (B.3)$$

If equation (B.3) cannot be satisfied by choosing δ_{i+1} , then δ_1 -regulation cannot be achieved. A bigger upper bound δ_1 or a smaller control loop time Δt is needed. If equation (B.3) can be satisfied, then determine control gain k_i and desired trajectory $x_{i+1,d}$ for $(i+1)th$ sliding surface such that if $i < m$

$$\begin{aligned} \frac{1}{(1-C_i)\sigma_i(\delta_i)} [B_{1i} + B_{2i} + B_{3i} + |g_i^k \delta_{i+1}|] < k_i < \\ \frac{1}{(1+C_i)\sigma_i(\delta_i)} \left[\frac{2\delta_i}{\Delta t} - B_{1i} - B_{2i} - B_{3i} - |g_i^k \delta_{i+1}| \right] \end{aligned} \quad (B.4)$$

$$x_{i+1,d} = \frac{1}{\hat{g}_i} \left[\hat{x}_{i,d} - k_i \sigma_i(s_i) - \hat{f}_i \right] \quad (B.5)$$

and if $i = m$

$$\begin{aligned} \frac{1}{(1-C_m)\sigma_m(\delta_m)} [B_{1m} + B_{2m} + B_{3m}] < k_m < \\ \frac{1}{(1+C_m)\sigma_m(\delta_m)} \left[\frac{2\delta_m}{\Delta t} - B_{1m} - B_{2m} - B_{3m} \right] \end{aligned} \quad (B.6)$$

$$u = \frac{1}{\hat{g}_m} \left[\hat{x}_{md} - k_m \sigma_m(s_m) - \hat{f}_m \right] \quad (\text{B.7})$$

where $x^k = x(t_k)$ and “^” indicates estimated values.

Next we will show that design step 5 can be achieved if and only if equation (B.3) is satisfied.

In order to calculate k_i in design step 5, the following equation must be satisfied,

$$\frac{1}{1 - C_i} (B_{1i} + B_{2i} + B_{3i} + |g_i^k \delta_{i+1}|) < \frac{1}{1 + C_i} \left(\frac{2\delta_i}{\Delta t} - B_{1i} - B_{2i} - B_{3i} - |g_i^k \delta_{i+1}| \right) \quad (\text{B.8})$$

we can verify directly that the above equation can be satisfied if and only if the following equation can be satisfied,

$$\frac{\delta_i}{\Delta t} > \frac{1}{(1 - C_i)} (B_{1i} + B_{2i} + B_{3i} + |g_i^k \delta_{i+1}|)$$

Following the controller design procedure, the convergence condition (a) in Lemma B.1 will be satisfied, that is, the $(j-1)$ th sliding condition will be satisfied if j -th tracking error is within the boundary layer. Next, we will describe the sufficient condition for the satisfying of convergence condition (b) in Lemma B.1. In Theorem B.1, it will be proved that if the stated sufficient condition is satisfied, then the system described by equations (B.1) and (B.2) will be “ δ - regulated” with the designed discrete-time controller.

Theorem B.1. Consider the system described by equation (B.1) and (B.2) and the control designed from the design steps, if the following conditions are satisfied

$$\frac{1}{\Delta t} \geq k_i \cdot \frac{\partial \sigma_i}{\partial s_i} \quad \forall s_i \in [-\delta_i, \delta_i], \quad i = 1 \dots m \quad (\text{B.9})$$

then there is some t_p such that $|x_1(t) - x_{1d}(t)| \leq \delta_1$, $\forall t \geq t_p$, where Δt is the control loop time and δ_1 is the desired bound of the output tracking error.

Proof:

Using equation (B.1), (B.2), and controller design step 5,

$$\begin{aligned} \dot{S}_i &= \dot{x}_i - \dot{x}_{id} = (\dot{x}_i^k - \dot{\hat{x}}_{id}^k) + (\dot{x}_i - \dot{x}_i^k) + (\dot{\hat{x}}_{id}^k - \dot{x}_{id}) \\ &= -k_i \sigma_i(s_i^k) + \Delta f_i^k + \Delta g_i^k x_{i+1,d}^k + \varepsilon_i h_i^k + g_i^k S_{i+1}^k + (\dot{x}_i - \dot{x}_i^k) + (\dot{\hat{x}}_{id}^k - \dot{x}_{id}) \\ &= -(1 + \frac{\Delta g_i^k}{\hat{g}_i^k}) k_i \sigma_i(s_i^k) + [\Delta f_i^k + \varepsilon_i h_i^k + \frac{\Delta g_i^k}{\hat{g}_i^k} (\dot{\hat{x}}_{id}^k - f_i^k)] + g_i^k S_{i+1}^k + (\dot{x}_i - \dot{x}_i^k) + (\dot{\hat{x}}_{id}^k - \dot{x}_{id}) \end{aligned}$$

From controller design step 2, step 3, step 4, and above equation,

$$\begin{aligned} -(1 + \frac{\Delta g_i^k}{\hat{g}_i^k}) k_i \sigma_i(s_i^k) + g_i^k S_{i+1}^k - B_{1i} - B_{2i} - B_{3i} < \dot{S}_i < \\ &-(1 + \frac{\Delta g_i^k}{\hat{g}_i^k}) k_i \sigma_i(s_i^k) + g_i^k S_{i+1}^k + B_{1i} + B_{2i} + B_{3i} \end{aligned} \quad (B.10)$$

Next we will show that with control designed from the design steps, the system described by equation (B.1) and (B.2) will be δ_1 -regulated if condition (B.9) is satisfied.

Three different cases are discussed for three different situations of the sliding surfaces:

Case A. $|S_{i+1}^k| \leq \delta_{i+1}$, $|S_i^k| > \delta_i$, $S_i^k < 0$

From controller design step 5 and equation (B.10),

$$\begin{aligned} 0 \leq -(1 + \frac{\Delta g_i^k}{\hat{g}_i^k}) k_i \sigma_i(s_i^k) + g_i^k S_{i+1}^k - B_{1i} - B_{2i} - B_{3i} < \dot{S}_i \\ < -(1 + \frac{\Delta g_i^k}{\hat{g}_i^k}) k_i \sigma_i(s_i^k) + g_i^k S_{i+1}^k + B_{1i} + B_{2i} + B_{3i} \leq -2 \frac{S_i^k}{\Delta t} \end{aligned}$$

Integrating above equation,

$$0 < \int_k^t \dot{S}_i(\tau) d\tau < -2S_i^k$$

Case B. $|S_{i+1}^k| \leq \delta_{i+1}$, $|S_i^k| > \delta_i$, $S_i^k > 0$

From controller design step 5 and equation (B.10),

$$\begin{aligned} -2\frac{S_i^k}{\Delta t} &\leq -(1 + \frac{\Delta g_i^k}{\hat{g}_i^k})k_i\sigma_i(s_i^k) + g_i^k S_{i+1}^k - B_{1i} - B_{2i} - B_{3i} < \dot{S}_i \\ &< -(1 + \frac{\Delta g_i^k}{\hat{g}_i^k})k_i\sigma_i(s_i^k) + g_i^k S_{i+1}^k + B_{1i} + B_{2i} + B_{3i} \leq 0 \end{aligned}$$

Integrating above equation,

$$-2S_i^k < \int_k^t \dot{S}_i(\tau) d\tau < 0$$

Case C. $|S_{i+1}^k| \leq \delta_{i+1}$, $|S_i^k| \leq \delta_i$

From controller design step 5, equation (B.10), (B.3), and (B.9),

$$\begin{aligned} \frac{-S_i^k - \delta_i}{\Delta t} &\leq -(1 + \frac{\Delta g_i^k}{\hat{g}_i^k})k_i\sigma_i(s_i^k) + g_i^k S_{i+1}^k - B_{1i} - B_{2i} - B_{3i} \leq \dot{S}_i \\ &\leq -(1 + \frac{\Delta g_i^k}{\hat{g}_i^k})k_i\sigma_i(s_i^k) + g_i^k S_{i+1}^k + B_{1i} + B_{2i} + B_{3i} \leq \frac{-S_i^k + \delta_i}{\Delta t} \end{aligned}$$

Integrating above equation, we will get that

$$-S_i^k - \delta_i \leq \int_k^t \dot{S}_i(\tau) d\tau \leq -S_i^k + \delta_i$$

From above discussions and Lemma B.1, $(j-1)$ th sliding condition will be satisfied if j -th

tracking error is within the boundary layer, that is, $|S_i^k| \rightarrow \delta_i$ if $|S_{i+1}^k| \leq \delta_{i+1}$. Also from

controller design step 5, the m -th sliding condition is satisfied, that is, $|S_m^k| \rightarrow \delta_i$. Using induction, there is some t_p such that $|S_1(t)| \leq \delta_i$ for $t \geq t_p$.

Lemma B.2: The condition (B.3) can be rewritten as follows,

$$\frac{\delta_q}{\Delta t} > \sum_{i=q+1}^m \left[\left(\prod_{p=q}^i \frac{1}{1-C_p} \right) \left(\prod_{p=q}^{i-1} |g_p| \right) \left(\sum_{j=1}^3 B_{ji} \right) \right] + \frac{1}{1-C_q} \left(\sum_{j=1}^3 B_{jq} \right) \quad \forall q = 1..m \quad (\text{B.11})$$

Proof:

(Omitted, it can be verified directly from condition (B.3))

Remark B.1. Conditions (B.3) (or (B.11)), and (B.9) indicate that for continuous-time system, using continuous control can achieve δ - regulation for any non-zero bound δ . However, with discrete-time control, when the system changing rate or uncertainties are large, the control loop time needs to be significantly small to preserve the tracking performance.

B.3. References

Wang, W. J., G. H. Wu, and D. C. Yang, "Variable Structure Control Design for Uncertain Discrete-Time Systems," *IEEE Trans. Automatic Control*, AC-39, pp. 99-102, 1994.

APPENDIX C. ACCELERATION ESTIMATION SCHEMES

In this Appendix, theorems for the proposed acceleration estimators are derived. The Estimation Scheme A shown in Figure 5.1 will be discussed in Theorem C.3. It is proved that the maximum estimation error is bounded and the estimation will always improve upon the base-line estimation if certain condition is satisfied. The Estimation Scheme B shown in Figure 5.2 is described in Theorem C.4. It is proved that the estimation with the bandwidth adapter will always be better than that without it if certain conditions are satisfied.

The following derivations in this Appendix will be derived based on the expression of signals in Fourier series. The approximation property of Fourier series is introduced in Lemma C.1. Some properties of first order low pass filters are discussed in Lemma C.2-C.4.

Lemma C.1. If $x(t) \in C^1(T)$, its Fourier series, $\sum c_n s_n(t)$, converges uniformly to x , where $C^n(T) \equiv \{x(t) | t \in T, x(t) \text{ is continuous and has continuous } n\text{-th derivative}\}$, n is an integer, $s_0(t)=1$, $s_i(t)=\sin(\omega_i t)$ if i is odd, $s_i(t)=\cos(\omega_i t)$ if i is even, and $T=[t_0, t_0+\Delta T]$.

Lemma C.2. For low pass filter $g=a/(s+a)$, there exists constant gains $K_{gi} = a^2 / (\omega_i^2 + a^2)$ and $K'_{gi} = (-1)^i a \omega_i / (\omega_i^2 + a^2)$, such that $g * s_i(t) = K_{gi} s_i(t) + K'_{gi} s'_i(t)$ when $t \rightarrow \infty$, where $s'_i = s_{i-1}$ if i is even, $s'_i = s_{i+1}$ if i is odd.

Lemma C.3. For low pass filter $g = a/(s+a)$, $|g * x(t)| \leq |g * \varepsilon|$ if $|x(t)| \leq |\varepsilon|$.

Assumptions of band-limit and bounded of the signals are introduced in

Assumption C.1.

Assumption C.1.

$$\text{a) } \dot{v}(t) = \sum_{i=0}^{2N} \dot{v}_i s_i(t) \in V, \quad \dot{w}(t) = \sum_{i=2N+1}^{\infty} \dot{w}_i s_i(t) \in W, \quad \sum_{i=0}^{2N} |\dot{v}_i| \leq M_1, \text{ and}$$

$$\sum_{i=2N+1}^{\infty} |\dot{w}_i| \leq M_2, \text{ where } W \text{ and } V \text{ are defined as follows,}$$

$$V \equiv \left\{ x(t) = \sum c_i s_i(t) \mid t \in T, 0 < \delta_0 \leq K_{g_i} \leq 1 \right\}$$

$$= \left\{ x(t) = \sum_{i=0}^{2N} c_i s_i(t) \mid t \in T, K_{g_i} \geq \delta_0 \right\}$$

$$W \equiv \left\{ x(t) = \sum c_i s_i(t) \mid t \in T, 0 < K_{g_i} < \delta_0 \right\}$$

$$= \left\{ x(t) = \sum_{i=2N+1}^{\infty} c_i s_i(t) \mid t \in T, K_{g_i} < \delta_0 \right\}$$

$$\text{b) } u = u_v + u_w, u_v = \sum_{i=0}^{2N} u_{vi} s_i \in V, u_w = \sum_{i=2N+1}^{\infty} u_{wi} s_i \in W, \sum_{i=0}^{2N} |u_{vi}| < M_3, \sum_{i=2N+1}^{\infty} |u_{wi}| < M_4$$

$$\text{c) } \tilde{A} = \tilde{A}_v + \tilde{A}_w, \tilde{A}_v = \sum_{i=0}^{2N} \tilde{A}_{vi} s_i \in V, \tilde{A}_w = \sum_{i=2N+1}^{\infty} \tilde{A}_{wi} s_i \in W$$

$$, \sum_{i=0}^{2N} |\tilde{A}_{vi}| < M_5, \sum_{i=2N+1}^{\infty} |\tilde{A}_{wi}| < M_6$$

The following paragraphs will describe the proof of Theorem C.1-C.4. In order to describe the results for the estimation schemes in Theorem C.3 and Theorem C.4, we will derive the system equations for the systems shown in Figure 5.1 and Figure 5.2 in

Theorem C.1. Also, the lowest upper bound of the tracking error for systems with feedback signal uncertainties is needed, which is derived in Theorem C.2.

Generic system equations for these two schemes will be derived and rewritten in different forms in Theorem C.1. Upper bound of some of states will also be derived.

Theorem C.1. Consider the schematics shown in Figure 5.1 and Figure 5.2, the system is described by the following equations,

$$\dot{e}(t) = -ae(t) + a[\hat{A} - \dot{v} - \dot{w}] \quad (C.1)$$

$$f: \dot{A}'(t) = -c(t)A'(t) + c(t)\tilde{A}(t) \quad (C.2)$$

where v is the speed signal, w is the noise, $\hat{A}(t) = A'(t) + u(t)$, f is a function of $c(t)$, $A'(t_0)$ and $e(t_0)$ are initial conditions, and $0 < c_{min} \leq c(t) \leq c_{max}$. Uniqueness of the solutions is assumed.

(a) The equations (C.1)-(C.2) can be rewritten as follows,

$$\dot{e}(t) = -ae(t) + a \left[\sum_i (K_{f_i}(c) \tilde{A}_i s_i(t) + K'_{f_i}(c) \tilde{A}_i s'_i(t)) - \dot{v} - \dot{w} + \varepsilon_f + u \right] \quad (C.3)$$

$$\dot{\varepsilon}_f(t) = -c(t)\varepsilon_f(t) - \sum_i \dot{K}_{f_i}(c) \tilde{A}_i s_i(t) - \sum_i \dot{K}'_{f_i}(c) \tilde{A}_i s'_i(t) \quad (C.4)$$

where

$$\varepsilon_f(t_0) = A'(t_0) - \sum_i (K_{f_i}(c) \tilde{A}_i s_i(t_0) + K'_{f_i}(c) \tilde{A}_i s'_i(t_0)) \quad (C.5)$$

$$\hat{A}(t) = \sum_i (K_{f_i}(c) \tilde{A}_i s_i(t) + K'_{f_i}(c) \tilde{A}_i s'_i(t)) + \varepsilon_f + u \quad (C.6)$$

$$K_{f_i} = c^2 / (\omega_i^2 + c^2) \quad (C.7)$$

$$K'_f = (-1)^i c \omega_i / (\omega_i^2 + c^2) \quad (\text{C.8})$$

(b) The equations (C.3)-(C.8) can be rewritten as follows,

$$\dot{e}_1(t) = -ae_1(t) + a \left[\sum_{i=0}^{2N} (K_{f_i}(c) \tilde{A}_i s_i(t) + K'_{f_i}(c) \tilde{A}_i s'_i(t)) - \dot{v} + u_v \right] \quad (\text{C.9})$$

$$\dot{e}_2(t) = -ae_2(t) + a \left[\sum_{i=2N+1}^{\infty} (K_{f_i}(c) \tilde{A}_i s_i(t) + K'_{f_i}(c) \tilde{A}_i s'_i(t)) - \dot{w} + u_w \right] \quad (\text{C.10})$$

$$\dot{e}_3(t) = -ae_3(t) + a \varepsilon_f \quad (\text{C.11})$$

$$\dot{\varepsilon}_f(t) = -c(t) \varepsilon_f(t) - \sum_i \dot{K}_{f_i}(c) \tilde{A}_i s_i(t) - \sum_i \dot{K}'_{f_i}(c) \tilde{A}_i s'_i(t) \quad (\text{C.12})$$

and $e(t) = e_1(t) + e_2(t) + e_3(t)$.

(c) The solutions of (C.9)-(C.12) can be described as follows,

$$\begin{aligned} e_1(t) = & \sum_{i=0}^{2N} K_{g_i} [K_{f_i}(c) \tilde{A}_i - \dot{v}_i + u_{v_i}] s_i(t) + \sum_{i=0}^{2N} K'_{g_i} [K_{f_i}(c) \tilde{A}_i - \dot{v}_i + u_{v_i}] s'_i(t) \\ & + \sum_{i=0}^{2N} K_{g_i} K'_{f_i}(c) \tilde{A}_i s'_i(t) - \sum_{i=0}^{2N} K'_{g_i} K_{f_i}(c) \tilde{A}_i s_i(t) + \varepsilon_{f1} = K_G (\hat{A} - \dot{v}) + e_4(t) \end{aligned} \quad (\text{C.13})$$

$$\begin{aligned} e_2(t) = & \sum_{i=2N+1}^{\infty} K_{g_i} [K_{f_i}(c) \tilde{A}_i - \dot{w}_i + u_{w_i}] s_i(t) + \sum_{i=2N+1}^{\infty} K'_{g_i} [K_{f_i}(c) \tilde{A}_i - \dot{w}_i + u_{w_i}] s'_i(t) \\ & + \sum_{i=2N+1}^{\infty} K_{g_i} K'_{f_i}(c) \tilde{A}_i s'_i(t) - \sum_{i=2N+1}^{\infty} K'_{g_i} K_{f_i}(c) \tilde{A}_i s_i(t) + \varepsilon_{f2} \end{aligned} \quad (\text{C.14})$$

$$e_3(t) = g(t - t_o) (e(t_o) - e_1(t_o) - e_2(t_o)) + \int_{t_o}^t g(t - \tau) \varepsilon_f(\tau) d\tau \quad (\text{C.15})$$

where

$$\varepsilon_{f1}(t) = - \int_{t_o}^t g(t - \tau) \left[\sum_{i=0}^{2N} K_{g_i} \dot{K}_{f_i}(c) \tilde{A}_i s_i(\tau) + \sum_{i=0}^{2N} K'_{g_i} \dot{K}'_{f_i}(c) \tilde{A}_i s'_i(\tau) \right]$$

$$+ \sum_{i=0}^{2N} K_{g_i} \dot{K}'_{f_i}(c) \tilde{A}_i s'_i(\tau) - \sum_{i=0}^{2N} K'_{g_i} \dot{K}_{f_i}(c) \tilde{A}_i s_i(\tau)] d\tau \quad (C.16)$$

$$\begin{aligned} \varepsilon_{f_2}(t) = & - \int_{t_0}^t g(t-\tau) \left[\sum_{i=2N+1}^{\infty} K_{g_i} \dot{K}_{f_i}(c) \tilde{A}_i s_i(\tau) + \sum_{i=2N+1}^{\infty} K'_{g_i} \dot{K}'_{f_i}(c) \tilde{A}_i s'_i(\tau) \right. \\ & \left. + \sum_{i=2N+1}^{\infty} K_{g_i} \dot{K}'_{f_i}(c) \tilde{A}_i s'_i(\tau) - \sum_{i=2N+1}^{\infty} K'_{g_i} \dot{K}_{f_i}(c) \tilde{A}_i s_i(\tau) \right] d\tau \end{aligned} \quad (C.17)$$

$$\begin{aligned} e_4(t) = & \sum_{i=0}^{2N} (K_{g_i} - K_G) [K_{f_i}(c) \tilde{A}_i - \dot{v}_i + u_{v_i}] s_i(t) + \sum_{i=0}^{2N} K'_{g_i} [K_{f_i}(c) \tilde{A}_i - \dot{v}_i + u_{v_i}] s'_i(t) \\ & + \sum_{i=0}^{2N} (K_{g_i} - K_G) K'_{f_i}(c) \tilde{A}_i s'_i(t) - \sum_{i=0}^{2N} K'_{g_i} K_{f_i}(c) \tilde{A}_i s_i(t) + (1 - K_G) \varepsilon_{f_1} \\ & - K_G \sum_{i=2N+1}^{\infty} [(K_{f_i}(c) \tilde{A}_i + u_{w_i}) s_i(t) + K'_{f_i}(c) \tilde{A}_i s'_i(t)] \end{aligned} \quad (C.18)$$

(d) The upper bounds of some the solutions can be described as follows,

$$|\varepsilon_f(t)| \leq |\varepsilon_f(t_0) \exp(-c_{\min}(t-t_0))| + \frac{3|\dot{c}|_{\max}}{4c_{\min}} (M_5 + M_6) \quad (C.19)$$

$$|\varepsilon_{f_1}(t)| \leq \frac{9|\dot{c}|_{\max}}{8c_{\min}} M_5 \quad (C.20)$$

$$|\varepsilon_{f_2}(t)| \leq \frac{3|\dot{c}|_{\max}}{2c_{\min}} \cdot \delta_o \cdot M_6 \quad (C.21)$$

$$|e_2(t)| \leq \left(\frac{a^2}{\omega_{2N+1}^2 + a^2} + \frac{1}{2} \right) \cdot (M_2 + M_4 + \frac{c_{\max}^2}{\omega_{2N+1}^2 + c_{\max}^2} M_6 + \frac{1}{2} M_6) + |\varepsilon_{f_2}(t)| \quad (C.22)$$

$$|e_3(t)| \leq |e_3(t_0) g(t-t_0)| + |\varepsilon_f(t_0) \exp(-c_{\min}(t-t_0))| + \frac{3|\dot{c}|_{\max}}{4c_{\min}} (M_5 + M_6) \quad (C.23)$$

Proof:

(a) Assume $A'(t) = \sum_i [K_{fi}(c)\tilde{A}_i s_i(t) + K'_{fi}(c)\tilde{A}_i s'_i(t)] + \varepsilon_f$ and substitute into equation

(C.2), by using Lemma C.2,

$$\dot{\varepsilon}_f(t) = -c(t)\varepsilon_f(t) - \sum_i \dot{K}_{fi}(c)\tilde{A}_i s_i(t) - \sum_i \dot{K}'_{fi}(c)\tilde{A}_i s'_i(t)$$

$$\varepsilon_f(t_0) = A'(t_0) - \sum_i (K_{fi}(c)\tilde{A}_i s_i(t_0) + K'_{fi}(c)\tilde{A}_i s'_i(t_0))$$

(b) We can easily verify that the solution satisfying equations (C.9)-(C.12) will satisfy equations (C.3)-(C.8) and vice versa. That is, they have the same solution.

(c) Assume $e_1(t)$ and $e_2(t)$ can be expressed as in equation (C.13)-(C.14), and substitute into equation (C.9) and (C.10), we can get

$$\begin{aligned} \dot{\varepsilon}_{f1}(t) &= -a\varepsilon_{f1}(t) - \sum_{i=0}^{2N} K_{gi} \dot{K}_{fi}(c)\tilde{A}_i s_i(t) - \sum_{i=0}^{2N} K'_{gi} \dot{K}'_{fi}(c)\tilde{A}_i s'_i(t) \\ &\quad - \sum_{i=0}^{2N} K_{gi} \dot{K}'_{fi}(c)\tilde{A}_i s'_i(t) + \sum_{i=0}^{2N} K'_{gi} \dot{K}_{fi}(c)\tilde{A}_i s_i(t) \\ \dot{\varepsilon}_{f2}(t) &= -a\varepsilon_{f2}(t) - \sum_{i=2N+1}^{\infty} K_{gi} \dot{K}_{fi}(c)\tilde{A}_i s_i(t) - \sum_{i=2N+1}^{\infty} K'_{gi} \dot{K}'_{fi}(c)\tilde{A}_i s'_i(t) \\ &\quad - \sum_{i=2N+1}^{\infty} K_{gi} \dot{K}'_{fi}(c)\tilde{A}_i s'_i(t) + \sum_{i=2N+1}^{\infty} K'_{gi} \dot{K}_{fi}(c)\tilde{A}_i s_i(t) \\ \dot{\varepsilon}_3(t) &= -a\varepsilon_3(t) + a\varepsilon_f \end{aligned}$$

and equations (C.13)-(C.18) can be verified directly.

(d) Consider equation (C.12), assume $\varepsilon_f(t) = \varepsilon_{fh}(t) + \varepsilon_{fp}(t)$, we can easily verify that the homogeneous solution

$$\varepsilon_{fh}(t) = \varepsilon_f(t_0) - \int_{t_0}^t c(\tau)\varepsilon_{fh}(\tau)d\tau$$

and the particular solution

$$\varepsilon_{fp}(t) = \varepsilon_{fp}(t) \int_{t_0}^t \varepsilon_{fp}^{-1}(\tau) \left[\sum_i \dot{K}_{fi}(c(\tau)) \tilde{A}_i s_i(\tau) + \sum_i \dot{K}'_{fi}(c) \tilde{A}_i s'_i(\tau) \right] d\tau$$

$$\varepsilon_{fp}(t) = 1 - \int_{t_0}^t c(\tau) \varepsilon_{fp}(\tau) d\tau$$

From equations (C.7)-(C.8), we will get that

$$\dot{K}_{fi} = \omega_i^2 2c\dot{c} / (\omega_i^2 + c^2)^2 \quad (C.24)$$

$$\dot{K}'_{fi} = (-1)^i \dot{c} \omega_i (\omega_i^2 - c^2) / (\omega_i^2 + c^2)^2 \quad (C.25)$$

By using above equations and Lemma C.3, the upper bound of the solutions can be verified directly.

Some properties of low pass filters are described in the following lemma.

Lemma C.4. For low pass filter $g : \dot{e}(t) = -a \cdot e(t) + a u(t)$, if $u(t) = \sum_{i=0}^{2N} u_i s_i(t) \in \mathcal{V}$, then

$$e(t) = g(t - t_o)(e(t_o) - \sum_{i=0}^{2N} u_i (K_{gi} s_i(t_o) + K'_{gi} s'_i(t_o)))$$

$$+ K_G u(t) + \sum_{i=0}^{2N} u_i [(K_{gi} - K_G) s_i(t) + K'_{gi} s'_i(t)] \quad (C.26)$$

Before we introduce the main result for Estimation Scheme A (shown in Figure 5.1) in Theorem C.3, we will derive the lowest upper bound of the tracking error for systems with measurement uncertainties. The result will be used in Theorem C.3 to design a feedback control such that the lowest upper bound of the tracking error can be achieved and high frequency control signal can be minimized.

Theorem C.2. Given a system described by the following equations

$$\dot{e}_1(t) = -a e_1(t) + a[u(t) - \dot{v}(t)] \quad (\text{C.27})$$

$$e(t) = e_1(t) + \psi(t) \quad (\text{C.28})$$

or

$$\dot{e}_1(t) = -a e_1(t) + a[u(t) - \dot{v}(t)] \quad (\text{C.29})$$

$$\dot{e}_2(t) = -a e_2(t) - a\dot{w}(t) \quad (\text{C.30})$$

$$e(t) = e_1(t) + e_2(t) \quad (\text{C.31})$$

the objective is to drive $e_1(t)$ to zero using control input $u(t)$, where $e(t)$ is the measurable feedback signal and $w(t)$ is unmeasurable high frequency noise. If $|\psi(t)| \leq \delta_o$ (or $|e_2(t)| \leq \delta_o$), then

(a) the lowest upper bound of $|e_1(t)|$, $\delta \geq \delta + \delta_o$ and the lowest upper bound of $|e(t)|$ is δ_o .

(b) in order to avoid high frequency chatter of the control signal, the control objective and feedback signal can be defined as

$$\text{fuzzy}(e(t)) = \left[\sum_j W_j \cdot \text{Mem}_j^u(e) \right] \cdot e(t) \quad (\text{C.32})$$

The lowest upper bound of the tracking error can be guaranteed by designing the control

$$u(t) = -K_p \cdot \text{fuzzy}(e(t)) \quad (\text{C.33})$$

where $\text{fuzzy}(e)$ is a monotonous function of e and

$$K_p \cdot |\text{fuzzy}(e)|_{|e(t)| \geq \delta} \geq |\dot{v}|_{\max} \quad (\text{C.34})$$

Proof:

(a) Assume $u(t) \cdot \text{sign}(e(t)) \leq 0$, then

$$e_1 \dot{e}_1(t) = -a[e_1^2(t) + e_1 \dot{v}(t) - e_1 \cdot u(t)]$$

$$\text{sign}(e(t)) = \text{sign}(e_1(t)) \text{ iff } e(t) \cdot e_1(t) = e(t) \cdot e(t) - e(t) \cdot e_2(t) > 0 \quad (\text{C.35})$$

$\Rightarrow e_1 \dot{e}_1(t) < 0$ can be guaranteed only when $|e(t)| \geq \delta \geq \delta_o$.

From $|e(t)| \leq \delta$, we can get that

$$|e_1(t)| - \delta_o \leq |e_1(t)| - |e_2(t)| \leq |e_1(t) + e_2(t)| = |e(t)| \leq \delta \Rightarrow |e_1(t)| \leq \delta_o + \delta.$$

(b) By choosing the weighting, W_j , and membership functions, Mem_j^u , the following equation can be satisfied,

$$\text{fuzzy}(e) = 0 \Leftrightarrow |e_1| \leq \delta + \delta_o$$

i.e. the lowest upper bound of the tracking error can be achieved by controlling $\text{fuzzy}(e) \rightarrow 0$. From equation (C.35), we know that the control direction can be determined only when $|e_1| \geq \delta + \delta_o$, i.e. $\text{fuzzy}(e) \neq 0$.

Also we can see that using $\text{fuzzy}(e)$ as feedback signal can avoid the high frequency control signal because $u = 0$ when $\text{fuzzy}(e) = 0$. If we use $e(t)$ as feedback signal, the measurement uncertainty of $e(t)$ must be considered in designing the controller.

Remark C.1. From Theorem C.2, we can choose a proper bound of $e_1(t)$ by estimating the upper bound of $|e_2(t) + e_3(t)|$ from equation (C.10) and (C.11) and a proper control gain from equation (C.9). This will reduce the high frequency control signal [Xu et al.,1989].

With the results of Theorem C.2, we will establish in Theorem C.3 the result for Estimation Scheme A. The controller design will be described. The upper bound of the

steady state estimation error and some criterion for performance improvement are derived.

Theorem C.3. Consider the schematic shown in Figure 5.1, the system is described by equations (C.1)-(C.2). The control $u(t) = -K_p \cdot \text{fuzzy}(e(t))$ is designed such that

$$K_p \cdot |\text{fuzzy}(e)|_{|e(t)| \geq \phi} \geq \left| \sum_{i=0}^{2N} \tilde{A}_i s_i(t) - \dot{v} \right|_{\max} \quad (\text{C.36})$$

then the estimation error is bounded,

$$\left| K_G (\hat{A}(t) - \dot{v}(t)) \right| \leq \phi + |e_4(t)| \quad (\text{C.37})$$

where $e_4(t)$ is described in equation (C.18), $\text{fuzzy}(e)$ is a monotonous function of e ,

$$\text{fuzzy}(e(t)) = \left[\sum_j W_j \cdot \text{Mem}_j^u(e) \right] \cdot e(t) \quad (\text{C.38})$$

and

$$\begin{aligned} |e_2(t) + e_3(t)| + \left| \sum_{i=0}^{2N} A''_{vi} [(K_{gi} - K_G) s_i(t) + K'_{gi} s'_i(t)] - K_G \sum_{i=2N+1}^{\infty} A''_{wi} s_i(t) \right| \\ + \left| \sum_{i=2N+1}^{\infty} A''_{wi} [K_{gi} s_i(t) + K'_{gi} s'_i(t)] \right| \leq \phi \end{aligned} \quad (\text{C.39})$$

The performance of the acceleration estimation \hat{A} is improved upon A' if the filter g can be designed such that the following condition is satisfied for $u = 0$

$$|e(t)| \geq 2|e_4(t)| + 2\phi \quad (\text{C.40})$$

Proof:

Substituting the control law in equation (C.36) into equation (C.9), we can verify directly

using Theorem C.2 that for $|e(t)| > |e_2(t) + e_3(t)|$

$$e_1(t) \cdot \dot{e}_1(t) < 0$$

That is, the following equation can be satisfied

$$\left| K_G(\hat{A}(t) - \dot{v}(t)) + e_4(t) \right| \leq 2|e_2(t) + e_3(t)| \leq 2\phi$$

If equation (C.40) is satisfied for $u = 0$, from equation (C.36), the performance of acceleration estimation is improved in the sense that the maximum error is reduced.

Remark C.2. From Theorem C.3, the filter g is designed to minimize $|e_2(t) + e_3(t)|$ and $|e_4(t)|$. If condition (C.40) can be satisfied by designing the filter g , the performance can be improved. And condition (C.40) means that the frequency bands of the signal and the noise are not heavily overlaid.

Before we establish the result for Estimation Scheme B (shown in Figure 5.2), we will introduce some assumptions.

Assumption C.2.

1. $\left| \sum_{i=0}^{2N} (K_f(c)\tilde{A}_i s_i + K'_f(c)\tilde{A}_i s'_i) - \dot{v} - (e_1 - \varepsilon_{f1}) \right| \leq$

$$MAX(\varepsilon_a, \delta_a \left| \sum_{i=0}^{2N} (K_f(c)\tilde{A}_i s_i + K'_f(c)\tilde{A}_i s'_i) - \dot{v} \right|)$$
2. $\left| \sum_{i=0}^{2N} \tilde{A}_i s_i - \dot{v} \right| \leq \tilde{\varepsilon}$
3. $\left| \sum_{i=0}^{2N} \frac{K'_f}{c} \tilde{A}_i s'_i \right| \leq \tilde{\delta}_c$

$$4. \left| \frac{\partial}{\partial c} \left[\sum_{i=0}^{2N} (K_{\beta}(c) \tilde{A}_i s_i + K'_{\beta}(c) \tilde{A}_i s'_i) \right] \right| \geq M_8 \left(\left| \sum_{i=0}^{2N} (K_{\beta}(c) \tilde{A}_i s_i + K'_{\beta}(c) \tilde{A}_i s'_i) - \dot{v} \right| - \tilde{\varepsilon} \right) - \tilde{\delta}_c \quad \text{if}$$

$$\left| \sum_{i=0}^{2N} (K_{\beta}(c) \tilde{A}_i s_i + K'_{\beta}(c) \tilde{A}_i s'_i) - \dot{v} \right| \geq |e_2 + e_3 + \varepsilon_{f1}|$$

It is worth mention that Assumption C.2.4 means that the changing of signal distortion w.r.t. bandwidth is big when the distortion is big. Next, we will introduce the result for Estimation Scheme B, it is shown that the estimation with adaptive bandwidth filter is better than that with constant bandwidth filter if some conditions are satisfied.

Theorem C.4. For the system described by equations (C.1)-(C.2) and the schematic shown in Figure 5.2, a cost function of the integration of the square of the estimation error, $J(c, \dot{c})$, is considered. There exists some adaptively tuned $c(t) = f(t, r, n) > c_0$, $\forall t \in (t_1, t_2)$, $c(t_1) = c(t_2) = c_0$, such that $J(c(t), \dot{c}) < J(c_0, 0)$, if the following conditions are satisfied

1. $(\partial J^1 / \partial c)_{c=c_0} \leq -\eta < 0$
2. $J^2(c, 0) = 0$
3. $|J^2| \leq \max|\dot{c}(t)| \cdot M_7$
4. $M_7 |(\partial \max|\dot{c}| / \partial r)_{c=c_0}| \leq \eta |(\partial c / \partial r)_{c=c_0}|$

where

$$J^1 = \int_1^2 \left(\sum_{i=0}^{2N} [(K_{\beta}(c) \tilde{A}_i - \dot{v}_i) s_i + K'_{\beta}(c) \tilde{A}_i s'_i] + \sum_{i=2N+1}^{\infty} \tilde{A}_i [K_{\beta}(c) s_i + K'_{\beta}(c) s'_i] \right)^2 dt \quad (\text{C.41})$$

$$J^2 = \int_1^2 \varepsilon_{f1} \left(2 \sum_{i=0}^{2N} [(K_{\beta}(c) \tilde{A}_i - \dot{v}_i) s_i + K'_{\beta}(c) \tilde{A}_i s'_i] \right) dt$$

$$+ \int_1^2 \varepsilon_{f1} (2 \sum_{i=2N+1}^{\infty} \tilde{A}_i [K_{\beta}(c)s_i + K'_{\beta}(c)s'_i] + \varepsilon_{f1}) dt \quad (C.42)$$

$$J = \int_1^2 (\hat{A} - \dot{v})^2 dt = J^1 + J^2 \quad (C.43)$$

and $f(t, 0, n) = c_0$, $\dot{c}(t) = \dot{f}(t, r, n)$ is a continuous differentiable function of r , $(\partial c / \partial r) \geq 0$.

That is, there exists some n_0 and $r_0 > 0$ such that $J(c(t, r_0, n_0), \dot{c}) < J(c(t, 0, n_0), 0)$. In other words, the performance J of the acceleration estimation with adaptive bandwidth filter is better than that with constant bandwidth filter. A possible candidate

$$c(e(t)) = \begin{cases} c_0 & \text{if } e(t) \leq e_0 \\ c_0 + (c_{max} - c_0)(1 - \exp^{-r(e-e_0)^n}) & \text{if } e(t) > e_0 \end{cases} \quad (C.44)$$

where $e_0 \geq |e_2 + e_3 + \varepsilon_{f1}| + \Phi$ and Φ satisfies the following equation

$$\begin{aligned} & |MIN(\Phi - \varepsilon_a, \Phi / (1 + \delta_a))| \cdot |M_8(MIN(\Phi - \varepsilon_a, \Phi / (1 + \delta_a)) - \tilde{\varepsilon}) - \tilde{\delta}_c| \geq \\ & \left(\frac{c_{max}^2}{c_{max}^2 + \omega_{2N+1}^2} \right) M_6 \cdot \left(|M_8(MIN(\Phi - \varepsilon_a, \Phi / (1 + \delta_a)) - \tilde{\varepsilon}) - \tilde{\delta}_c| + \frac{3M_6}{4c_{min}} \right) + \\ & |MIN(\Phi - \varepsilon_a, \Phi / (1 + \delta_a))| \cdot \frac{3M_6}{4c_{min}} + \eta \end{aligned} \quad (C.45)$$

Proof:

From stated condition 3 and 4,

$$\left| \left(\frac{\partial J^2}{\partial r} \right)_{r=0} \right| \leq \left| \left(\frac{\partial J^2}{\partial \max|\dot{c}|} \right)_{r=0} \cdot \left(\frac{\partial \max|\dot{c}|}{\partial r} \right)_{r=0} \right| \leq \eta \cdot \left(\frac{\partial |c|}{\partial r} \right)_{r=0}$$

Because $J = J^1 + J^2$,

$$(\partial J / \partial r)_{r=0} = (\partial J^1 / \partial r)_{r=0} + (\partial J^2 / \partial r)_{r=0} \leq 0$$

That is, if conditions (1)-(4) are satisfied, there exists some adaptive $c(t)$ which will have better estimation than that with constant $c(t)=c_0$. Also $c(t_1)=c(t_2)=c_0$, and $c(t) > c_0$, $\forall t \in (t_1, t_2)$.

Next, we will consider the system described by equation (C.1)-(C.2) and shown in Figure 5.2. Consider J^1 , the following equations can be verified directly from equation (C.7)-(C.8) and Assumption C.1,

$$\left| \sum_{i=2N+1}^{\infty} K_{f_i}(c) \tilde{A}_i s_i \right| \leq \frac{c_{max}^2}{c_{max}^2 + \omega_{2N+1}^2} M_6 \quad (C.46)$$

$$\left| \sum_{i=2N+1}^{\infty} K'_{f_i}(c) \tilde{A}_i s'_i \right| \leq \frac{1}{2} M_6 \quad (C.47)$$

$$\left| \frac{\partial}{\partial c} \left[\sum_{i=2N+1}^{\infty} K_{f_i}(c) \tilde{A}_i s_i \right] \right| \leq \frac{1}{2c_{min}} M_6 \quad (C.48)$$

$$\left| \frac{\partial}{\partial c} \left[\sum_{i=2N+1}^{\infty} K'_{f_i}(c) \tilde{A}_i s'_i \right] \right| \leq \frac{1}{4c_{min}} M_6 \quad (C.49)$$

If $|e(t)| \geq |e_2 + e_3 + \varepsilon_{f1}| + \Phi$, using equation (C.9), (C.13)-(C.15), and Assumption C.2,

we can get that

$$\left| \sum_{i=0}^{2N} (K_{f_i}(c) \tilde{A}_i s_i + K'_{f_i}(c) \tilde{A}_i s'_i) - \hat{v} \right| \geq \text{MIN}(\Phi - \varepsilon_a, \Phi / (1 + \delta_a))$$

$$\left| \frac{\partial}{\partial c} \sum_{i=0}^{2N} (K_{f_i}(c) \tilde{A}_i s_i + K'_{f_i}(c) \tilde{A}_i s'_i) \right| \geq M_8 (\text{MIN}(\Phi - \varepsilon_a, \Phi / (1 + \delta_a)) - \tilde{\varepsilon}) - \tilde{\delta}_c$$

Using equations (C.45)-(C.49), we can get that

$$\left(\frac{\partial J^1}{\partial c}\right)_{c=c_0} \leq -\eta < 0$$

Also, from equation (C.42), we can get that

1. J^2 is a continuous function of \dot{c} and $J^2(c,0) = 0$.
2. There exists a constant M_7 , such that $|J^2| \leq \max|\dot{c}| \cdot M_7$.

And it can be verified directly that there exists n_0 and r_0 such that the candidate of $c(t)$

described in equation (C.44) will satisfy condition 4 if $e_0 \geq |e_2 + e_3 + \varepsilon_{f1}| + \Phi$.

Finally, it is proved that the stated conditions (1)-(4) are satisfied for the system shown in Figure 5.2 with $c(t)$ described in equation (C.45).

VITA

Jing-Shiun Lai was born in Taiwan, R.O.C., July 10, 1962. He received his B.S. and M.S. degrees in Control Engineering in May 1984 and May 1986 from National Chiao-Tung University, Taiwan. After serving his military service in the Army for two years, he was a lecturer at the Da-Hwa College. He also received an M.S. degree in Mechanical Engineering in December 1990 from New Jersey Institute of Technology and continued his doctoral study in Mechanical Engineering at The Pennsylvania State University in August 1991.